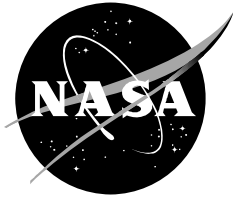


NASA/TM-2008-214765



C-9 and Other Microgravity Simulations

Summary Report

Report prepared by
Space Life Sciences Directorate
Human Adaptation & Countermeasures Division
Johnson Space Center, Houston

Lyndon B. Johnson Space Center
Houston, Texas

September 2008

THE NASA STI PROGRAM OFFICE . . . IN PROFILE

Since its founding, NASA has been dedicated to the advancement of aeronautics and space science. The NASA Scientific and Technical Information (STI) Program Office plays a key part in helping NASA maintain this important role.

The NASA STI Program Office is operated by Langley Research Center, the lead center for NASA's scientific and technical information. The NASA STI Program Office provides access to the NASA STI Database, the largest collection of aeronautical and space science STI in the world. The Program Office is also NASA's institutional mechanism for disseminating the results of its research and development activities. These results are published by NASA in the NASA STI Report Series, which includes the following report types:

- **TECHNICAL PUBLICATION.** Reports of completed research or a major significant phase of research that present the results of NASA programs and include extensive data or theoretical analysis. Includes compilations of significant scientific and technical data and information deemed to be of continuing reference value. NASA's counterpart of peer-reviewed formal professional papers but has less stringent limitations on manuscript length and extent of graphic presentations.
- **TECHNICAL MEMORANDUM.** Scientific and technical findings that are preliminary or of specialized interest, e.g., quick release reports, working papers, and bibliographies that contain minimal annotation. Does not contain extensive analysis.
- **CONTRACTOR REPORT.** Scientific and technical findings by NASA-sponsored contractors and grantees.

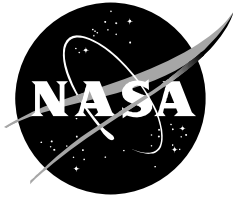
- **CONFERENCE PUBLICATION.** Collected papers from scientific and technical conferences, symposia, seminars, or other meetings sponsored or cosponsored by NASA.
- **SPECIAL PUBLICATION.** Scientific, technical, or historical information from NASA programs, projects, and mission, often concerned with subjects having substantial public interest.
- **TECHNICAL TRANSLATION.** English-language translations of foreign scientific and technical material pertinent to NASA's mission.

Specialized services that complement the STI Program Office's diverse offerings include creating custom thesauri, building customized databases, organizing and publishing research results . . . even providing videos.

For more information about the NASA STI Program Office, see the following:

- Access the NASA STI Program Home Page at <http://www.sti.nasa.gov>
- E-mail your question via the Internet to help@sti.nasa.gov
- Fax your question to the NASA Access Help Desk at (301) 621-0134
- Telephone the NASA Access Help Desk at (301) 621-0390
- Write to:
NASA Access Help Desk
NASA Center for AeroSpace Information
7115 Standard
Hanover, MD 21076-1320

NASA/TM-2008-214765



C-9 and Other Microgravity Simulations

Summary Report

Report prepared by
Space Life Sciences Directorate
Human Adaptation & Countermeasures Division
Johnson Space Center, Houston

National Aeronautics and Space Administration
Lyndon B. Johnson Space Center
Houston, Texas

September 2008

**C-9 and Other Microgravity Simulations
Summary Report – September 30, 2008**

National Aeronautics and Space Administration
Lyndon B. Johnson Space Center

Prepared by: Noel C Skinner 8/21/08
Noel C. Skinner, MS
C-9 Coordinator
Wyle
Date

Wanda L Thompson 8/21/08
Wanda L. Thompson, RN, BC, NMCC
Alternate C-9 Coordinator
JES Tech, LLC
Date

Approved by: Jeanie L Nillen 8/20/08
Jeanie L. Nillen, MT (ASCP)
Manager
Human Adaptation & Countermeasures Group
Wyle
Date

Approved by: Todd T. Schlegel, MD 8/18/08
Todd T. Schlegel, MD
Technical Monitor
Human Adaptation & Countermeasures Division
Reduced-Gravity Program
NASA Johnson Space Center
Date

Available from:

NASA Center for Aerospace Information
7115 Standard Drive
Hanover, MD 21076-1320

National Technical Information Service
5285 Port Royal Road
Springfield, VA 22161

This report is also available in electronic form at <http://ston.jsc.nasa.gov/collections/TRS>

PREFACE

This document represents a summary of medical and scientific evaluations conducted aboard the C-9 or other NASA sponsored aircraft from June 23, 2007, to June 23, 2008. Included is a general overview of investigations manifested and coordinated by the Human Adaptation & Countermeasures Division. A collection of brief reports that describe tests conducted aboard the NASA-sponsored aircraft follows the overview. Principal investigators and test engineers contributed significantly to the content of the report describing their particular experiment or hardware evaluation. Although this document follows general guidelines, the format of individual reports varies to accommodate differences in experiment design and procedures. This document concludes with an appendix that provides background information about the Reduced-Gravity Program.



CONTENTS

| | |
|---|----------|
| Overview of Flight Activities Sponsored by the Human Adaptation & Countermeasures Division | 1 |
| Medical and Scientific Evaluations during Parabolic Flights..... | 2 |
| The Effects of Microgravity on Enzyme Kinetic Reactions | 3 |
| Human Vestibular Orientation and Posture in Variable Force Backgrounds – Flight Week 1 | 7 |
| Robotic Surgery in Flight..... | 12 |
| Integrated Immune Flight Study (SMO-015, SDBI-1900) – Evaluation of In-flight Sample Collection Hardware and Recording of Training Video for STS and ISS Crewmembers | 19 |
| Rapid Development of Colorimetric-Solid Phase Extraction Technology for Water Quality Monitoring: Evaluation of C-SPE Total Iodine Analysis Methods in Microgravity | 23 |
| Manned Evaluation of the Second-Generation International Space Station Treadmill during Parabolic Flight..... | 36 |
| Space Medicine C-9 Familiarization Flight | 46 |
| NASA Explorer School – NASA’s Weightless Wonder Simulates Microgravity Mass Determination via Inertial Balance Technology | 52 |
| NASA Explorer School – Reaction Time | 58 |
| NASA Educator Astronaut Teacher Program – Nutrient Delivery Systems for Plant Growth Chambers in Micro Gravity | 66 |
| NASA Educator Astronaut Teacher Program – Capillary Conundrum..... | 75 |
| NASA Educator Astronaut Teacher Program – Effect of Microgravity on the Lateral Movement of Hair Cell Bundles (HCB) within the Otolithic Membrane | 83 |
| NASA Educator Astronaut Teacher Program – The Effects of Microgravity on the Motion of Stereocilia in the Semi-Circular Canals of the Inner Ear..... | 93 |
| NASA Educator Astronaut Teacher Program – Soil Porosity at Reduced Gravity | 102 |
| NASA Educator Astronaut Teacher Program – Physics of Plant Growth in Micro, Lunar, and Martian Gravity | 109 |
| NASA Educator Astronaut Teacher Program – Project MEGA (Microgravity Experimental Growth Activity) | 118 |
| NASA Educator Astronaut Teacher Program – Uptake of Nutrients by Plants in Microgravity | 121 |
| Transgenic Arabidopsis Gene Expression System and Advanced Biological Research System..... | 127 |
| Human Vestibular Orientation in Variable Force Backgrounds – Flight Week 2 | 132 |
| Undergraduate Program – Multimission Space Suit EVA Drink Bag Filling Process | 137 |
| Undergraduate Program – Gravitational Effects on Human Immune Complexes and Flame Dynamics..... | 142 |
| Undergraduate Program – Study of Damping Effects of Grass-like Crops in a Microgravity Environment..... | 147 |
| Appendix | A |
| Background Information about the C-9 and the Reduced-Gravity Program..... | 1 |

Overview of Flight Activities Sponsored by the Human Adaptation & Countermeasures Division

Four weeks of the year from June 23, 2007, to June 23, 2008, were specifically reserved for flights sponsored by the Human Adaptation & Countermeasures Division (HACD). In addition, we were able to obtain seating for HACD customers during 6 flight weeks sponsored by other organizations. A total of 30 flights with approximately 40 parabolas per flight were completed. The average duration of each flight was 2 hours. The C-9 coordinator assisted the principal investigators and test engineers of 23 different experiments and hardware evaluations in meeting the necessary requirements for flying aboard the C-9 and in obtaining the required seating and floor space. HACD customers purchased a total of 229 seats. The number of seats supported and number of different tests flown by flight week are provided below:

| Flight Week | Seats | # Tests Flown | Sponsor |
|----------------------|--------------|----------------------|--|
| July 31–Aug. 2, 2007 | 42 | 2 | HACD |
| Sept. 25–28 | 33 | 2 | HACD |
| Oct. 23–26 | 45 | 3 | HACD |
| Feb. 15, 2008 | 5 | 1 | NASA Explorer School |
| Feb. 26–27 | 4 | 1 | NASA Explorer School |
| Mar. 11–14 | 32 | 8 | NASA Educator Astronaut Teacher Program |
| Mar. 18–21 | 52 | 2 | HACD |
| Apr. 9 | 4 | 1 | Undergraduate Program |
| Apr. 22–23 | 4 | 1 | Undergraduate Program |
| June 12–13 | 8 | 2 | Undergraduate Program |

Support was provided to the NASA Explorer School teacher program during February, to the NASA Educator Astronaut Teacher program during March, and to the Undergraduate Program during weeks in April and June. A large ground crew from the respective institutions supported the in-flight experiments.

Other HACD-sponsored flight opportunities are scheduled for weeks during July, August, and September 2008. Additional flights will be added throughout the remainder of calendar year 2008 to accommodate customers, as needs arise.

Medical and Scientific Evaluations during Parabolic Flights

TITLE

The Effects of Microgravity on Enzyme Kinetic Reactions

FLIGHT DATES

July 31, 2007–August 3, 2007

PRINCIPAL INVESTIGATOR

Vince LiCata, Louisiana State University

CO-INVESTIGATORS

Chin-Chi Liu, Louisiana State University

Allison J. Richard, Louisiana State University



GOAL

The overall goal is to determine if microgravity alters protein kinetics and equilibria.

OBJECTIVES

The objective is to test the effects of microgravity on several enzyme kinetic reactions: fast and slow acetylcholinesterase, and alkaline phosphatase.

METHODS AND MATERIALS

Materials

Enzymes and all other standard reagents were purchased from Sigma Chemical (St. Louis, MO).

Over the course of several parabolic microgravity flights, we measured:

Ligand concentration dependence for the enzyme kinetics of the acetylcholinesterase (AChE) and alkaline phosphatase reactions. Two different AChE variants were examined: fast (from electric eel) and slow (bovine). Six to 8 data points were collected, in duplicate, for each full Michaelis-Menten (MM) curve. Each full parabola yielded one 0 G data sequence (kinetics collected for 10 s) and one 1.7 G data sequence. Each data sequence was analyzed linearly (see below) to obtain the rate of reaction at that substrate concentration. Each rate point was then plotted versus substrate concentration to obtain a full MM curve. Full MM curves were collected at 0%, 10%, 20%, and 30% glycerol concentrations for fast AChE only.

Data Analysis

The initial portion of each kinetic trace was fit to a linear equation to obtain the effect rate at that substrate concentration. A plot of rate (slope) versus [substrate] yields a standard MM kinetics curve:

$$v = V_{MAX} [S] / K_M + [S] \quad (\text{Equation 1})$$

The curve (v versus [S]) was then nonlinearly fit to determine the V_{max} and K_m parameters.

RESULTS

All reactions were measured both during the microgravity portion of each parabola and during the 1.7 G portion of each parabola. The 1.7 G measurements served as the control measurements in flight. All reactions were also measured at 1 G either in the laboratory or on the C-9 while it was parked in the hangar at Johnson Space Center.

Significant spectrophotometer drift occurs during parabolic flight. The drift is linear, and the slope of the drift is different for 0 G and 1.8 G. However, drift slopes are highly consistent from one parabola to the next, and so raw kinetic data are processed by

subtracting the spectrophotometric drift, as described in the flight report for May 2007.

Michaelis-Menten curves for slow AChE, fast AChE, and alkaline phosphatase at 0 G and 2 G are shown in figures 1-1 and 1-2.

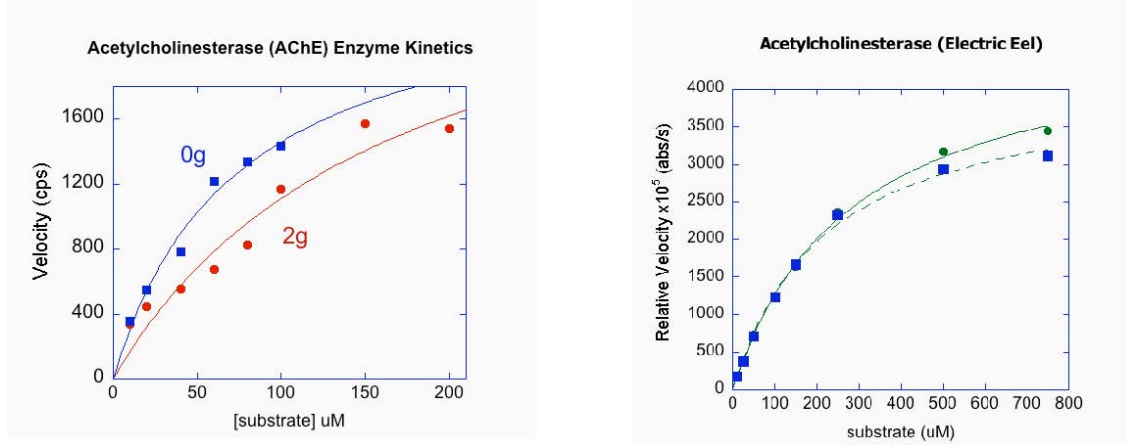


Figure 1-1. Michaelis-Menten kinetic curves for slow (left) and fast (right) AChE at 0 G (top curve in both) and 1.8 G (bottom curve in both).

The data of figure 1-1 indicate a possible change in the enzyme kinetics for slow AChE in microgravity versus macrogravity. The increased V_{max} in microgravity suggests that the reaction rate for slow acetylcholinesterase is enhanced in microgravity. Full statistical analysis of these data is still in progress.

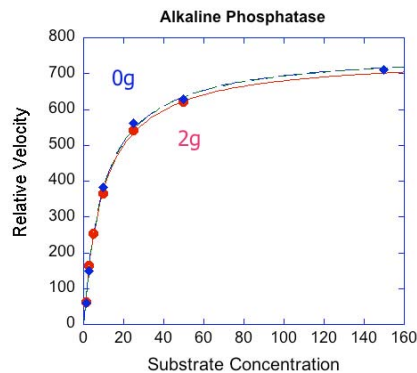


Figure 1-2. Michaelis-Menten kinetic curves for alkaline phosphatase at 0 G and 2 G .

DISCUSSION AND CONCLUSIONS

The goal of this project is to determine if microgravity alters the reaction rates for very rapid biological reactions. Small apparent effects of microgravity have been observed in several systems; however, the harsh measurement conditions during flight consistently result in much higher random, and sometimes systematic, error for in-flight data. Continued redesign of the experimental equipment continues to improve data quality. Further data collection is necessary to confirm these conclusions.

REFERENCES

Cantor, C. R. and Schimmel, P. R. (1980) Biophysical Chemistry, Part III, The Behavior of Biological Macromolecules. W. H. Freeman and Company. San Francisco, CA. USA.

Hammes, G. G. (2000) Thermodynamics and Kinetics for the Biological Sciences. A. J. Wiley and Sons. New York, NY. USA.

Schoeffler, A. J., Ruiz, C. R., Joubert, A. M., Yang, X., and LiCata, V. J. (2003) Salt modulates the stability and lipid binding affinity of the adipocyte lipid binding protein, *J. Biol.Chem.* 278, 33268-33275.

PHOTOGRAPHS

JSC2007EO38976

JSC2007EO38980 to JSC2007EO38982

JSC2007EO38984 to JSC2007EO38986

JSC2007EO38989 to JSC2007EO38991

JSC2007EO38997

JSC2007E040833 to JSC2007E040835

JSC2007E040841 to JSC2007E040844

JSC2007E040849

JSC2007E040852 to JSC2007E040855

JSC2007E040858 to JSC2007E040852

JSC2007E040953

JSC2007E040955 to JSC2007E040960

JSC2007E0409558 to JSC2007E040960

JSC2007E040962 to JSC2007E040964

JSC2007E040968 to JSC2007E040973

JSC2007E040975 to JSC2007E040977

VIDEO

- Zero G flight week July 31–August 3, 2007, Master: PROV.DV

Videos available from Imagery and Publications Office (GS4), NASA JSC.

CONTACT INFORMATION

Vince LiCata, PhD

Department of Biological Sciences

Louisiana State University

Baton Rouge, LA 70803

Phone: (225) 578-5233

FAX: (225) 578-2597

licata@lsu.edu

TITLE

Human Vestibular Orientation and Posture in Variable Force Backgrounds –
Flight Week 1

FLIGHT DATES

July 31–August 2, 2007

PRINCIPAL INVESTIGATOR

James R. Lackner, Brandeis University

Paul DiZio, Brandeis University



OBJECTIVES

The experiment we conducted during July 31–August 2, 2007, in parabolic flights on board the C-9 was a continuation of our effort to develop a predictive model of human vestibular orientation and posture in variable force backgrounds.

We conducted 3 experiments, which are designated by their project name and specific aim, as follows:

1. Models and Mechanisms – Vestibular Orientation
2. Predicting and Assessing – Bipedal Control
3. Predicting and Assessing – Limb Mass Adaptation

BACKGROUND

During the past few years, we have developed a model of static orientation (Bortolami et al. 2006). Past parabolic flight experiments have confirmed a novel prediction of this model, that localization of the subjective vertical during recumbent yaw axis tilts is not influenced by increases in gravito-inertial force (GIF) background above 1 G. This finding contrasts with the well-known influence of GIF on subjective vertical estimates for pitch and roll tilts (Correia et al. 1968). A further prediction of our model is that tilt about 1 axis will cause systematic variations in estimates of the subjective vertical, not only about the physical axis of head tilt but also about the orthogonal axes.

The specific aim of the present Experiment 1, *Models and Mechanisms – Vestibular Orientation*, was to collect the first comprehensive data set assessing the subjective vertical as a function of static, 3-dimensional body orientation and force background. Four subjects were tested with a new multi-axis tilting chair. Each subject was blindfolded and securely strapped into the device. The subject indicated the perceived vertical with a joystick while being held briefly in various static tilted positions. The joystick orientation data were collected with a magnetic tracking system. Static tilts included 1) all 3 tilt axes – roll, pitch, and recumbent yaw; 2) the full range of possible tilt angles, 0–360°; 3) multiple force backgrounds – 0 G, 1 G, and 1.8 G. This data set, when analyzed, will allow the development and evaluation of the first true 3-dimensional model of static orientation. The procedure has been approved by the Brandeis Committee for the Protection of Human Subjects (CPHS) as well as by the Johnson Space Center (JSC) CPHS.

The specific aim for the present Experiment 2, *Predicting and Assessing – Bipedal Control*, was to assess bipedal patterns of ground reaction force when subjects stand without moving their feet in 1 G and 1.8 G. A dual force plate was used to collect ground 1 G and parabolic flight 1.8 G data from both feet while subjects stood with their feet side by side. Eight subjects participated. Their tasks included 1) standing as still as possible; 2) voluntarily executing rectilinear oscillations of their center of mass, $\approx \pm 2$ cm, in 3 directions – anterior-posterior, medial-lateral, and diagonal; 3) voluntarily moving their center of mass in a circle with a radius of ~ 2 cm. The results will be used to evaluate a model of bipedal control of stance and voluntary postural rhythms. The procedure has been approved by the Brandeis CPHS and the JSC CPHS.

The specific aim for the present Experiment 3, *Predicting and Assessing – Limb Mass Adaptation*, was to understand how altering arm mass affects arm movement control. Eight subjects participated. Subjects executed planar reaching movements before, during, and after either donning a weighted (400 g) glove or grasping an equivalent mass. Movements were performed only in 0 G, so that the glove added mass but not weight to the arm. An accelerometer package connected to a laptop computer was used to collect kinematic data about the arm. When data have been processed, we hope to learn the time course required for subjects to internalize the added mass of a worn versus a hefted mass.

METHODS AND MATERIALS

The specific procedures for each experiment were as follows:

Models and Mechanisms – Vestibular Orientation

Each subject was tested in parabolas 1 through 40 of 1 flight day. The subjects selected for testing were all experienced fliers who have never had any of the severe motion sickness symptoms in parabolic flight. Subjects were blindfolded and tightly restrained in a motorized 2-axis device capable of tilting them in pitch (horizontal, medial-lateral body axis), roll (horizontal, anterior-posterior body axis) or recumbent yaw (horizontal, foot-to-head body axis). Subjects wore earplugs and noise-canceling earphones and listened to white noise to mask the sound of the aircraft as much as possible. The experimenter could interrupt the white noise to speak to the subject at any time. The experimenter triggered a 2-axis device movement when he or she judged that a stable 1.8 G or 0 G force period (during parabolas) or 1 G period (during straight-and-level flight) had been reached, by viewing accelerometer readout on a computer console. The 2-axis device moved to a randomly selected tilt angle (from a set of angles covering the full 360° range at 15° increments) about 1 of the 3 axes. Tilt velocity profiles were raised cosines with peak velocities of 30°/s to 180°/s and durations of 0.5 s to 4 s. These profiles mimic natural head turns in speed and amplitude. When the tilt was complete, the subject heard a computer-generated command instructing him or her to indicate the subjective vertical by orienting a pointer held by both hands so that its top pointed “up.”

Two tilts and 2 judgments were conducted in each of the 1.8 G and 0 G force phases during parabolas. Rests were given every sixth parabola, with the subject positioned upright.

Predicting and Assessing – Bipedal Control

Each subject participated in parabolas 1 through 20 or in parabolas 21 through 40, as well as in the periods of straight and level flight preceding these parabola sets. Trials consisted of having the subject stand for 20 s on dual force plates, with their eyes open, and with their feet in a comfortable side-by-side stance. Subjects were instructed to attempt to stand without support from their hands, but a safety bar was available for them in case of loss of balance. A spotter was stationed behind the subject. No motion tracking of body segments was done; data from the force plates were recorded using a laptop computer. In each trial, the experimenter told the subject to do 1 of the 5 practiced tasks, in random order, when the force level was 1.8 G (during parabolas) or 1 G (in straight-and-level flight) and started data collection when the subject said “ready.” Analyses will focus on the center of foot pressure and the weight distribution (vertical force) under each foot.

Predicting and Assessing – Limb Mass Adaptation

Each subject was tested in parabolas 1 through 40 of 1 flight day. Testing was done with the subject seated in any one of the standard aircraft seats on the right (starboard) side of the cabin. The portable work surface was secured to the arms of the chair with Velcro® straps after takeoff. Marked on the table surface were a starting location for all reaches, and 4 target locations. In the 0 G phase of each parabola, the experimenter gave verbal

commands for the subject to move from the start location to one of the targets, and to return when done. Four movements per parabola were executed. In parabolas 1 through 4, the subjects made moves with their hand free. In parabolas 5 through 36, they wore a glove weighing 400 g, and in parabolas 37 through 40, they again moved with their hand free. A laptop computer collected kinematic data about the arm movement from a set of accelerometers mounted on elastic cuffs worn on the arm.

RESULTS

Analysis of the data is currently underway.

CONCLUSION

Because data analysis is still in progress, we have no scientific conclusion yet. However, an important outcome was that the multi-axis tilt device used for the Vestibular Orientation experiment functioned well in parabolic flight. This is important because it is a major, novel device that will be important for the future of our experiment program.

REFERENCES

- Bortolami SB, Rocca S, DiZio P, Lackner J (2006) Mechanisms of human static spatial orientation. *Exp Brain Research* 173: 374-388
- Correia MJ, Hixson WC, Niven JI (1968) On predictive equations for subjective judgments of vertical and horizon in a force field. *Acta Otolaryngol (Stockh.) Suppl.* 230: 1 -20

PHOTOGRAPHS

JSC2007EO39008
JSC2007EO38983
JSC2007EO38987 to JSC2007EO38988
JSC2007EO38992 to JSC2007EO38993
JSC2007EO38996
JSC2007EO38975
JSC2007EO38977 to JSC2007EO38979
JSC2007EO38983
JSC2007EO38987 to JSC2007EO38988
JSC2007EO38992 to JSC2007EO38993
JSC2007EO38996
JSC2007EO39000 to JSC2007EO39020
JSC2007E040831 to JSC2007E040840
JSC2007E040886 to JSC2007E040890
JSC2007E040894 to JSC2007E040917
JSC2007E 040846 to JSC2007E040848
JSC2007E040850 to JSC2007E040851
JSC2007E040856 to JSC2007E040857
JSC2007E040859 to JSC2007E040864

JSC2007E040954
JSC2007E040961
JSC2007E040965 to JSC2007E040967
JSC2007E040974
JSC2007E040978 to JSC2007E041010

VIDEO

- Zero G flight week July 31–August 3, 2007, Master: PROV.DV

Videos available from Imagery and Publications Office (GS4), NASA JSC.

ACKNOWLEDGEMENT

Grant Support: Air Force Grant # FA9550-06-1-0102

CONTACT INFORMATION

| | |
|------------------------------------|--|
| Dr. James R. Lackner, Director | lackner@brandeis.edu |
| Dr. Paul DiZio, Associate Director | dizio@brandeis.edu |

Ashton Graybiel Spatial Orientation Laboratory
Brandeis University MS 033
Waltham MA 02454-9110
Tel: 781-736-2033
Fax: 781-736-2031

TITLE

Robotic Surgery in Flight

FLIGHT DATES

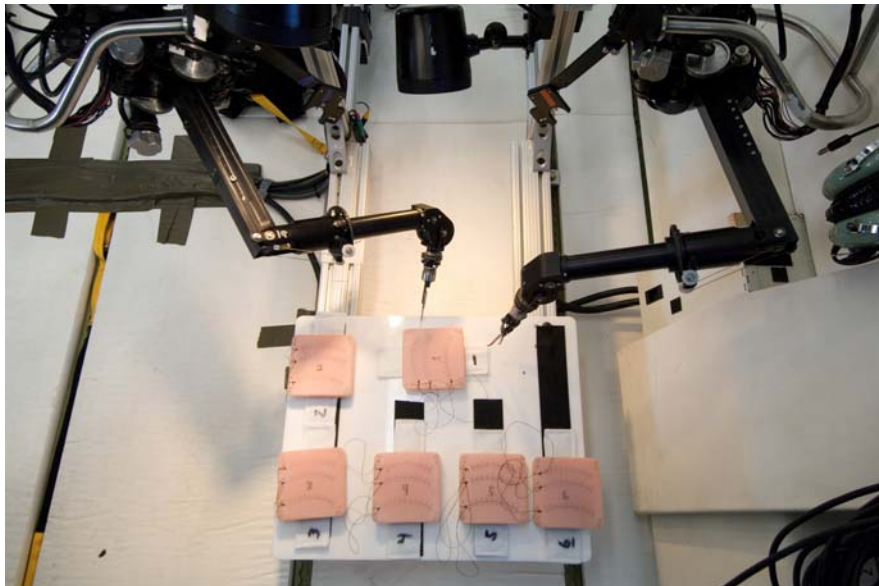
September 25–28, 2007

PRINCIPAL INVESTIGATOR

Timothy J. Broderick, University of Cincinnati

CO-INVESTIGATOR

Charles R. Doarn, University of Cincinnati



GOAL AND OBJECTIVES

This project was designed to evaluate the feasibility of using robotic technology to improve access to and quality of surgical care during flight. Robotic surgery and telesurgery can interject expert surgical care into remote extreme environments and thereby serve as a key component of future military medical care from the battlefield to critical care transport to geographically dispersed medical facilities. In addition, such a capability can serve as an effective tool in addressing medical care needs in long-duration space flight missions. As a critical element of a smart medical system, supervisory-controlled autonomous therapeutics represents a foundation of evolving medical care in these extreme environments.

Performance of surgeons and astronauts was evaluated using the SRI International M7 surgical robot to perform simulated robotic surgery during parabolic flight. The surgeons included trauma surgeons from the University of Cincinnati, the United States Air Force Center for Sustainment of Trauma and Readiness Skills, and a military Critical Care Air Transport team. For these flights, the M7 robot was modified to include acceleration compensation and permit installation on the C-9 aircraft.

The goal was to evaluate the feasibility of robotic surgery in flight and evaluate the effectiveness of acceleration compensation. Operators used the M7 robot to perform simulated surgical tasks throughout parabolic flight. Performance was evaluated using the robot with and without acceleration compensation. The experiments were performed over 4 days on board the NASA C-9 parabolic laboratory.

The science objectives for this research were

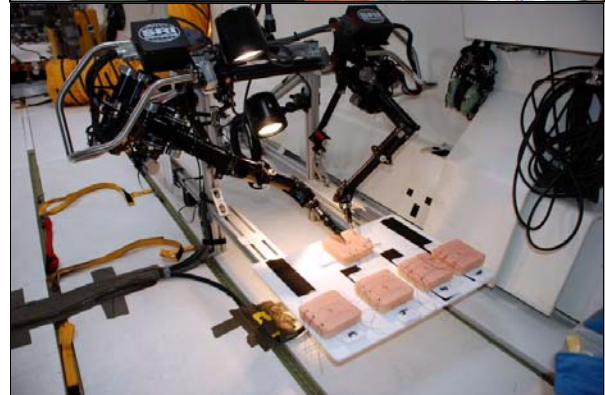
- 1) To evaluate the feasibility of robotic surgery during variable-G flight
- 2) To evaluate the effectiveness of acceleration compensation during variable-G flight
- 3) To obtain initial robotic surgical flight experience
- 4) To launch development of an exploration-enabling autonomous therapeutics system

METHODS AND MATERIALS

Over the course of 4 flights, 24 individuals (astronauts, surgeons, and non-surgeons) participated in this research. Eight participants conducted a series of surgical tasks incising and suturing simulated tissue using (1) the SRI M7 surgical robot with and without acceleration compensation and (2) a manual surgical workstation without the robot. The rest of the personnel (16) provided technical support including robot operations and data acquisition. Eight participants were evaluated during 4 parabolic flights, 2 different participants per flight. During each flight, an additional individual served as safety officer and backup surgeon.



Figure 3.1. Left photo is the manual workstation. The 2 photos on the right represent the M7 workstation.



Participants operated on the same simulated tissue using both the robot and normal surgical instruments (see fig. 3.1).

One surgeon operated the robot while restrained in a standard aircraft passenger seat and the second surgeon operated using his hands while restrained in the kneeling position. During parabolic flight, each surgeon was assessed during both microgravity (0 G) and variable gravity (V G).

The following protocol was designed for use during all flight days. The 2 participants (surgeons) completed tasks on both systems.

Flight Experiment Protocol (Robot):

Acclimation (parabolas 1 through 2)

Normal M7 settings (parabolas 3 through 20)

Three lines per simulated tissue to be incised with sutures at end of each line

Surgeon 1 (parabolas 3 through 10)

Cut Line 1 in 0 G (3)

Cut Lines 2 and 3 in V G (4 through 5)

Switch right (R)-hand instrument to needle driver (6)

Suture Line 1 in 0 G (7 through 8)

Suture Lines 2 and 3 in V G (9 through 10)

Switch to surgeon 2, switch simulated tissues, and switch R-hand instrument to scalpel during aircraft turn

Surgeon 2 (parabolas 11 through 20)

Cut Line 1 in 0 G (11)

Cut Lines 2 and 3 in V G (12 through 13)

Switch R-hand instrument to needle driver (14)

Suture Line 1 in 0 G (15 through 16)

Suture Lines 2 and 3 in V G (17 through 18)

Complete unfinished tasks as necessary (19 through 20)

Reconfigure M7; switch simulated tissues and switch R-hand instrument to scalpel during aircraft turn.

M7 variable-G compensation (parabolas 21 through 40)

Three lines per simulated tissue to be incised with sutures at end of each line

Surgeon 1 (parabolas 21 through 30)

Cut Line 1 in 0 G (21)

Cut Lines 2 and 3 in V G (22 through 23)

Switch R-hand instrument to needle driver (24)

Suture Line 1 in 0 G (25 through 26)

Suture Lines 3 and 4 in V G (27 through 28)

Complete unfinished tasks as necessary (29 through 30)

Switch to surgeon 2, switch simulated tissue, and switch R-hand instrument to scalpel during aircraft turn

Surgeon 2 (parabolas 31 through 40)

- Cut Line 1 in 0 G (31)
- Cut Lines 2 and 3 in V G (32 through 33)
- Switch R-hand instrument to needle driver (34)
- Suture Line 1 in 0 G (35 through 36)
- Suture Lines 2 and 3 in V G (37 through 38)
- Complete unfinished tasks as necessary (39 through 40)

Each simulated tissue had 3 identical curved lines and suture entry and exit points to facilitate comparison of data (figure 3-2). Using the line as a guide, the surgeon sequentially incised simulated skin, fat, and fascia as time permitted during the designated parabola. Using suture entry and exit dots, the surgeon closed the skin and fat of each incision using a running 2-0 silk suture as time permitted during the designated parabola. Sutures were placed at the end of the incision and tied before flight, and the needle was embedded in the simulated tissue for stowage. Therefore, suture needles were not free-floating.

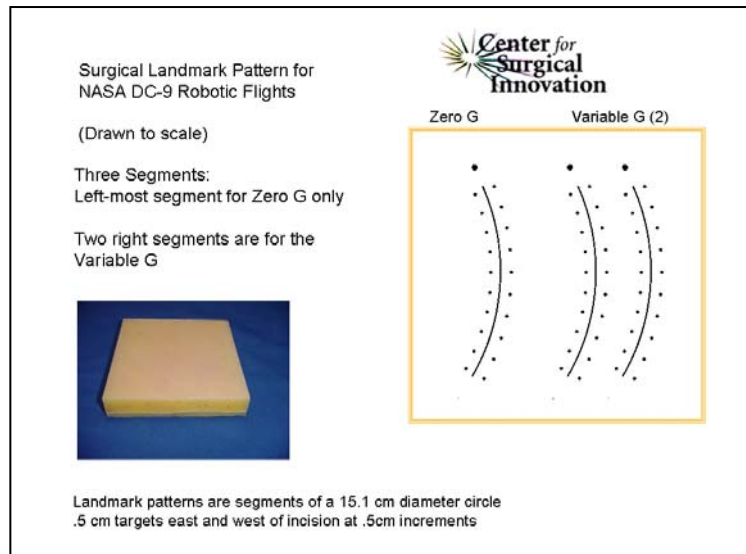


Figure 3-2. Simulated tissue with pre-marked lines.

RESULTS

Over the 4 days of flying, performance data were collected from the robotic system and users. Data included robot kinematics, high-definition video, and user questionnaires. The data are currently being evaluated.

CONCLUSION

The robotic surgery in-flight experiments were very successful. Participants, including NASA astronauts and surgeons, were able to suture simulated tissue throughout all phases of parabolic flight using the surgical robot. Presumably because the robotic system allowed optimal head and body position, operators experienced much less motion sickness with robotic suturing than manual suturing. Preliminary data analysis reveals that the M7 robot performed well and acceleration compensation ameliorated the effects of

variable acceleration encountered in parabolic flight. Furthermore, surgeons and astronauts considered acceleration compensation valuable and believe future robotic surgery research and development is indicated. We plan to follow user recommendations to incorporate users in the iterative development process and will provide users additional time for system familiarization before the next flight. Finally, these successful experiments represent an important initial step in the development of exploration-enabling smart medical systems and autonomous therapeutics.

The comprehensive final report will contain appropriate detail, data analysis, and references to peer-reviewed presentations and publications.

REFERENCES

1. Speich JE, Cagle YD, Rafiq A, Merrell RC, Doarn CR, Broderick TJ. Evaluation of surgical skills in microgravity using force sensing. *Medical Engineering & Physics* 2005; 27(8): 687-93.
2. Rafiq A, Merrell RC, Williams DR, Doarn CR, Jones JA, Broderick TJ. Assessment of surgical skill performance in parabolic microgravity. *Aviat Space Environ Med* 2005; 76(4):385-91.
3. Panait L, Broderick T, Rafiq A, Speich J, Doarn CR, Merrell RC. Measurement of laparoscopic skills in microgravity anticipates the space surgeon. *Am J Surg* 2004; 188(5):549-52.
4. Panait L, Rafiq A, Mohamed A, Doarn CR, Merrell RC. Surgical skill facilitation in videoscopic open surgery. *J Laparoendosc Adv Surg Tech* 2003; 13(6):387-95.
5. Doarn CR. Telemedicine in tomorrow's operating room: a natural fit. *Semin Laparosc Surg* 2003; 10(3):121-26.
6. Merrell RC, Doarn CR. Meeting summary: A Department of Defense agenda for development of the surgical suite of tomorrow -- implications for telemedicine. *Telemed J E Health* 2003; 9(3):297-301.
7. Panait L, Doarn CR, Merrell RC. Applications of robotics in surgery. *Chirurgia (Bucur)* 2002; 97(6):549-55.
8. Rodas EB, Latifi R, Cone S, Broderick TJ, Doarn CR, Merrell RC. Telesurgical presence and consultation for open surgery. *Arch Surg* 2002; 137(12):1360-363.
9. Broderick TJ, Russell KM, Doarn CR, Merrell RC. A novel method for visualizing the open surgical field. *J Laparoendosc Adv Surg Tech* 2002; 12(4):293-98.
10. Doarn CR, Fitzgerald S, Rodas E, Harnett B, Praba-Egge A, Merrell RC. Telemedicine to integrate intermittent surgical services in to primary care. *Telemed J E Health* 2002; 8(1):131-37.
11. Broderick TJ, Harnett BM, Merriam NR, Kapoor V, Doarn CR, Merrell RC. Impact of varying transmission bandwidth on image quality in laparoscopic telemedicine. *Telemed J E Health* 2001; 7(1):47-53.

12. Williams DR, Bashshur RL, Pool SL, Doarn CR, Merrell RC, Logan JS. A strategic vision for telemedicine and medical informatics in space flight. *Telemed J E-Health* 2000; 6(4):441-48.
13. Kirkpatrick AW, Campbell MR, Jones JA, Broderick TJ, Ball CG, McBeth PB, McSwain NE, Hamilton DR, Holcomb JB. Extraterrestrial hemorrhage control: Terrestrial developments in technique, technology, and philosophy with applicability to traumatic hemorrhage control in long-duration spaceflight. *J Am Coll Surg*. 2005 Jan; 200(1):64-76.
14. Marescaux J, Soler L, Mutter D, Leroy J, Vix M, Koehl C, Clement JM. Virtual university applied to telesurgery: from tele-education to telemanipulation. *Stud Health Technol Inform*. 2000; 70:195-201.
15. Fabrizio MD, Lee BR, Chan DY, Stoianovici D, Jarrett TW, Yang C, Kavoussi LR. Effect of time delay on surgical performance during telesurgical manipulation. *J Endourol*. 2000; 14(2):133-38.
16. Guillonneau B, Jayet C, Tewari A, Vallancien G. Robot assisted laparoscopic nephrectomy. *J Urol*. 2001; 166(1):200-01.
17. Larkin M. Transatlantic, robot-assisted telesurgery deemed a success. *Lancet*. 2001 Sep 29; 358(9287):1074.
18. Marescaux J, Smith MK, Folscher D, Jamali F, Malassagne B, Leroy J. Telerobotic laparoscopic cholecystectomy: initial clinical experience with 25 patients. *Ann Surg*. 2001; 234(1):1-7.
19. Marescaux J, Leroy J, Gagner M, Rubino F, Mutter D, Vix M, Butner SE, Smith MK. Transatlantic robot-assisted telesurgery. *Nature*. 2001 Sep 27; 413(6854):379-80.
20. Smithwick M. Network options for wide-area telesurgery. *J Telemed & Telecare* 1995; 1(3):131-38.
21. Thompson JM, Ottensmeyer MP, Sheridan TB. Human factors in telesurgery: effects of time delay and asynchrony in video and control feedback with local manipulative assistance. *Telemed J*. 1999; 5(2):129-37.
22. Jourdan IC, Dutson E, Garcia A, Vleugels T, Leroy J, Mutter D, Marescaux J. Stereoscopic vision provides a significant advantage for precision robotic laparoscopy. *Br J Surg*. 2004; 91(7):879-85.
23. Allen D, Bowersox J, Jones GG. Current status of telesurgery. *Telemedicine Today* 1997.
24. Moore RG, Adams JB, Partin AW, Docimo SG, Kavoussi L. Telesurgical mentoring. Initial clinical experience. *Surg Endosc* 1996; 10(2):107-10.
25. Janetschek G, Bartsch G, Kavoussi LR. Transcontinental interactive laparoscopic telesurgery between the United States and Europe. *J Urol* 1998; 160(4):1413.
26. Cubano M, Poulouse B, Talamini M et al. Long distance telerobotics: A novel tool for laparoscopy aboard the USS Abraham Lincoln. *Surg Endosc* 1999; 13(7): 673-78.

27. Bove P, Stoianovici D, Micali S, Patriciu A et al. Is telesurgery a new reality? Our experience with laparoscopic and percutaneous procedures. *J Endourol* 2003; 17(3):137-42.
28. Netto NR, Mitre AI, Lima SV, et al. Telementoring between Brazil and the United States: initial experience. *J Endourol* 2003; 17(4):217-20.
29. Marescaux J, Leroy J, Rubino F, Smith M et al. Transcontinental robot-assisted remote telesurgery: feasibility and potential applications. *Ann Surg* 2002; 235(4):487-92.
30. Pirisi, A. Telerobotics brings surgical skills to remote communities. *Lancet* 2003; 351:1794-95.
31. Anvari M, McKinley C, Stein H. Establishment of the world's first telerobotic remote surgical service: for provision of advanced laparoscopic surgery in a rural community. *Ann Surg* 2005; 241(3):460-64.

PHOTOGRAPHS

JSC2007E048069 to JSC2007E048070
JSC2007E047742 to JSC2007E047829
JSC2007E047991 to JSC2007E048037
JSC2007E048324 to JSC2007E048351
JSC2007E048069 to JSC2007E048070
JSC2007E048103 to JSC2007E048158

VIDEO:

- Zero G flight week September 25–28, 2007, Master: 306387, 385

Videos available from Imagery and Publications Office (GS4), NASA JSC.

CONTACT INFORMATION

Charles R. Doarn, MBA
Deputy Director, Advanced Center for Telemedicine and Surgical Innovation
Associate Professor of Surgery and Biomedical Engineering
Department of Surgery
University of Cincinnati
231 Albert Sabin Way, SRU 1466
ML 0558
Cincinnati, OH 45267-0558
Voice: (513) 558-6148
Fax : (513) 558-2026
Cell: (513) 403-9604
charles.doarn@uc.edu

TITLE

Integrated Immune Flight Study (SMO-015, SDBI-1900) – Evaluation of In-flight Sample Collection Hardware and Recording of Training Video for STS and ISS Crewmembers

FLIGHT DATES

September 28, 2007

PRINCIPAL INVESTIGATOR

Brian Crucian, Wyle
Clarence Sams, NASA Johnson Space Center



GOAL

The goal of the current on-orbit study is to develop and validate a strategy for monitoring the immune system that is consistent with operational flight requirements and constraints. No procedures are currently in place to monitor immune function or its effect on crew health. Immune dysregulation has been demonstrated to occur during space flight, yet precious little in-flight immune data have been generated to assess this clinical problem. This Supplemental Medical Objective (SMO) assesses the clinical risks resulting from the adverse effects of space flight on the human immune system and will validate a flight-compatible immune monitoring strategy. The clinical risk must be characterized and a monitoring strategy must be developed as necessary prerequisite activities before countermeasures can be validated. Ample evidence suggests that space flight leads to immune system dysregulation. This may be a result of microgravity, confinement, physiological stress, radiation, environment, or other mission-associated factors. The

clinical risk from prolonged immune dysfunction could be significant and may include increased incidence of infection, allergy, hypersensitivity, hematological malignancy, or altered wound healing. Each of the clinical events resulting from immune dysfunction could have an impact on mission-critical objectives during long-duration space flight. In the *Integrated Immune* study, the overall status of the immune system during flight (activation, deficiency, dysregulation) and the response of the immune system to specific latent virus reactivation (known to occur during space flight) will be thoroughly assessed.

OBJECTIVES

The objective of the evaluation conducted on the current parabolic flight was to validate the procedure for collecting samples of whole blood during reduced gravity and to film a video of Vacutainer® filling in reduced gravity to be used during training of Space Shuttle and International Space Station crewmembers.

On-orbit filling of the tubes has been a significant discussion point during Shuttle crew training sessions. Anecdotal flight reports indicate filling is altered during reduced gravity and it may be difficult to ascertain if the tube is full. The intent on this flight was to evaluate and record the phenomenon on digital media.

METHODS AND MATERIALS

The basic equipment used for this experiment consisted of the following items:

- 450-mL bag containing dyed H₂O, with port
- Butterfly blood collection unit (single needle and tubing)
- ACD (acid-citrate-dextrose) (yellow top) Vacutainer tubes
- EDTA (ethylenediaminetetraacetic acid) (purple top) Vacutainer tubes

For this C-9 activity, dyed water was the primary fluid used for evaluation. A single needle was used that was opened briefly before the beginning of parabolas. The needle was secured during the parabolas within sample collection tubing, and re-stowed after the parabolas ended.

RESULTS

The evaluation was successful. Novel information about the collection of blood samples using Vacutainer technology was obtained and recorded. The images and videos obtained will be used in astronaut training for the *Integrated Immune* flight study.

During the reduced-gravity conditions of parabolic flight, it did not seem difficult to determine if the tubes were indeed full. However, the appearance and operation of the EDTA vs. ACD tubes was entirely different. The EDTA (plastic) tubes appeared to be more hydrophobic, and in fact the tubes filled top to bottom (when inverted), allowing easy visualization (see figure 4-1). The ACD (glass) tubes seemed to be more hydrophilic, and the liquid appeared to adhere to the sides more, which could hinder visualization of the full tube.

Figure 4-1. Right: evaluation of Vacutainer operation during conditions of zero gravity. “Foaming” effect of tube filling is evident, and the effect seemed different in glass ACD tubes (lower right) vs. plastic EDTA evacuated tubes (lower left).



DISCUSSION AND CONCLUSION

This evaluation was conducted to investigate anecdotal crew comments that, in space, it was difficult to ascertain if a Vacutainer was full. The problem was attributed to a foaming effect caused by the absence of gravity. This effect was successfully captured on video, and will be used to properly train Shuttle and Space Station crewmembers before collection of in-flight samples. It was a successful parabolic flight experiment.

PHOTOGRAPHS

JSC2007EO48301 to JSC2007EO48315

VIDEO

- Zero G flight week September 25–28, 2007, Master: 306387, 385

Videos available from Imagery and Publications Office (GS4), NASA JSC.

CONTACT INFORMATION

Brian Crucian, PhD

Wyle

1290 Hercules Suite 120

Houston, Texas 77058

281-483-7061

brian.crucian-1@nasa.gov

TITLE

Rapid Development of Colorimetric-Solid Phase Extraction Technology for Water Quality Monitoring: Evaluation of C-SPE Total Iodine Analysis Methods in Microgravity

FLIGHT DATES

October 24–26, 2007

PRINCIPAL INVESTIGATOR

Marc D. Porter, University of Utah

CO-INVESTIGATORS

Torin McCoy, NASA Johnson Space Center

April Hill, Iowa State University

Bob Lipert, Iowa State University

Lorraine Siperko, University of Utah

Dan Gazda, Wyle

Jeff Rutz, Wyle

John Straub, Wyle

Danny Nolan, Wyle

Jim Alverson, Wyle

John Schultz, Wyle



GOALS

To develop procedures for effectively collecting 10.0-mL bubble-free samples after extracting water through an Oxone® cartridge in microgravity for in-flight determination of total iodine (total I).

To verify the functionality of sample collection procedures and colorimetric-solid phase extraction (C-SPE) test methods in microgravity by demonstrating analysis for total I in water samples consisting of standard solutions of potassium iodide (KI) that were analyzed by ground tests using the leuco crystal violet (LCV) method to certify total I concentrations.

OBJECTIVES

Flight 1: Syringe filling and bubble mitigation for total I analysis of I₂ and I₂ + KI samples

To evaluate syringe filling strategies for 10.0-mL water sample collection through an Oxone® cartridge.

To determine a procedure for manual bubble mitigation and expulsion of air and excess sample before passing 10.0 mL of bubble-free sample through a C-SPE membrane.

To evaluate use of a 3-way valve connected to a syringe, sample bag, and waste bag as a means of simplifying sample handling.¹

Flight 2: Test total I analysis as KI

To use methods developed in Flight 1 to compare ground and flight data from total I analyses.

Flight 3: Refine total I analysis from test of single concentration of KI

To determine if 10.0 mL of sample can be drawn accurately into a syringe through an Oxone® cartridge present in line between the sample collection bag and syringe by comparing multiple in-flight determinations of a single KI concentration to the certified ground measurement value.

To evaluate reproducibility of new and existing sample collection and manipulation methods by comparing the results from multiple runs using only one KI concentration.

Flight 4: Evaluate Oxone® introduction and sampling procedures for total I analysis as KI

To analyze a range of KI concentrations for total I using procedures developed in previous flights.

To construct calibration curves and determine precision of the method using certified ground analysis concentrations.

To tabulate results and compare to ground measurements to determine accuracy of the method under microgravity conditions.

MATERIALS AND METHODS

Instrumentation

Both in-flight and ground-based measurements were made for the Rapid Development of Colorimetric-Solid Phase Extraction study using BYK Gardener Color Guide spin d/8° diffuse reflectance spectrophotometers. All mass measurements were performed using a calibrated, certified Mettler Toledo model AG205 analytical balance.

Iodine-sensitive membranes

A solution was prepared by dissolving 14.988 g polyvinylpyrrolidone (PVP: MW = 10,000) in 250 mL of 1:1 methanol:water in a 500-mL volumetric flask. The solution was brought to volume with 1:1 methanol:water. An Empore SDB-XC 47-mm extraction membrane was placed in a Millipore glass filter holder assembly, and 10.0 mL of the PVP solution were pipetted into the funnel. Next, a vacuum pump was used to apply a pressure differential (~3.5 in Hg) across the membrane to force this solution through the membrane. Once the solution had passed through the membrane, the pressure difference was maximized by setting the vacuum valve to its full-open position for 30 s to remove residual solvent. The prepared membranes were allowed to air dry for ~12 h and stored in ziplock bags in the dark before being cut into 13-mm disks.

Oxone® glass fiber filters

Oxone® (Aldrich) was used as an oxidizing agent to convert iodide to iodine. An Oxone® solution was prepared by weighing 7.4977 g in a weighing boat, transferring it to a 25-mL volumetric flask, and bringing it to volume with deionized water. Glass fiber filters (Millipore AP20047000) were placed in 60 × 15 mm (Dia × H) glass Petri dishes, and 1.0 mL of Oxone® solution was pipetted onto the center of each filter to ensure wetting of the entire filter. The dishes containing the treated filters were heated in an oven at 110°C for 2 h, after which the filters were removed and stored in ziplock bags before being cut into 13-mm reagent chads just before use.²

C-SPE cartridges

All C-SPE membranes and Oxone®-coated glass fiber filters were prepared the day before their corresponding flight. A few hours before flight, the PVP-treated membranes and Oxone®-treated filters were cut into 13-mm disks and loaded into Swinnex® polypropylene cartridges. One end of the filter holder cartridge has a Luer fitting that readily forms a leak-tight connection with a syringe; the opposite end of the cartridge has a slip fit that mates with the sample or waste collection bag. A Teflon gasket contained in the cartridge forms an internal seal and defines the area of the membrane disk exposed to the water sample.

Standard solutions

A 50-ppm standard iodide stock solution was prepared by dissolving 0.0696 g KI in deionized water in a volumetric flask and diluting to 1.0 L. The stock solution for iodine and total I was prepared by diluting 1 ampule of FIXANAL® standard (Riedel-de Haen, #38060, containing 12.690 g I₂ and 20 g KI) to 1.0 L with deionized water, producing 0.1N iodine. Working solutions of iodide, iodine, and total I were prepared by appropriate dilution of the stock with deionized water. The actual solution concentrations of I₂ and total I were certified by Wyle personnel, by means of the LCV method.³

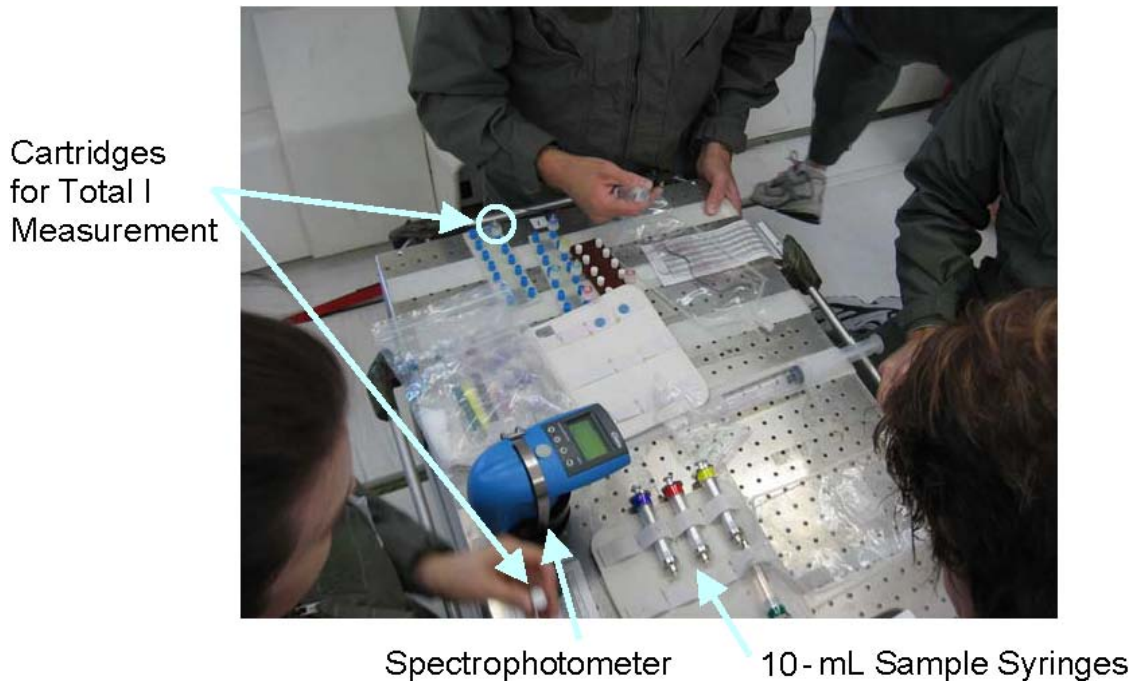


Figure 5-1. Photograph taken during flight illustrating the layout of the worktable and positioning of the 4 fliers.

Sample and waste bags

Bags for the closed-loop system were acquired from American Fluoroseal. Sample bags (#1P-0072-K) that hold approximately 72 mL and waste bags (#1PF-0270) that hold ~1.0 L were used for sample passing (through the membrane) and membrane drying steps, respectively. The bag used for sampling (#1P-0012) holds ~12 mL).

Microgravity bench setup

The positions of fliers and analytical accessories on and around the flight bench are shown in figure 5-1.

PROCEDURES, RESULTS, AND DISCUSSION

General Observations

During the first 2 flights of this series, challenges were encountered in accurately filling syringes with 10.0 mL of sample during the ~25-s microgravity period of each parabola. Careful reassessment of the test procedures during the third flight resulted in a marked

reduction in the measurement error. By identifying problem areas and making corrections, the team was able to demonstrate the use of C-SPE methodology for total I analysis in microgravity environments. It is important to note that we expect even better performance on the International Space Station (ISS), since many of the challenges encountered on these flights resulted from the limitation of the 25-s microgravity simulation time. The time constraints generated by C-9 microgravity simulations will not be applicable on the ISS. Once verified by additional microgravity testing to further refine the analytical procedure, this methodology will place C-SPE in a strategic position as a means to strictly manage biocidal iodine concentration levels in drinking water on the ISS and future lunar and/or Mars missions.

Flight 1: Syringe filling and bubble mitigation for total I analysis of I₂ and I₂ + KI samples

Table 5-1. Test matrix Flight 1: flier tasks for each parabola.

| Parabola # | Flier 1 | Flier 2 | Flier 3 | Flier 4 |
|------------|---------|---------|-----------|----------|
| 1 | Open | Open | Fill 1 | Fill 1 |
| 2 | Pass 1 | Open | Fill 2 | Fill 2 |
| 3 | Pass 2 | Dry 1 | Fill 3 | Fill 3 |
| 4 | Pass 3 | Dry 2 | Measure 1 | Record 1 |
| 5 | Open | Dry 3 | Measure 2 | Record 2 |
| 6 | Fill 4 | Fill 4 | Measure 3 | Record 3 |
| 7 | Pass 4 | Open | Fill 5 | Fill 5 |
| 8 | Pass 5 | Dry 4 | Open | Open |
| 9 | Open | Dry 5 | Measure 4 | Record 4 |
| 10 | Open | Open | Measure 5 | Record 5 |

Procedures

Various sampling manipulations were evaluated on the first half (20 parabolas) of Flight 1. Glass syringes (10.0 mL, SGE International Pty, Ltd.) were fitted with (1) an Oxone® cartridge connected to a 72-mL Teflon® sample bag filled with colored water to enhance air bubble visualization or (2) a 3-way valve¹ with attached 10-mL waste bag incorporated in line between the syringe and sample bag. In either case, the syringe was first overfilled by withdrawing the plunger to the end of the syringe and then detaching the sample bag from the port (that is, the exit) end. The syringe was then swung in an arc to separate the entrapped air from the water by driving the liquid to the plunger end and the air to the port end of the syringe, where the air could be expelled into the waste bag along with any excess liquid. In tests without the 3-way valve, the syringe with a cartridge attached to the port end was affixed to a waste bag and the plunger was depressed to expel air and excess liquid. This step was not required when the 3-way valve was used, since a waste bag was already attached to 1 port of the valve. The 2 experimental procedures seemed to produce comparable results.

On the third set of 10 parabolas, iodine measurements were made at 5 different concentrations using procedures verified on previous C-9 flights to confirm that all previous developmental procedures were working effectively. For the last set of 10 parabolas, the total I procedures tested earlier in the flight were used for a total I analysis, using dilutions of the FIXANAL® standard as a simulant for water. To maximize the number of samples handled (5), each of the 4 fliers had multiple tasks. Syringe filling required fliers to work in teams of 2 to complete each task in the microgravity portion (~25 s) of each parabola. The task/test matrix is shown in table 5-1.

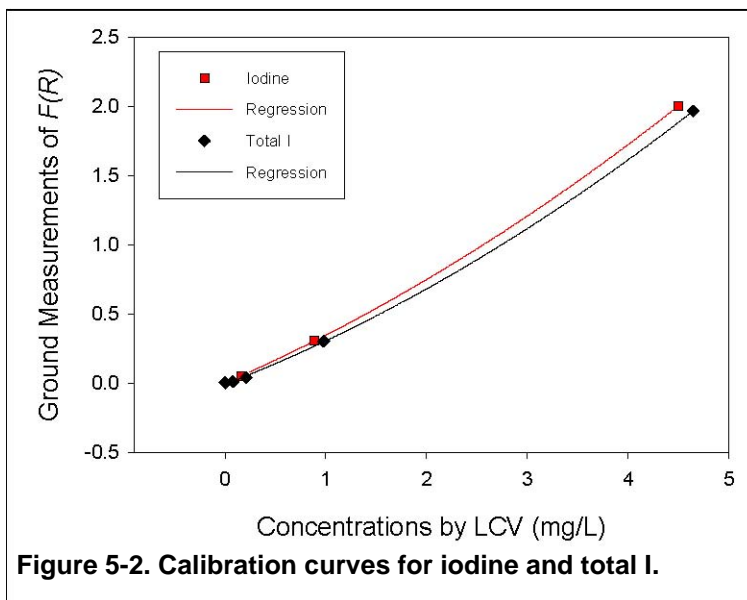
During the procedure, one member of the team held the syringe and another held the sample bag to ensure that the Luer slip fitting of the cartridge remained connected to the sample bag. After filling, debubbling, and expelling air and excess liquid, this team member handed the syringe to a second flier, who metered the liquid sample through the PVP membrane; a third flier dried the membrane, and a fourth flier measured spectral response and recorded the data. An observer was also present on this flight to become familiar with the procedure to be used on subsequent flights.

Table 5-2. Comparison of Flight 1 results with laboratory determination of I₂.

| Number of Samples | Iodine Conc. (mg/L) Ground LCV | Iodine Conc. (mg/L) C-9 Flight | Error | Target Error |
|-------------------|--------------------------------|--------------------------------|------------|--------------|
| 1 | 0.046 | 0.035 | -24% | ±50% |
| 1 | 0.16 | 0.095 | -41% | ±50% |
| 1 | 0.89 | 0.58 | -35% | ±50% |
| 1 | 4.5 | 3.08 | -1.42 mg/L | ±1.25 mg/L |

Concurrent with the flight, samples taken from the same solutions used on the flight were analyzed by Wyle. Two measurements were taken. The concentrations of I₂ and total I

were determined using the LCV method.³ These solutions were also analyzed by C-SPE for I₂ and total I. Calibration curves for each analyte were constructed by plotting the Kubelka-Munk parameter⁴ (F(R)_{440nm}) vs. LCV values for iodine. These curves were fit to a second-order polynomial, which was subsequently used to determine the concentration of samples measured in flight from their F(R) values. The calibration curves are shown in figure 5-2.



Results

The results from four I₂ samples measured on this flight are shown in table 5-2 and the results for total I as I₂ + KI are given in table 5-3. The experimental error lies well within the target error for each concentration of I₂ analyzed by C-SPE, except for the highest concentrations. The target error above concentrations of 2.5 ppm has been set at ± 1.25 ppm, while for lower concentrations the target error has been set at ± 50%.

Table 5-3. Comparison of flight results with laboratory determination of total I from standard solutions containing I₂ + KI.

| Number of Samples | Total I Conc. (mg/L) Ground LCV | Total I Conc. (mg/L) C-9 Flight | Error | Target Error |
|-------------------|---------------------------------|---------------------------------|------------|--------------|
| 1 | 0.080 | 0.076 | -5.5% | ±50% |
| 1 | 4.65 | 3.27 | -1.38 mg/L | ±1.25 mg/L |

Discussion

Although use of an Oxone® cartridge had the effect of introducing large (~1 mL) volumes of air into the syringe, the process of overfilling the syringe to separate the entrapped air from the liquid sample proved highly effective. However, maintaining a leak-tight connection between the sample bag and syringe proved difficult because the outlet end of the Oxone® cartridge that mated the cartridge to the syringe was a Luer slip fitting as opposed to a Luer Lock fitting. The procedure of using teams of 2 fliers to fill syringes proved helpful in stabilizing the position and alignment of the sample bag with the syringe. In this arrangement, the flier holding the sample bag also had to ensure that the cartridge did not begin to detach from the sample bag. Unfortunately, the additional effort and maneuvering required to conduct this portion of the procedure proved difficult to complete in the time available in the microgravity segment of a parabola. This new set of procedures challenged the ability of even our most experienced fliers. As a consequence, the number of samples fully worked up in this portion of flight was less than originally planned. The errors in measurements for the high-concentration samples were also beyond the targeted level of acceptability.

Note that the calibration curve in figure 5-2 indicates that the diffuse reflectance response is not linearly dependent on iodine concentration, being fitted more effectively by a second-order polynomial equation. Although the fundamental origin of such dependence remains to be determined, we suspect that the optical characteristics of the membrane used to support the PVP reagent play an important role.⁵

Flight 2: Test total I analysis as KI

Procedures

The procedure for Flight 2 was essentially that used in Flight 1. For this experiment, total I was determined as KI. Again, teams of 2 fliers filled syringes, following the test matrix in table 5-1. Syringes were overfilled, and air and excess sample were expelled before the syringe was handed off for the subsequent steps of passing the sample through the reagent cartridge, drying the membrane, measuring spectral response, and recording the data. An observer was also present on this flight.

Results

This new flight procedure also proved problematic, because volumes of air larger than expected were introduced into the sample syringe. As a result, only 3 of the planned 20 samples contained the required 10.0 mL.

Discussion

This test matrix was judged unacceptable, since its successful execution required a high level of coordinated activity in the 0-G and 2-G segments of each parabola as well as during flight turnarounds.

Flight 3: Refine total I analysis from test of single concentration of KI

Procedures

To overcome the problems experienced on the previous 2 flights and to ensure that a viable test procedure for microgravity analysis could be developed, only one concentration of KI (5 ppm) was used on this flight and the test matrix was modified. Efforts focused on (1) optimizing syringe filling, (2) debubbling, and (3) expelling air and excess sample. Only correctly filled syringes (those containing 10.0 mL of the iodide sample) were analyzed. Furthermore, the workup of a new sample was initiated only after the preceding sample was completely processed. An additional flier was also added (total of 5 team members) during this flight to improve the efficiency of the process. A detailed record was maintained to track the possible importance of timing during each processing step.

Table 5-4. Flight 3 evaluation of 3-way valve.

| Sample # | Valve (Y/N) | Successful (Y/N) |
|----------|-------------|------------------|
| 1 | Y | N |
| 2 | N | Y |
| 3 | Y | Y |
| 4 | Y | N |
| 5 | N | Y |
| 6 | N | Y |
| 7 | N | Y |
| 8 | N | N |
| 9 | N | Y |
| 10 | N | Y |
| 11 | N | Y |

Results

A total of 11 attempts (3 using the 3-way valve and 8 without it) were made to fill syringes with 10.0 mL of water through an Oxone® cartridge. Table 5-4 summarizes the results of obtaining a properly filled syringe.

Table 5-5. Results of Flight 3: replicate total I analysis of samples from a single concentration of KI.

| Number of Samples | Iodide Conc. (mg/L) Ground LCV | Iodide Conc. (mg/L), C-9 Flight | Standard Deviation, C-9 Flight | RSD | Error |
|-------------------|--------------------------------|---------------------------------|--------------------------------|------|-------|
| 8 | 4.85 | 4.97 | 0.21 | 4.1% | 3.0% |

RSD, relative standard deviation.

Three of the first 4 samples analyzed on this flight involved use of the 3-way valve. Of these 3 attempts, 2 failed to yield the required 10.0-mL samples. A decision was made to abandon the use of this accessory. Of the next 7 attempts made without the valve, only one attempt failed. The results presented in table 5-5 summarize measurements made on the successfully filled syringes (7 without the 3-way valve, 1 with the valve). The table also includes data reflecting the precision and accuracy of the method developed on this flight. Table 5-6 lists the recorded time data for this flight.

Table 5-6. Time record from Flight 3 (H:M:S).

| Syringe # | Start Fill | End Fill | Start Pass | Start Dry | Measure | Total Time |
|-----------|------------|----------|------------|-----------|---------|------------|
| 1 | | | | | | Misfill |
| 2 | 0:13:10 | 0:13:24 | 0:14:29 | 0:15:42 | 0:17:02 | 0:03:52 |
| 3 | 0:18:18 | 0:18:42 | 0:19:35 | 0:26:56 | 0:28:16 | 0:09:58* |
| 4 | | | | | | Misfill |
| 5 | 0:35:00 | 0:35:22 | 0:36:11 | 0:37:23 | 0:38:35 | 0:03:35 |
| 6 | 0:39:44 | 0:40:57 | 0:40:57 | 0:42:09 | 0:43:18 | 0:03:34 |
| 7 | 0:49:00 | 0:49:27 | 0:50:20 | 0:51:35 | 0:52:30 | 0:03:30 |
| 8 | | | | | | Misfill |
| 9 | 0:55:29 | 0:55:59 | 0:56:57 | 0:58:17 | 0:59:39 | 0:04:10 |
| 10 | 1:04:47 | 1:05:10 | 1:05:57 | 1:07:08 | 1:08:17 | 0:03:30 |
| 11 | 1:09:31 | 1:09:57 | 1:10:40 | 1:11:58 | 1:13:03 | 0:03:32 |

* Cycle interrupted due to aircraft technical issue.

DISCUSSION

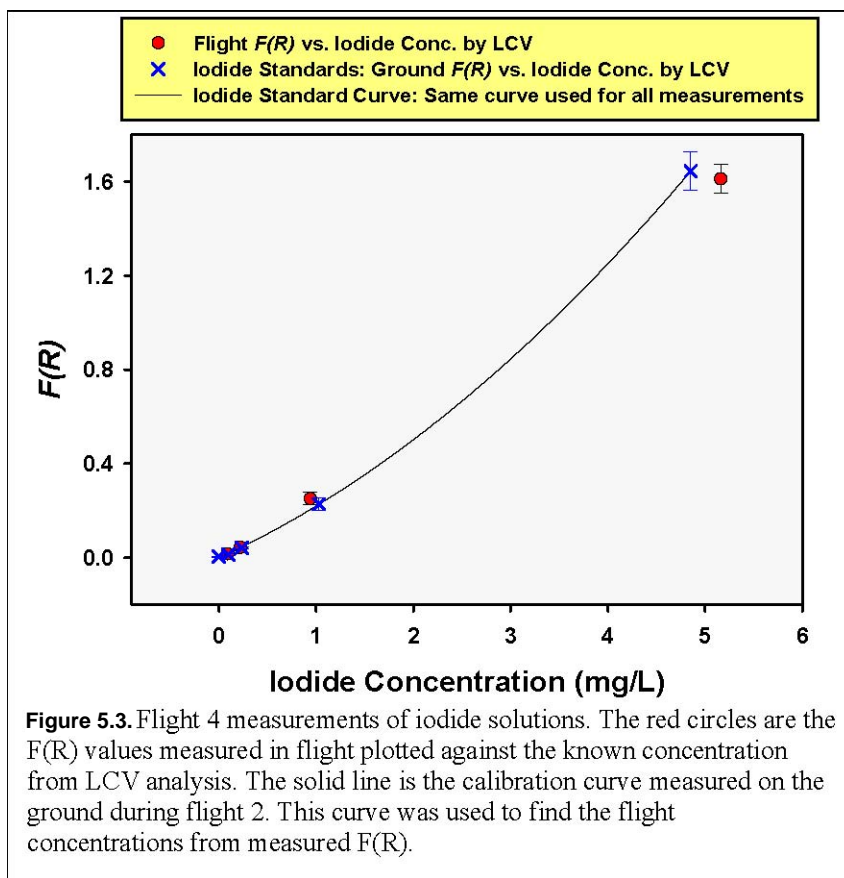
Terminating use of the 3-way valve resulted in boosting the percentage of successfully filled syringes from ~30 to >70%. The higher success rate was attributed to the ability of fliers to manipulate sample accessories in a more efficient manner, thereby preventing excess air from entering the syringe. With a resulting relative standard deviation of 4.1% and an error of 3%, the precision and accuracy of these results were well within the targeted level of acceptability. In addition, the length of time between sample filling and data recording had no observable effect on the precision and accuracy of these measurements.

Flight 4: Evaluate Oxone® introduction and sampling procedures for total I analysis as KI

PROCEDURES

Based on experience gained in the previous 3 flights, it was decided that a fifth flier was needed on Flight 4 to aid in the syringe-filling process. Three-way valves were not used, since it was previously determined that the valves contributed to problems associated with accurate syringe filling. Only 1 syringe was filled during a given parabola, and 2 fliers worked in teams; 1 flier held the sample bag while the other extracted a sample through an Oxone® cartridge. After the entrapped air was separated from the liquid sample by the previously described procedure, air and excess sample were expelled into a

waste bag. The syringe was handed to the next flier (sample pass step) for extraction of the sample through a PVP-modified membrane, followed by removal of the membrane cartridge. The cartridge was handed to the next flier (sample dry step) for membrane drying by forcing 60 mL of air through the cartridge. The cartridge was then disassembled (sample measure step), and the lower half of the cartridge containing the membrane was placed in the spectrophotometer for measurement and data recording.



RESULTS

Results from flight 4 are presented in figure 5-3 and table 5-7. A total of 12 samples, taken from freshly prepared solutions of 5.0, 1.0, 0.25, and 0.10 ppm KI, were analyzed. In table 5-7, concentrations determined from C-9 flight data are compared with laboratory LCV data for an assessment of accuracy and precision of the newly developed microgravity analytical method. Errors are well within the target error of $\pm 50\%$, attesting to the feasibility of using C-SPE for total iodine analysis in onboard flight management of biocidal concentrations in drinking water.

Table 5-7. Results from Flight 4 total I analysis of a range of concentrations of standard solutions of KI.

| Number of Samples | Iodide Conc. (mg/L) Ground LCV | Iodide Conc. (mg/L) C-9 Flight | Standard Deviation C-9 Flight | RSD | Error |
|-------------------|--------------------------------|--------------------------------|-------------------------------|------|-------|
| 3 | 0.09 | 0.091 | 0.0094 | 10% | 1.1% |
| 3 | 0.22 | 0.223 | 0.0048 | 2.1% | 1.6% |
| 3 | 0.94 | 1.1 | 0.12 | 11% | 19% |
| 3 | 5.16 | 4.8 | 0.13 | 2.7% | 7.0% |

DISCUSSION

The results from this flight demonstrate that experience gained from the previous 3 flights allowed us to modify and refine our total I analytical method to markedly reduce the measurement error from a range of 24% to 41% (table 5.2) to 1.1% to 19% (table 5.7), which readily meets the targeted levels of performance listed in table 5-2. This reduction in error is attributed to the ability of the fliers to more accurately meter a 10.0-mL sample for C-SPE analysis. Four factors contributed to this improvement: 1) eliminating the use of 3-way valves, which were cumbersome in flight and allowed excess air to enter the syringe; 2) working in teams of 2 fliers to fill each syringe with the sample; 3) overfilling the syringe to allow expulsion of air in conjunction with excess sample; 4) increasing the number of fliers involved in the analysis procedure from 4 to 5. By identifying problem areas and making corrections, the team demonstrated the use of C-SPE methodology for total I analysis in microgravity environments. Once verified by additional microgravity testing to further refine the analytical procedure, this methodology will place C-SPE in a strategic position for onboard flight as a means to strictly manage biocidal iodine concentration levels in drinking water on the ISS and future lunar and/or Mars missions.

REFERENCES AND NOTES

1. This approach represents a new procedure developed specifically for total I analysis on this flight.
2. This approach represents a newly developed procedure that replaces glass wool with glass fiber filters.
3. *Standard Methods for Examination of Water and Wastewater*, 18th ed., American Public Health Association: Washington, DC, 1992.
4. G. Kortum, *Reflectance Spectroscopy: Principles, Methods, Applications*, Springer: New York, 1969, pp. 106-16.

5. S. Dmitrienko, W. Sviridova, L. Pvatkova, V. Senvavin, *Analytical and Bioanalytical Chemistry* 2004, 374, 361-8.

PHOTOGRAPHS

JSC2007E093365 to JSC2007E093387

JSC2007E093088 to JSC2007E093114

JSC2007E054359 to JSC2007E054379

VIDEO

Zero G flight week October 23–26, 2007, Master: 306447

Videos available from Imagery and Publications Office (GS4), NASA JSC.

CONTACT INFORMATION

Marc D. Porter, PhD

Center for Nanobiosensors, University of Utah

383 Colorow Drive Salt Lake City, UT 84108

Email: marc.porter@utah.edu

Office: (801) 587-1505

TITLE

Manned Evaluation of the Second-Generation International Space Station
Treadmill during Parabolic Flight

FLIGHT DATES

October 23–26, 2007

PRINCIPAL INVESTIGATOR

John K. De Witt, Wyle

CO-INVESTIGATORS

Curt Wiederhoeft, Wyle

SUPPORTING PERSONNEL:

Jason Bentley, Wyle

Cassie Wilson, JES Tech

Kirk English, JES Tech

Leah Stroud, Wyle

James Loehr, Wyle

Meghan Everett, University of Houston

David Smoot, Wyle

David Chesney, Wyle

Susan Rullis, Wyle



ABSTRACT

The purpose of this experiment was to compare the kinematics of locomotion in microgravity and in normal gravity on the prototype second-generation International Space Station (ISS) treadmill (T2). Four subjects (1 male and 3 female) completed locomotion trials in microgravity during parabolic flight on board the NASA C-9 aircraft and in normal gravity. Subjects walked at 1.34 m s^{-1} and ran at 3.13 m s^{-1} and 5.36 m s^{-1} . During parabolic flight trials, the subjects wore a harness similar to that normally used during exercise on the ISS and were loaded with bungees to approximately 55% and 80% of body weight. Joint kinematics were determined using a motion-capture system. There were no differences in contact time and stride time between normal and microgravity conditions at any speed. Joint segment range of motion was also not different between conditions within speed. The only kinematic difference detected was that the thigh angle was greater at heel strike during walking in microgravity under the high external load. Our results indicate that segment kinematics were similar in microgravity and normal gravity during locomotion on the T2. Furthermore, subjects were able to complete sprinting locomotion in microgravity without difficulty.

INTRODUCTION

The ISS is scheduled to have a 6-person crew by spring of 2009. All 6 crewmembers will be required to complete a daily exercise regimen that includes exercise on a treadmill. Operational limits prevent the exclusive use of the existing treadmill (TVIS) to meet the requirement. Therefore, to accommodate the increased usage, a second treadmill has been proposed to fly on board the ISS.

The new treadmill (T2) is a modified commercial treadmill designed by Woodway (Waukesha, WI) and is shown in figure 6-1. The flight version will have the rails and control panel customized for use on the ISS. The current prototype has the rails removed and operates via a custom-made interface and workstation.



Figure 6-1. Woodway treadmill.

Groups from NASA and Wyle have completed preliminary tests of the T2. All of these tests have occurred in the laboratory, and have been used to collect data pertaining to the force between the treadmill and the ground from subjects locomoting at various speeds.

However, no data document the biomechanics of locomotion on the treadmill. Furthermore, no data have been collected in microgravity on the T2.

Although locomotive data have been collected in microgravity in the past (Schaffner et al., 2005; De Witt et al., 2004; De Witt et al., 2003), all trials were completed at speeds of 7 mph or less on a treadmill with a tread area that was restricted in size to the dimensions of TVIS (44 cm × 16 cm). The tread area of T2 is wider, and T2 can operate at speeds up to 15 mph. Therefore, it is unclear if previous findings during microgravity locomotion on another treadmill apply to this device.

The purpose of this experiment was to evaluate walking and running kinematics on the second-generation ISS treadmill prototype in microgravity and normal gravity. We hypothesized that contact time, stride time, and lower-extremity segment range of motion in microgravity and normal gravity environments will be different. We further hypothesized that segment angles at heel strike will differ between environments within speeds.

METHODS AND MATERIALS

Seven subjects completed locomotion trials in microgravity during parabolic flight on board the NASA C-9 aircraft. However, during post-processing, motion-capture data for 3 subjects were found to be unusable. Therefore, data from 4 subjects (1 M, 3 F; mass = 64.4 ± 15.3 kg) were analyzed. Data were collected during 4 flights, and each flight consisted of 40 microgravity parabolas. This investigation was reviewed and approved by the NASA JSC Committee for the Protection of Human Subjects. Subjects provided written informed consent before participating in the study.

Data Collection

Parabolic Flight Locomotion Trials

Upon arrival at the C-9 aircraft hangar, each subject was provided with running tights (Spandex) and running shoes (Xccelerator TR, Nike, Inc, Beaverton, OR) and completed a health questionnaire. During each flight, subjects walked (W) at 1.34 m s^{-1} (3 mph), ran (R) at 3.13 m s^{-1} (7 mph) and sprinted (S) at 5.36 m s^{-1} (12 mph) while loaded with bungees and wearing the US TVIS harness.

Subjects completed locomotion at each speed under 2 external load (EL) conditions. During the light EL condition (L), the bungee load was adjusted to approximately 55% of body weight (BW). During the heavy EL condition (H), the bungees were adjusted to approximately 80% of BW. Appropriate EL levels were obtained by adding carabiner clips in series with single bilateral bungees as used during normal exercise on board the ISS.

Before each flight, the carabiner clip-bungee configurations that elicited the desired load for each condition were determined for each subject using a bathroom scale mounted to a stable platform. Each subject's BW was recorded, and the subject then stood on the scale

while loaded with bungees and carabiner clips until an appropriate configuration was found. The configuration was noted and used during the subsequent flight (table 6-1). Subjects completed a single trial at each speed and EL condition.

Table 6-1. Mean external load (% BW) for each subject and loading configurations during walking and running in microgravity.

| Subject | BW (kg) | 55% EL (kg) | 80% EL (kg) | 55% Configuration | 80% Configuration |
|---------|---------|-------------|-------------|-----------------------------|---------------------|
| A | 63.2 | 34.8 | 56.9 | 2 clips to Y intersect | 2 clips to center D |
| B | 86.0 | 47.3 | 77.4 | 4 clips to center D | 0 clips to center D |
| C | 50.9 | 28.0 | 45.8 | 2 clips to bottom Y | 3 clips to center D |
| D | 57.5 | 31.6 | 51.7 | no clips; bottom of Y strap | 3 clips to center D |

Ground-Based Locomotion

Each subject completed locomotion in normal gravity on the treadmill while the aircraft was parked in the hangar. Therefore, all trials for each gravity level were completed under identical conditions. Subjects walked or ran for 30 s at each speed wearing normal exercise apparel without the harness.

External Load Measurement

To measure applied load, a load cell (Entran, Inc., Fairfield, NJ) was attached to a cable that was fed through a pulley and connected to the subject harness via the bungee loading system. The pulley arrangement was used so that the amount of linear space taken up by the load cell would not significantly reduce the extension of a bungee, which would have lowered the amount of load that could be provided to the subject. A displacement transducer (Ergotest Technology, Langesund, Norway) was mounted on the left side of the subject and used to measure the linear displacement of the load attachment point at the subject's harness.

In addition to measuring the external load during each trial, load was also measured for each subject before locomotion in each configuration during a static trial as the subject stood still on the treadmill during a period of microgravity. If the approximate load was significantly different from the target load, the harness was adjusted to appropriately alter the bungee tension. Load and displacement data were captured at 120 Hz and recorded by a data acquisition system (LabVIEW v8.1, National Instruments, Austin, TX). The load data were reduced by determining a maximum, minimum, mean, and standard deviation for each 10-s trial.

Kinematics

Reflective markers were attached to each subject's left side. Markers were placed arbitrarily on the upper and lower thigh, the upper and lower shank, and the heel and toe (figure 6-2). The body was modeled as 3 rigid, linked segments. This configuration allowed each segment to be represented as the vector connecting the proximal marker to the distal marker. Three-dimensional marker locations were found using the 6-camera

motion-capture system (SMART Elite System, BTS Engineering, Padova, Italy) with a sampling frequency of 60 Hz.



Figure 6-2. Marker positions during data collection.

All 3-dimensional data were expressed relative to an inertial reference frame that was established during calibration. The inertial reference frame was arbitrarily oriented so that the vertical axis was normal to the treadmill surface. A treadmill reference frame was created so that the x-axis was oriented to approximate the lateral direction of the treadmill belt, the y-axis was perpendicular to the treadmill surface, and the z-axis was parallel to the fore-aft axis of the treadmill in the direction of locomotion.

Raw motion-capture data were examined for missing points, which were replaced using cubic spline interpolation. The motion-capture data were then filtered using a fourth-order Butterworth low-pass filter with an optimal cutoff frequency for each marker determined using an autocorrelation procedure (Challis, 1999). The autocorrelation was executed independently for each coordinate of each marker, and the highest cutoff frequency determined for each coordinate was used for each marker. Cutoff frequencies ranged from 6 Hz to 28 Hz (mean = 16.65 Hz).

Processed motion-capture data were then rotated into the treadmill reference frame. All kinematic analyses then proceeded using 2-D (y,z) data, with the assumption that any motion in the lateral direction by the legs was negligible. Three or more strides from each trial were analyzed, depending on the quality of the data. The instances of heel strike and toe off were found using the heel and toe markers as described by De Witt and Hagan (2007).

Joint segment trajectories of the thigh, shank, and foot were found for each sample of each trial. Segment angles were computed relative to the horizontal. All segment angles were corrected relative to the anatomical position by subtracting joint angles found during a static (standing) trial. Positive segment angles represent forward (clockwise) motion relative to the anatomical position.

Dependent Variables and Statistical Analysis

Contact time (CT), stride time (ST), and kinematic data were processed using custom software programmed in MATLAB v7.1 (The MathWorks, Inc., Natick, MA). Kinematic variables of interest included the range of motion (ROM) of the thigh, shank, and foot segments, and the position of each segment at heel strike. Differences in CT, ST, and kinematic means between conditions were tested using a repeated-measures analysis of variance (ANOVA). Separate analyses were conducted for each speed. Significance was defined as $p < 0.05$.

RESULTS

External Load

Load cell measures indicated that during static trials, the group mean EL was near the target loads desired for testing with the exception of subject d being underloaded during the L trials (see table 6-2). During motion trials, slight decreases occurred in EL, as has been reported during previous EL evaluations in parabolic flight (Schaffner et al., 2005). Although not tested statistically, the drop in load during walking and running appears to be greater at low loads than at high loads.

Table 6-2. Mean (\pm SD of the entire trial) EL for each subject at each speed and condition during microgravity trials.

| Load Level | Subject | Static | Speed | | |
|------------------------------------|---------|---------------|----------------|---------------|----------------|
| | | | Walking | Running | Sprinting |
| EL = L (55% BW) | a | 67% | 61% \pm 1% | 64% \pm 3% | 58% \pm 1% |
| | b | 55% | 55% \pm 0.3% | 57% \pm 1% | 56% \pm 0.4% |
| | c | 66% | 59% \pm 2% | 57% \pm 2% | 51% \pm 3% |
| | d | 42% | 34% \pm 4% | 24% \pm 5% | NA |
| Mean (\pm SD of the group mean) | | 58% \pm 12% | 52% \pm 13% | 50% \pm 18% | 55% \pm 4% |
| EL = H (80% BW) | a | 91% | 84% \pm 1% | 87% \pm 2% | 84% \pm 2% |
| | b | 74% | 70% \pm 1% | 71% \pm 1% | 71% \pm 1% |
| | c | 82% | 74% \pm 1% | 71% \pm 1% | 75% \pm 4% |
| | d | 77% | 76% \pm 1% | 76% \pm 1% | 76% \pm 5% |
| Mean (\pm SD of the group mean) | | 81% \pm 8% | 76% \pm 6% | 76% \pm 7% | 76% \pm 5% |

NA = data unavailable

During locomotion, the subject's center of mass will oscillate vertically during the stride. Because bungee tension is a function of length, the vertical oscillation may cause the EL

to vary. Table 6-2 shows the standard deviation of the EL for each subject at each speed. These data indicate that EL variations were approximately 1% to 3% BW, and were similar among speeds and EL levels.

Gait Parameters

CT and ST means are presented for each gait type (see table 6-3). Gravity level did not affect CT or ST at any speed.

Table 6-3. Mean CT and ST for microgravity trials with each EL level and in normal gravity.

| | Gravity | Load | Speed | | |
|------------------|---------|-------|-------------|-------------|-------------|
| | | | Walking | Running | Sprinting |
| Contact Time (s) | Micro | Light | 0.65 ± 0.05 | 0.29 ± 0.04 | 0.21 ± 0.03 |
| | Micro | Heavy | 0.64 ± 0.08 | 0.31 ± 0.01 | 0.22 ± 0.01 |
| | Normal | – | 0.67 ± 0.01 | 0.31 ± 0.02 | 0.22 ± 0.01 |
| Stride Time (s) | Micro | Light | 1.03 ± 0.06 | 0.71 ± 0.03 | 0.55 ± 0.03 |
| | Micro | Heavy | 0.99 ± 0.09 | 0.66 ± 0.02 | 0.55 ± 0.04 |
| | Normal | – | 0.99 ± 0.02 | 0.67 ± 0.03 | 0.54 ± 0.01 |

Kinematics

Means of the thigh, shank, and foot ROM are shown in table 6-4. The repeated-measures ANOVA revealed no difference in ROM of any segment between the microgravity load conditions and the normal gravity condition, at any speed. Figure 6-3 shows the thigh, shank, and foot segment orientations at heel strike for each speed. During walking, thigh angle at the highest EL was greater than during normal gravity.

Table 6-4. Mean thigh, shank, and foot ROM for microgravity trials at each EL level and in normal gravity.

| Segment ROM | Gravity | Load | Speed | | |
|-----------------|---------|-------|---------------|----------------|----------------|
| | | | Walking | Running | Sprinting |
| Thigh ROM (deg) | Micro | Light | 51.21 ± 13.85 | 63.46 ± 13.34 | 64.11 ± 8.46 |
| | Micro | Heavy | 55.22 ± 15.50 | 61.31 ± 12.34 | 60.77 ± 7.43 |
| | Normal | – | 41.58 ± 1.72 | 48.51 ± 3.60 | 51.18 ± 6.79 |
| Shank ROM (deg) | Micro | Light | 76.58 ± 15.93 | 90.40 ± 9.55 | 114.99 ± 12.67 |
| | Micro | Heavy | 67.54 ± 12.29 | 86.20 ± 11.14 | 125.54 ± 22.43 |
| | Normal | – | 76.14 ± 7.66 | 92.36 ± 7.70 | 116.93 ± 11.92 |
| Foot ROM (deg) | Micro | Light | 85.87 ± 12.41 | 104.15 ± 13.45 | 131.83 ± 18.72 |
| | Micro | Heavy | 86.88 ± 17.25 | 106.39 ± 11.88 | 131.75 ± 9.71 |
| | Normal | – | 95.67 ± 4.91 | 108.07 ± 4.49 | 132.32 ± 10.90 |

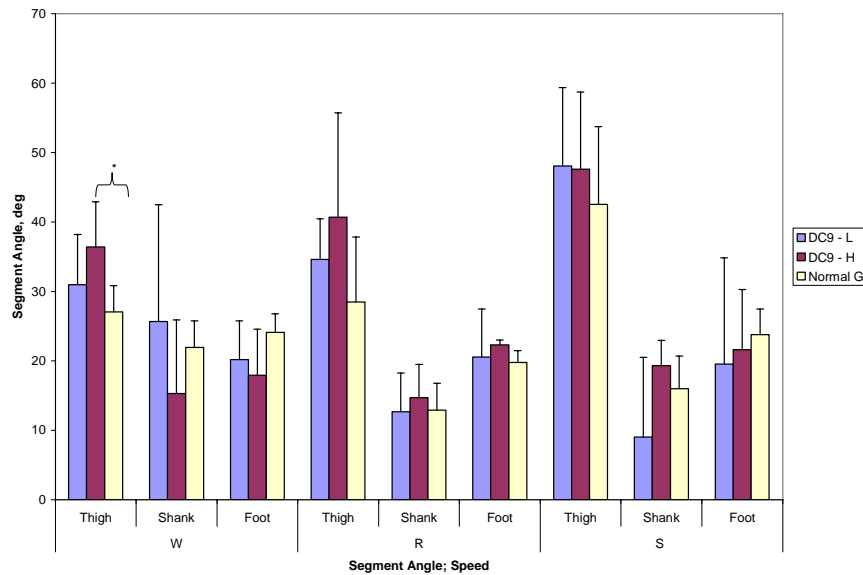


Figure 6-3. Mean thigh, shank, and foot segment angles at heel strike during walking, running, and sprinting in normal and microgravity.

DISCUSSION

During this investigation, subjects exercised on the second-generation ISS treadmill prototype in microgravity while loaded to approximately 80% and 55% of their BW using bungees, and in normal gravity. Gait kinematics in microgravity and normal gravity conditions were compared. Our results suggest that gait kinematics are similar for microgravity and normal gravity conditions, with the exception of an increase in walking thigh angle at heel strike during high external loading (80% BW) in microgravity. The thigh angle graphically seems to be very different in different conditions, but our small sample size may have limited our power to detect a significant difference. Future evaluations would benefit from a larger sample size.

The temporal kinematics during walking and running were similar to those found by Schaffner et al. (2005). Stride time and contact time were similar to those reported by Swanson and Caldwell (1999). These findings suggest that our subjects did not choose contact and stride patterns different from those chosen by other populations on different treadmills at similar speeds.

We did not find any differences in segment motion between normal gravity and parabolic flight conditions. Although we report segment angles rather than joint angles, one can easily infer that joint ranges of motion were not different in different conditions. The only difference that we did find was that thigh angle was greater at heel strike during our H EL walking condition. The greater thigh angle suggests that the hip was in greater flexion at heel strike.

De Witt et al. (2008, in preparation) found increased maximal hip flexion during walking in microgravity when loaded with bungees to approximately 90% of BW, which is similar to our findings. The increased hip flexion may be an adaptation that occurs to accommodate the increased EL, resulting in a gait style referred to as “Groucho running” (McMahon et al., 1987). During Groucho running, locomotion is completed with increased knee and hip flexion. This running style occurs with the increased EL, and has been estimated to increase the locomotion oxygen cost by about 25% for each 5-degree increase in midstance knee angle (Valiant, 1990). Although there was a difference in thigh angle at heel strike, this finding is not different from past evaluations of locomotion in microgravity, suggesting that the difference was not caused by the treadmill, but rather by the loading placed on our subjects.

CONCLUSION

Our hypothesis that locomotion would be different for different gravitational conditions was rejected. Overall, we found no differences between locomotion in microgravity and normal gravity, which suggests that subjects perform locomotion similarly in microgravity and normal gravity on the T2. Furthermore, our findings are in agreement with past research using different treadmills, suggesting that subjects do not change their locomotion styles on the T2. Although we had a small sample size, findings were consistent across subjects. We do not believe that subject locomotion on the T2 will differ from that on other treadmills.

REFERENCES

- Challis, JH. (1999) A procedure for the automatic determination of filter cutoff frequency for the processing of biomechanical data. *J. Appl. Biomechanics* 15:303-317.
- De Witt JK, Perusek GP, Lewandowski BE, Gilkey KM, Savina M, Samorezov S, and Edwards WB. (submitted). Comparison of locomotion in normal gravity, simulated microgravity and actual microgravity. *Med. Sci. Sports Exerc.*
- De Witt JK, Schaffner G, Laughlin MS, Loehr J, and Hagan RD. (2004). External load affects ground reaction force parameters non-uniformly during running in weightlessness. Presented at the 2004 Annual Meeting of the American Society of Biomechanics, Portland, OR.
- De Witt JK, Schaffner G, Blazine K, Bentley JR, Laughlin MS, Loehr J, and Hagan RD. (2003). Loading configurations and ground reaction forces during treadmill running in weightlessness. Presented at the 2003 Annual Meeting of the American Society of Biomechanics, Toledo, OH.
- McMahon TA, Valiant G., and Frederick E.C. (1987). Groucho running. *J. Appl. Physiol.* 62:2326–2337.
- Schaffner G, DeWitt JK, Bentley JR, Yarmanova E, Kozlovskaya I, and Hagan RD. (2005). Effect of subject loading device load levels on gait. NASA Technical Report TP-2005-213169.

Swanson SC and Caldwell GE. (2000). An integrated biomechanical analysis of high speed incline and level treadmill running. *Med. Sci. Sports Exerc.* 32:1146–1155.

Valiant, GA. (1990). Transmission and attenuation of heelstrike accelerations. In: *Biomechanics of Distance Running*, P. R. Cavanagh (Ed.). Champaign, IL. Human Kinetics, 225–247.

PHOTOGRAPHS

JSC2007E093406 to JSC2007E093430

JSC2007E093115 to JSC2007E093147

JSC2007E054380 to JSC2007E054427

VIDEO:

- Zero G flight week October 23–26, 2007, Master: 306447

Videos available from Imagery and Publications Office (GS4), NASA JSC.

CONTACT INFORMATION:

John De Witt, PhD

Wyle

1290 Hercules Suite 120

Houston, Texas 77058

john.k.dewitt@nasa.gov

281-483-8939

TITLE

Space Medicine C-9 Familiarization Flight

FLIGHT DATE

October 23, 2007

PRINCIPAL INVESTIGATOR

David Stanley, Wyle

CO-INVESTIGATORS

Tyler Carruth, Wyle

Chris Van Velson, Wyle

Robert Tweedy, Barrios

Heather Van Velson, Wyle



GOAL

Our goal was to test new equipment for the Space Medicine familiarization flight (MED OPS FAM Flight). The purpose of the MED OPS FAM Flights is to familiarize Space Medicine Branch personnel with the effects of a 0 G environment through performing activities that utilize the medical equipment and procedures. This helps facilitate crew training and biomedical engineering support for International Space Station (ISS) and Space Shuttle crew procedures.

OBJECTIVES

All co-investigators accomplished some or all of the following objectives:

BEFORE FLIGHT

1. Attended preflight briefing and participated in ground-based practice session
2. Attended Test Readiness Review (TRR)
3. Attended Medical Briefing
4. Conducted final inventory of all hardware and supplies and transported equipment to Ellington Field for scheduled reporting time
5. Properly loaded and secured hardware in the aircraft

DURING FLIGHT

1. Experienced and evaluated the effects of microgravity on intravenous insertion, drug administration, and medical fluids
2. Tested new mannequins and hardware
3. Experienced and evaluated the effects of microgravity on cardiopulmonary resuscitation (CPR), patient restraint, and rescuer restraint
4. Experienced and evaluated the effects of microgravity on using 2 different types of instruments for intubation

AFTER FLIGHT

1. Unloaded hardware from aircraft
2. Prepared a C-9 final report

INTRODUCTION

As new personnel join the Space Medicine Branch, it is critical that the co-investigators understand the effects of microgravity on using medical procedures, hardware, and supplies. The familiarization flight provides personnel with a better understanding of the effects of microgravity for use of (1) medical procedures, (2) patient and rescuer restraint, and (3) medical training for space flight. Using medical procedures to perform tasks on the familiarization flight allows the operator to understand the limitations imposed by microgravity, helps in the composition of procedures for space flight, and helps operators assist astronauts in onboard execution of procedures.

The flight process also provided experience in preparation and execution of flight lesson plans, and preparation of final reports. In addition, first-time fliers gained insight into their performance level in microgravity for future flights.

METHODS AND MATERIALS

An initial training session was held to familiarize the new fliers with the documentation and skills necessary to fly on the C-9. The documentation required for requesting and reporting a C-9 flight was covered in detail and the co-investigators were given a template for writing their final reports. A skill session on the medical procedures that would be attempted during flight was also held. Fliers were introduced to the tasks required at each station and were given additional time to build confidence in their skills by practicing these tasks.

The procedures and equipment were divided into 3 stations: a CPR station, an intravenous (IV) administration station, and an intubation station.

The CPR station was established to practice the performance of cardiopulmonary resuscitation on a simulated ill crewmember. The Crew Medical Restraint System (CMRS) was deployed and utilized to immobilize the simulated ill crewmember. Three approaches to the performance of CPR were practiced for the designated crew medical officer (CMO): (1) CMO beside the patient, (2) CMO straddled on patient, and (3) handstand position (inverted).

The IV administration station consisted of an artificial human arm with the correct anatomic landmarks for practicing intravenous catheter insertion. The arm and IV equipment (figure 7-1) were fixed to a small metal table. The procedures for establishing peripheral intravenous access were followed and procedures for injecting medication into the intravenous line were practiced. A Tubex drug injection system was used for this purpose. The established medical checklist procedure for this technique was followed.

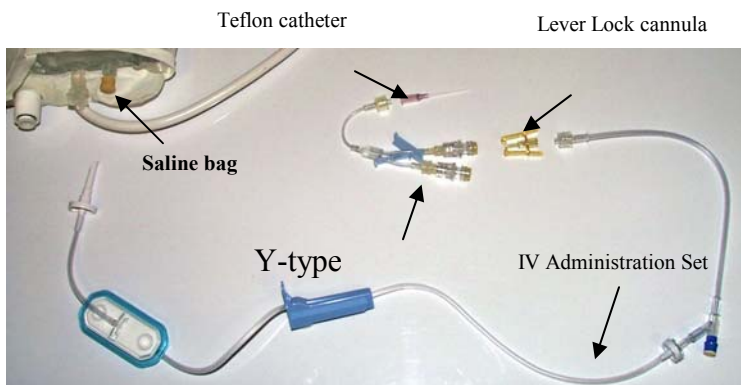


Figure 7-1. IV equipment.

The intubation station was composed of a plastic model of the human head, neck, and chest that is designed specifically for practicing the establishment of an airway. Intubation with 2 different devices was practiced: the laryngoscope (figure 7-2) and the Intubating

Laryngeal Mask Airway (ILMA) device (figure 7-3) and endotracheal tube. The established medical checklist procedures for the insertion of these devices were followed.



Figure 7-2. Laryngoscope



Figure 7.3. ILMA

During the flight, the co-investigators were stationed as outlined in table 7-1.

Table 7-1. C-9 familiarization flight procedure assignments.

| <i>Parabolas</i> | | 0 – 10 | 11 – 20 | 21 – 30 | 31 – 40 |
|-------------------|------------|--------------|--------------|--------------|--------------|
| <i>Activities</i> | CPR | Tweedy | Tweedy | H. VanVelson | ----- |
| | CPR | H. VanVelson | C. VanVelson | Stanley | Stanley |
| | IV | Carruth | Carruth | C. VanVelson | Carruth |
| | Intubation | C. VanVelson | H. VanVelson | Tweedy | H. VanVelson |

RESULTS

CPR Station

The CMRS was deployed and secured to the aircraft floor before flight. The simulated ill crewmember (mannequin) was secured to the CMRS according to established procedures for the use of the restraint system. The designated CMO was able to perform CPR in all 3 of the positions desired: side-by-side, straddled, and inverted. The inverted position was clearly the most effective position, as the other 2 positions required significant counterpressure from restraints. All the objectives for this station were met.



Figure 7-4. Chris VanVelson – CPR.



Figure 7-5. Tyler Carruth – ILMA.

IV Station

The insertion of an intravenous catheter was achieved using the standard procedures. Intravenous fluid tubing was connected to the catheter. Afterward, Tubex drug injection was practiced. The management of sharp waste was particularly important due to the tendency of objects to float in simulated microgravity. All the objectives for this station were met.



Figure 7-6. Chris VanVelson – IV.



Figure 7-7. Tyler Carruth – IV.

Intubation Station

The medical checklist procedures were followed for the insertion of the ILMA. The lack of gravitational influence made it necessary to secure all small loose objects so that they would not drift away. The laryngoscope / endotracheal tube method of intubation was performed according to established procedures. Both of these methods were repeated twice. All the objectives for this station were met.

DISCUSSION

Performing the medical operations procedures on the C-9 flight gave the co-investigators a greater understanding of the conditions during space operations. This knowledge will prove very useful for the co-investigators, especially during contingency situations with the flight crew and/or training sessions.

Experiencing weightlessness presented many difficulties that the co-investigators did not originally expect. The co-investigators found the lack of control while floating to be the most difficult aspect of weightlessness. The lack of control was most apparent when investigators were performing time-critical medical activities. They spent a larger amount of time securing themselves and maintaining proper positioning than was originally anticipated. They thought this time would most likely be reduced with extended exposure to microgravity. With this information, the co-investigators will be able to make more accurate and effective recommendations to crewmembers during nominal and emergency situations.

This familiarization flight was extremely beneficial for supporting the crew and supporting console operations. A greater understanding and appreciation of the difficulties crewmembers face because of their working environment was gained. This

experience will give investigators a better ability to walk the crew through any procedure, not just the ones performed during the flight.

CONCLUSION

Overall, the objectives of the C-9 Familiarization Flight were met. All co-investigators agreed that the C-9 Familiarization Flight and associated training provided them with an excellent knowledge level from which to conduct their own flights. This was a very valuable training session and is highly recommended for all biomedical engineers (BMEs), flight surgeons, and instructors. It is especially beneficial for anyone who expects astronauts to perform complex tasks that require the use of many items of loose equipment.

PHOTOGRAPHS

JSC2007E093388 to JSC2007E093405

VIDEO:

- Zero G flight week October 23–26, 2007, Master: 306447

Videos available from Imagery and Publications Office (GS4), NASA JSC.

CONTACT INFORMATION

David Stanley
Wyle
1290 Hercules Suite 120
Houston, TX 77058
dstanley@wylehou.com

TITLE

NASA Explorer School – NASA’s Weightless Wonder Simulates Microgravity Mass Determination via Inertial Balance Technology

FLIGHT DATES

February 15, 2008

PRINCIPAL INVESTIGATOR

Pete Pompura, South Plantation High School

CO-INVESTIGATORS

Colleen Leonard, South Plantation High School

Akram Molaka, South Plantation High School

Arthur Kelly, South Plantation High School



GOAL

To assess a method for finding the mass of an object in 0 G.

South Plantation High School, hosted by Kennedy Space Center, joined 13 other school teams for a unique learning experience to test science concepts in a weightless laboratory aboard the Weightless Wonder, NASA’s C-9 aircraft. Additional goals of the NASA Explorer School (NES) consisted of connecting space, math, and science to Earthly classrooms. It is NASA’s goal to recruit and retain students in STEM (Science,

Technology, Engineering, and Math) education programs that encourage the pursuit of careers critical to future space exploration.

OBJECTIVES

- (1) Devise an experimental apparatus to determine an unknown mass in zero gravity.
- (2) Relate applicability of data and results to human physiology in the weightless environment of the International Space Station and future space travel.

METHODS AND MATERIALS

Participation in NASA's Reduced Gravity Flight Opportunity Program has been a fabulous and thrilling "out of this world" experience. The flight operations facility at Ellington Field served as the base of operations for scientific experiments performed by educators from across the nation aboard a modified McDonnell Douglas C-9 jet aircraft. A series of 32 parabolic maneuvers over a period of 1.7 hours provided gravitational forces ranging from 1.8 to 2g at the parabolic bottom to 0 G as the C-9 nosed "over the top" for 25 to 30 s. These intermittent maneuvers provided short periods of simulated lunar and martian gravitational forces for the experiment.



The Inertial Balance was attached to a camera pole on board the reduced-gravity aircraft. The balance oscillates horizontally and is unable to bend vertically, so varying levels of gravity will not affect the experiment results. A mass, either known or unknown, was loaded into the Inertial Balance. The arm was pulled to the side, then let go, and the number of oscillations in a given amount of time were measured using a light gate. When the allotted time had elapsed, the arm was stopped and the oscillation measurements were recorded on a clipboard. Depending on how many measurements were taken, a different

object could then be loaded. Finally, the Inertial Balance was reset for the next measurement.

The Inertial Balance apparatus was composed of wooden blocks, steel strips, a vinyl pouch, foam padding, duct tape, a Data Logger with a Light Gate attachment, and hose clamps.



RESULTS

The Inertial Balance performed as expected throughout the experiment. The data gathered under all 3 gravitational conditions (0 G, 1 G, 2 G) concurred with expectations and predictions. The percentage error was relatively small, and we were able to accurately identify the unknown mass of the mystery object.



DISCUSSION

Mass measurement in microgravity has been a concern for astronauts from the very beginning of the space program. It has been observed over the last 50 years that all space travelers lose body mass in space. To investigate this phenomenon, methods of determining the mass of an object in microgravity were developed.

Most Earth-bound methods of determining the mass of an object depend on the weight of that object, or the force due to gravity that the object exerts toward the center of the Earth. Without the effects of that force, the object has no “weight,” so other mass measurement techniques must be used. One method is to use an Inertial Balance.

Inertia is defined as the tendency of an object to resist a change in its velocity. The more massive the object, the more it resists any change to its current motion. An Inertial Balance simply places the object in an oscillation pattern. The more massive the object, the slower the Inertial Balance will oscillate. An object with less mass will cause the Inertial Balance to oscillate faster.

If a known mass is attached to an Inertial Balance, and the oscillation frequency is measured, then an unknown mass can be measured by the same Inertial Balance using simple proportions. An Inertial Balance is actually a compound spring system, which acts according to the equation $T^2 = [4\pi^2/k]*M$, where T is the period of oscillation, M is the mass of the object, and k is the spring constant of the system. So, from one object measurement to the next, if the oscillations decreased in period by one-half, then the mass of the object must have increased by a factor of 4.

The Inertial Balance is not affected by gravity, so this experiment will work on the ground as well as during any part of the reduced-gravity flight parabola. The purpose of

the experiment is to show that the mass of an object can be determined successfully in microgravity.

Our NASA JSC mentor, Mark Pape, was instrumental in the development of our inertial balance, and in the execution of the experiment on the day of the flight.

CONCLUSION

The apparatus as defined in this experiment is in fact the present basis of mass determination of astronauts aboard the International Space Station. This information was shared with me during experimentation by Johnson Space Center scientist Dr. Carlos Luongo. He complimented our work as being accurate and precise in logic and reasoning.

PHOTOGRAPHS

JSC2008EO14229 to JSC2008EO14230

JSC2008EO14250 to JSC2008EO1453

JSC2008EO14255

JSC2008EO14265

JSC2008EO14343

JSC2008EO14447 to JSC2008EO14448

JSC2008EO14450

JSC2008EO14486 to JSC2008EO14495

JSC2008EO14528

VIDEO

- Zero G flight week February 11–15, 2008, Master: 734487

Videos available from Imagery and Publications Office (GS4), NASA JSC.

REFERENCES

1. <http://en.wikipedia.org/wiki/Inertia>
2. http://dev.physicslab.org/Document.aspx?doctype=2&filename=Dynamics_InertialMass.xml

ACKNOWLEDGEMENTS

Principal investigator Pete Pompura derived the idea for this experiment with students in his physics class. He relied on the brilliance and imagination of students in his astronomy class to finalize the design and provide assistance in the construction of the apparatus. Also providing expertise were members of the flight team, including Akram Molaka, Science Department Chairman; Colleen Leonard, original NASA Explorer School team member; and Arthur Kelly, Environmental Science Magnet teacher.

We appreciate very much the support provided by our colleagues at the NASA Johnson Space Center – Mr. Mark Pape; Dr. Carlos Luongo; Mr. Dominic Del Rosso, who served as Test Director and was responsible for all major safety factors and equipment functionality; Mr. Douglas Goforth, Program Manager of the Education Office, who co-directed the NASA Reduced Gravity Student Flight Opportunities Program; and Sara Malloy and Alissa Kuseske, who coordinated the logistics of the 2-week program for visiting teachers.

CONTACT INFORMATION

Pete Pompura
South Plantation High School
peter.pompura@browardschools.com
poppapete@comcast.net
561-756-2235
1300 SW 54th Avenue
Plantation, Florida 33317-5402

TITLE

NASA Explorer School – Reaction Time

FLIGHT DATES

February 26–27, 2008

PRINCIPAL INVESTIGATOR

Phyllis Isbell, Key Peninsula Middle School

CO-INVESTIGATORS

Karen Lindberg, Key Peninsula Middle School

Patty Rivers, Key Peninsula Middle School

Rebecca Cutri-Kohart, NASA Johnson Space Center



GOAL

We will test the reaction rate of the chemical reaction of baking soda and vinegar. Investigation question: How does microgravity affect the rate of the reaction of baking soda and vinegar? An experiment will be conducted to compare the rate of the chemical reaction that occurs when baking soda and vinegar are mixed in microgravity with the rate of the same reaction in Lakebay, Washington. The reaction rate is the speed of the reaction. The reaction rate depends on how often the reactants collide (collision theory); that is, on how easily the particles of the reactants can get together. Reaction rate can be measured by measuring how quickly one of the reactants disappears or by measuring how quickly one of the products is made. The relative reaction rates will be determined by measuring the pressure produced by the product carbon dioxide.

OBJECTIVES

The purpose of this experiment is to determine how microgravity affects the rate of the reaction of baking soda and vinegar. For the purpose of this experiment, the reaction rate will be measured by determining the volume of carbon dioxide produced per unit time. This will be found by measuring the air pressure in an enclosed container containing the carbon dioxide gas generated in the first 20 s of the reaction. Control experiments will be carried out by students in a 1-G laboratory environment, and the results of these experiments will be compared with the results of the experiments carried out by teachers on the C-9 reduced gravity jet this year and those performed last year, when the reactants were mixed using a syringe to inject the vinegar into a test tube.

The reaction rate for this experiment is governed partly by collision theory, which is based on the concept that the frequency with which the reactants collide determines reaction rate. (The reaction rate can also be affected by a catalyst, heat, or surface area.) The greater the frequency of collisions, the faster the reaction rate and the faster the product (carbon dioxide in this case) is produced. It is expected that fewer collisions will occur in microgravity, and therefore the reaction rate will be slower. In a 1-G environment, gravity causes the vinegar to fall directly onto the baking soda, and the reactants are contained in a smaller volume. The reactants have greater opportunity to collide, resulting in a faster reaction rate.

In this experiment, the use of a syringe, which was used last year to mix the reactants, was eliminated. It was hypothesized that without the syringe to speed mixing, there would be fewer reactions in this year's microgravity experiment than in last year's. A ball valve pipe containing 5 mL of vinegar on one side of the valve and 0.05 g of baking soda on the other side of the valve was attached to a Vernier pressure sensor. During freefall, the chemical reaction was initiated by opening the valve between the vinegar and baking soda. If the reactants mixed, carbon dioxide gas was produced, and the air pressure inside the test tube increased. After 20 s had elapsed, the amount of carbon dioxide gas produced by the experiment was measured by reading the pressure sensor. This experiment was repeated 4 times in 4 pre-prepared test tubes housed in a test-tube rack. A fifth trial was conducted using vinegar only and no baking soda to determine a baseline pressure for comparing the pressures of the other 4 trials. This experiment was repeated on both flights. The experiment was conducted and contained in an enclosed glove box on the C-9.



METHODS AND MATERIALS

The filled pipe ball valves were secured with 2 cable ties (tie wraps) around each to prevent them from coming out of the test tube rack. The opening of the top of each pipe was secured with a nipple cap attached to ¼" clear tubing that was used to connect 6 Vernier PS-DIN pressure sensors. Each pressure sensor was connected to a Vernier LabPro data interface unit using a data interface cable, which passed through a single port on the glove box. The LabPro data interface unit was connected to a laptop computer using Logger Pro Software. The laptop was used to store and plot data from each trial of the experiment. The glove box, LabPro data interface unit, and laptop were stored inside a C-9 onboard storage container for takeoff and landing.

In flight, the glove box was removed from the C-9 onboard storage box and secured to the aircraft using Velcro® and cargo straps. Before the first parabola was flown, the Logger Pro graphing software and LabPro data interface unit were connected to the data interface cable attached to the first pressure sensor. During the first parabola, the valve separating the vinegar and baking soda was opened and data collection began. After 20 s had elapsed, the data collection software had stored the time and pressure vectors measured inside the first test tube. Before each subsequent parabola, the LabPro data interface unit was connected to the appropriate data interface cable, and the above procedure was repeated.

A secondary educational demonstration that allowed students to visualize the effect of microgravity on the chemicals was flown in 1-liter plastic bottles. These bottles were taped to the wall and on display to show what was happening in the test tubes.

Procedure

Preflight experiment setup

1. Draw 5 mL of vinegar into one half of pipe assembly.
2. Measure 0.05 g of baking soda with digital scale and place in other half of pipe assembly (ensuring valve is closed).
3. Secure 2 tie wraps to each pipe tube so that the pipe is securely braced on the mounting frame.
4. Connect clear plastic tubing to the nipple cap of the tubes.
5. Connect the PS-DIN pressure sensor to the clear plastic tubing.
6. Connect the black PS-DIN power and data link cable to the gray interface cable (flat gray 2" cable with a white analog connector on one end).
7. Secure mounting rack and pressure sensors inside glove box using Velcro.
8. Secure the black PS-DIN cable through a rubber stopper and insert in cable port in glove box top.
9. Attach LabPro to outside top of glove box with Velcro.
10. Attach laptop to the LabPro and secure to aircraft floor.
11. Close glove box, using Velcro.

In-flight setup

Unstow glove box and mount to aircraft floor using Velcro and cargo straps.

Set up laptop with PS-DIN Pressure Sensor and LabPro interface:

1. Plug the sensor into 1 of 4 CH slots on the LoggerPro.
2. Connect the data collector USB to the laptop.
3. Open LoggerPro from the desktop.
4. GOTO Experiment and select SET UP SENSORS and SHOW ALL INTERFACES.
5. Select CH1 and select the gas pressure sensor.
6. The time was preset to 30 s with 1 data item per second.

Experiment procedures for each parabola

1. Experimenter 1 selects “Collect” on LabPro.
2. Experimenter 2 puts her hand into the glovebox and moves the valve handle from perpendicular to the pipe to parallel. At “feet down,” the valve is returned to perpendicular.
3. Experimenter 2 uses GOTO Experiment and STORE LATEST RUN.

Post-parabola procedures

1. Save the file on the laptop as RGO 2008 A or B.
2. Select the next pressure sensor.

RESULTS

Table 9-1. Air pressure (kPa) in ball valves during 4 trials.

| Test One, First Valve | | | | Test Two, Second Valve | | | |
|-----------------------|----------|----------|----------|------------------------|----------|----------|----------|
| 15.49632 | 15.32606 | 20.03648 | 20.09324 | | | | |
| 15.55307 | 15.32606 | 20.03648 | 20.09324 | | | | |
| 15.55307 | 15.38281 | 20.03648 | 20.03648 | 15.49632 | 15.32606 | 20.03648 | 20.09324 |
| 15.60982 | 15.38281 | 20.03648 | 20.09324 | 15.55307 | 15.32606 | 20.03648 | 20.03648 |
| 15.60982 | 15.38281 | 20.09324 | 20.09324 | 15.55307 | 15.32606 | 20.03648 | 20.09324 |
| 15.55307 | 15.32606 | 20.03648 | 20.14999 | 15.55307 | 15.38281 | 20.03648 | 20.09324 |
| 15.55307 | 15.38281 | 20.03648 | 20.09324 | 15.55307 | 15.38281 | 20.09324 | 20.09324 |
| 15.55307 | 15.38281 | 20.03648 | 20.14999 | 15.55307 | 15.38281 | 20.03648 | 20.09324 |
| 15.55307 | 15.38281 | 20.03648 | 20.14999 | 15.60982 | 15.38281 | 20.03648 | 20.09324 |
| 15.60982 | 15.43957 | 20.03648 | 20.14999 | 15.60982 | 15.38281 | 20.03648 | 20.14999 |
| 15.60982 | 15.38281 | 20.09324 | 20.14999 | 15.60982 | 15.43957 | 20.03648 | 20.03648 |
| 15.60982 | 15.43957 | 20.03648 | 20.14999 | 15.60982 | 15.38281 | 20.03648 | 20.03648 |
| 15.55307 | 15.43957 | 20.03648 | 20.14999 | 15.66657 | 15.38281 | 20.14999 | 20.09324 |
| 15.60982 | 15.43957 | 20.03648 | 20.14999 | 15.66657 | 15.43957 | 20.09324 | 20.09324 |
| 15.60982 | 15.38281 | 20.03648 | 20.14999 | 15.60982 | 15.43957 | 20.09324 | 20.09324 |
| 15.66657 | 15.43957 | 20.03648 | 20.09324 | 15.66657 | 15.43957 | 20.03648 | 20.09324 |
| 15.66657 | 15.43957 | 20.03648 | 20.14999 | 15.66657 | 15.43957 | 20.03648 | 20.14999 |
| 15.66657 | 15.43957 | 20.03648 | 20.14999 | 15.66657 | 15.43957 | 20.09324 | 20.14999 |

| | | | | | | | |
|----------|----------|----------|----------|----------|----------|----------|----------|
| 15.66657 | 15.38281 | 20.03648 | 20.14999 | 15.66657 | 15.43957 | 20.09324 | 20.09324 |
| 15.72333 | 15.43957 | 20.03648 | 20.09324 | 15.72333 | 15.49632 | 20.03648 | 20.09324 |
| 15.66657 | 15.49632 | 20.03648 | 20.09324 | 15.66657 | 15.43957 | 20.03648 | 20.14999 |
| 15.66657 | 15.49632 | 20.03648 | 20.14999 | 15.72333 | 15.43957 | 20.09324 | 20.09324 |
| | | | | 15.72333 | 15.49632 | 20.09324 | 20.03648 |
| | | | | 15.66657 | 15.49632 | 20.09324 | 20.09324 |

Test Three, Third Valve

Test Four, Fourth Valve

| | | | | | | | |
|----------|----------|----------|----------|----------|----------|----------|----------|
| 15.55307 | 15.26931 | 20.09324 | 20.09324 | | | | |
| 15.49632 | 15.32606 | 20.09324 | 20.09324 | 15.66657 | 15.43957 | 20.03648 | 20.09324 |
| 15.55307 | 15.32606 | 20.09324 | 20.09324 | 15.66657 | 15.43957 | 20.09324 | 20.14999 |
| 15.55307 | 15.32606 | 20.14999 | 20.14999 | 15.66657 | 15.38281 | 20.14999 | 20.14999 |
| 15.55307 | 15.32606 | 20.09324 | 20.09324 | 15.66657 | 15.43957 | 20.09324 | 20.14999 |
| 15.60982 | 15.38281 | 20.09324 | 20.14999 | 15.66657 | 15.43957 | 20.09324 | 20.09324 |
| 15.60982 | 15.32606 | 20.09324 | 20.09324 | 15.66657 | 15.38281 | 20.03648 | 20.14999 |
| 15.60982 | 15.38281 | 20.14999 | 20.09324 | 15.72333 | 15.43957 | 20.09324 | 20.14999 |
| 15.55307 | 15.38281 | 20.09324 | 20.09324 | 15.66657 | 15.43957 | 20.14999 | 20.14999 |
| 15.60982 | 15.43957 | 20.03648 | 20.09324 | 15.66657 | 15.43957 | 20.03648 | 20.09324 |
| 15.66657 | 15.38281 | 20.09324 | 20.14999 | 15.66657 | 15.49632 | 20.09324 | 20.09324 |
| 15.60982 | 15.38281 | 20.09324 | 20.14999 | 15.72333 | 15.43957 | 20.14999 | 20.14999 |
| 15.66657 | 15.38281 | 20.09324 | 20.09324 | 15.66657 | 15.49632 | 20.09324 | 20.09324 |
| 15.60982 | 15.43957 | 20.03648 | 20.14999 | 15.72333 | 15.43957 | 20.09324 | 20.14999 |
| 15.66657 | 15.43957 | 20.09324 | 20.09324 | | | | |
| 15.66657 | 15.43957 | 20.03648 | 20.14999 | | | | |
| 15.60982 | 15.43957 | 20.03648 | 20.09324 | | | | |

The results from the flight (table 9-1, figure 9-1) indicate that minor fluctuations of about 0.1 to 0.15 kPa occurred in the measured air pressure. As a check, upon landing we ran the test and opened the valves (figure 9-2). The pronounced change in air pressure in each valve indicates that a chemical reaction occurred. If a chemical reaction had occurred during microgravity, then little or no reaction would have occurred after landing. Because the time in microgravity was different for different trials (parabolas), the data tables are not all the same length. We do not think that the results were affected by that. The results of control tests performed on the ground are shown in figure 9-3.

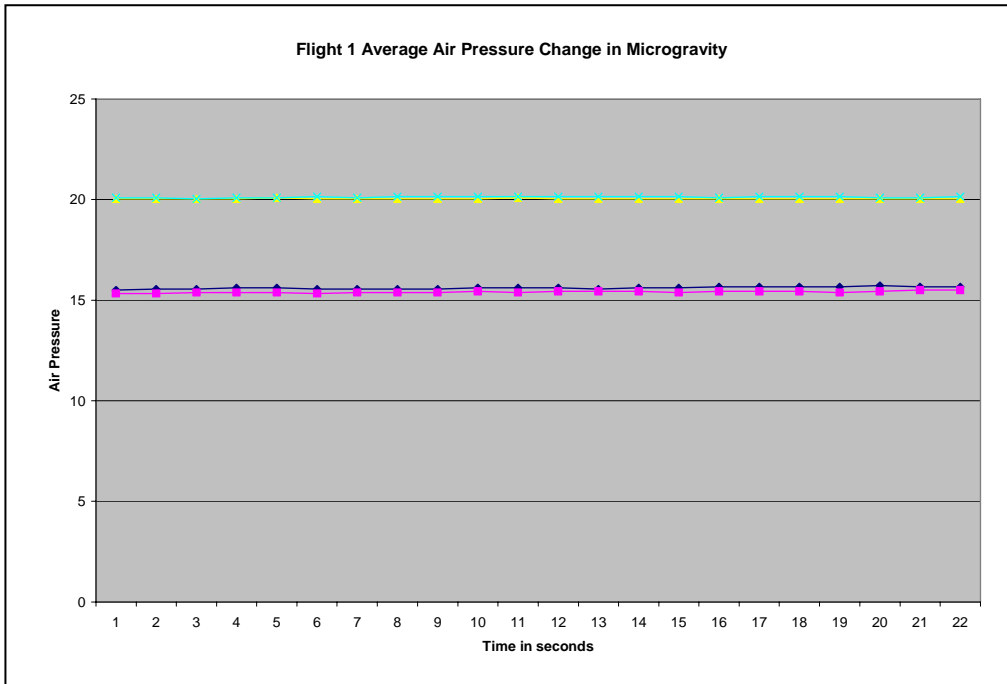


Figure 9-1. Average air pressure (kPa) change on Flight 1 for 4 trials (different symbols and colors).

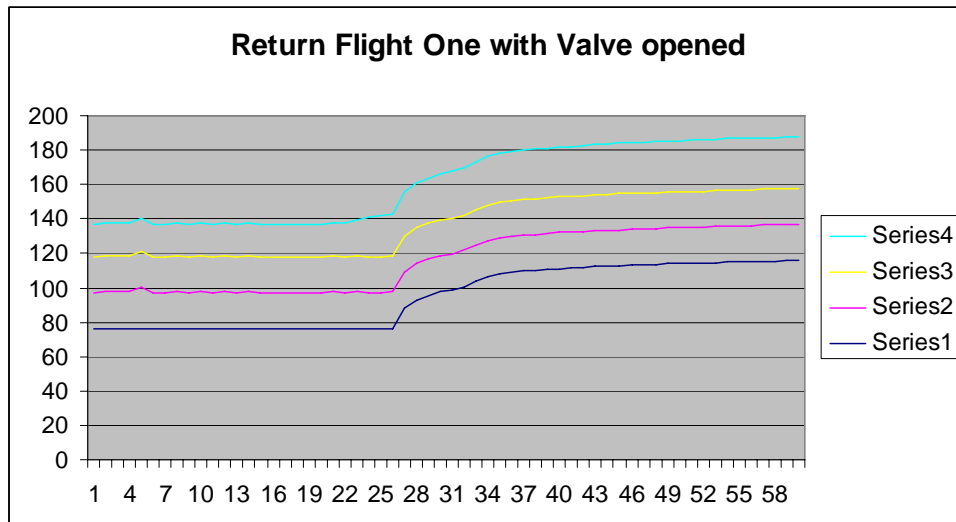


Figure 9-2. Air pressure (kPa) with time (seconds) after Flight 1 for the 4 valves.

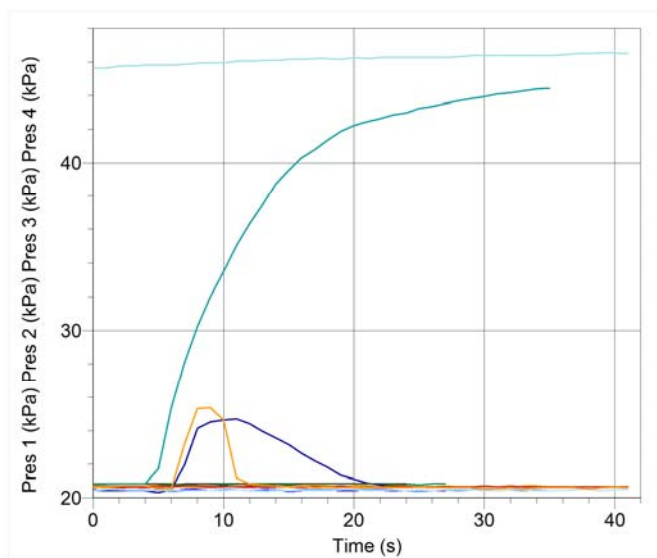


Figure 9-3. Reaction time control test, Earth gravity

DISCUSSION

Although cautioned not to make any changes in procedure the day before the test flight, we worried about the liquid going up into the pressure sensor tube, so we put crimps on each tube. Of course, in all the excitement, the crimps were forgotten and not removed. Immediately upon landing we connected the sensors and opened the valves. The measurement of the change in pressure was dramatic, as shown in figure 9-2. On the second day of the tests, the crimps were removed before the valves were opened and the results were the same.



The only test that indicated a reaction was the tube in which we placed the vinegar on the bottom section and the baking soda in the top section. We decided to change the position of the chemicals because a display, a 2-liter bottle with a cup of colored water in it, which

we had taped on the wall of the plane, showed activity of the liquid when we were in reduced gravity. What we surmise to be capillary action caused the water to spread out and up, and cover the sides of the bottle. We observed “wave action” at the top of the bottle, where the water went quickly to the top and crested over and started down the opposite side.

CONCLUSION

We feel confident in saying that the molecules stayed separated and did not collide, and there was virtually no reaction in microgravity. We think this happened because the liquid was placed in the top section of the tube and that our results would be different if we had placed the liquid on the bottom of the tube. We also think that if we had used more liquid, the results would be different because the liquid could have rebounded from the top with enough energy to send it to the lower half of the tube, where it would then react with the baking soda. The liquid did not stay in a bubble “clump” as we expected. We were envisioning a blob of liquid held together by surface tension floating in the tube. The 2-liter bottle display demonstrated that the liquid behaved differently from the way we expected. However, with the right amount of liquid, in a container of the correct size, a reaction can be avoided in microgravity.

PHOTOGRAPHS

JSC2008E015768
JSC2008E015778
JSC2008E015791 to JSC2008E015792
JSC2008E015796
JSC2008E015804
JSC2008E015825 to JSC2008E015826
JSC2008E015833 to JSC2008E015837
JSC2008E017942
JSC2008E017947
JSC2008E017877
JSC2008E017879 to JSC2008E017881
JSC2008E017888 to JSC2008E017894

VIDEO

- Zero G flight week February 21–27, 2008, Master: 734516

Videos available from Imagery and Publications Office (GS4), NASA JSC.

CONTACT INFORMATION

Phyllis Isbell
5510 Key Peninsula Middle School
Lakebay, WA 98349
253-530-4200
253-530-4256

TITLE

NASA Educator Astronaut Teacher Program – Nutrient Delivery Systems for Plant Growth Chambers in Micro Gravity

FLIGHT DATE

March 11–12, 2008

PRINCIPAL INVESTIGATORS

Daniel John Loewen, Alice Worsley School
Mark Ybarra, Alice Worsley School
Ted Munguia, Alice Worsley School
Mike Parker, Alice Worsley School

CO-INVESTIGATORS

Students at Alice Worsley School, Fresno County Office of Education

NASA MENTORS

Tim Pelischek, NASA Johnson Space Center
Mathew Kiel, Teaching from Space Office



GOAL

The goal of this research project was to build and test a system, researched and designed by students, for nutrient (water) delivery that could be used for plant growth chambers in

a microgravity environment. This goal was developed as part of the student work being done on NASA's plant growth chamber challenge aligned with the educational mission of STS 118.²

The student design team hypothesis stated that the nutrient delivery systems being tested would produce even soil saturation throughout the test chambers. The second hypothesis stated that the student-designed protocols for testing the nutrient delivery system would be effective in microgravity.

OBJECTIVES

The first major question that was addressed focused on the delivery apparatus itself. A system needed to be developed that could effectively deliver water to a plant and evenly saturate the soil being tested under conditions on the ground as well as in a microgravity environment.

The second objective focused on the testing apparatus itself. The design team focused on building a specially designed glove box and internal testing chambers that would effectively test multiple delivery systems for soil saturation and overall effectiveness of the design. Students designed appropriate protocols for laboratory testing that could be translated to short-duration microgravity conditions lasting 25 to 30 s in NASA's C-9 airplane.

The third objective was education. Broadening the minds of the students involved, giving them a deeper understanding of space science and the microgravity environment, was a priority. This objective was aligned with NASA's plant growth chamber challenge.² The students learned the importance of research along with research design, the scientific method, and analysis of experiment results.

METHODS AND MATERIALS

Materials used in the design were simple plastics including syringes, tubes, and fittings with no sharp edges, for student, teacher, and crew safety. The majority of the materials used were purchased from the local Lowe's outdoor and home warehouse and a Target home store. For purpose of safety, non-toxic food coloring was added to pure water and was used to test the delivery systems' effectiveness in microgravity.

After reviewing the literature, the students built 2 variations of a nutrient delivery system. Orbital Technologies Corporation, Orbitec, has completed much research concerning plant growth chambers for microgravity and developed the Space Garden that was flown on STS 118.⁴ The first system built by the students was a single-ring design similar to the Orbitec system used in the Space Garden.⁵ The students built System One using ¼-inch clear plastic tubing with 4 sets of two 1/16-inch holes drilled into its 4 quadrants (figure 10-1). System One had a total volume of 5 milliliters. System Two was developed using the same size tubing and same hole placement as the first system in a double-ring configuration (figure 10-2). System Two had a total volume of 12 milliliters.



Figure 10-1. Design 1, single ring.

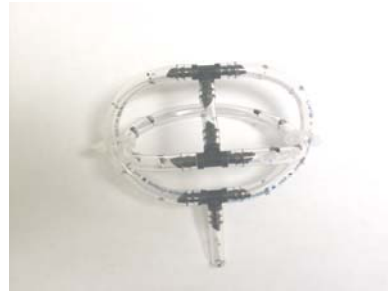


Figure 10-2. Design 2, double ring.

The delivery systems being tested were placed inside specially designed testing chambers and then placed in a specially designed glove box to keep the water in a sealed and safe environment (figures 10-3 and 10-4). The test apparatus flew twice and data were gathered with 2 separate teacher flight teams.

The students developed 3 phases of testing for both ground tests and microgravity tests. A protocol was written for each phase that kept in mind the short duration of microgravity that would be experienced during each parabola. The test protocol was written for 20-s increments and was tested and practiced in the classroom before flight. Redundancy in testing was developed to account for the unique environment of microgravity and to provide for multiple tests.

The objective of phase one was to film the nutrient delivery systems as they functioned in microgravity so further analysis of fluid flow could be completed upon return to the classroom. Using 1100-mL clear, locking food containers, an enclosed system was developed to test each nutrient delivery design. Both delivery systems were filmed against a grid of 1 cm \times 1 cm. Each system was filmed 4 times per flight. The systems were filmed once under martian gravity, once under lunar gravity, and 2 times under microgravity. The systems were filled with 35 mL of water using 35-mL syringes. Each syringe was depressed during a 3-s count (figure 10-3).



Figure 10-3. Video testing chamber.

The objective of phase two was to collect data on soil saturation levels in each system. Each system was tested 2 times per flight. The systems were tested under lunar gravity

and microgravity conditions. Using 850-mL clear, locking food containers, an enclosed system was developed to test each system (figure 10-4). Simple cat litter¹⁰ was used as the test growth medium because of its ability to absorb and hold water. Each container was filled with the test growth medium (cat litter) and the systems were injected with 35 mL of water using 35-mL syringes. Each syringe was depressed during a 3-s count. After the chambers were injected, the dry cat litter was carefully removed, leaving the water-filled cat litter in place around the plastic tubing of the delivery system. This procedure created a 3-dimensional casting of the water dispersal in the chamber, allowing further analysis of the effectiveness of the systems' ability to disperse the water evenly throughout the chamber. Each of these chambers was fitted with a simple moisture meter, purchased from Lowe's home and garden warehouse, as a secondary measure of water saturation in the soil. The meters were placed in such a way as to measure the soil moisture in the center of the plastic rings.



Figure 10-4. Cat litter testing chamber.

The third phase of the testing involved supersaturation of a single-ring design. An 1100-mL container was used and filled with cat litter. The system was filled with 140 mL of water to test for soil saturation patterns. Two moisture meters were fitted to the test chamber, 1 measuring the center of the ring and 1 measuring the outside of the system. Upon return from flight, the dry cat litter was removed from the chamber and the 3-dimensional casting of the water saturation pattern that was created by the cat litter was taken back to the classroom for further analysis. Photographs of the casts were taken and downloaded into a graphics program, with which 3-dimensional outlines of the water dispersion patterns were created for further analysis.¹

RESULTS

Ground testing of the nutrient delivery systems indicated a definite gravity-induced flow pattern. Both the video analysis in phase one and the casting in phase two reinforced the understanding of water percolation under 1 G on the planet Earth, creating a noticeable wedge shape in the cat litter casting (figure 10-5).

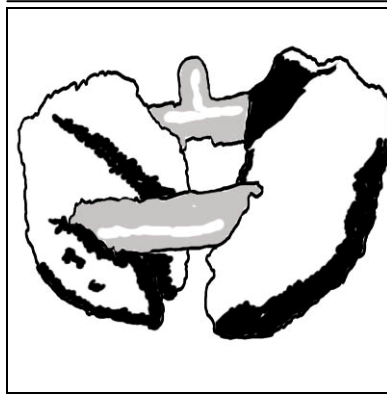


Figure 10-5. Cat litter cast, ground test. Saturated areas are shown in black.

The microgravity video results of phase one showed that although the water drained downward during both martian (38% of Earth) and lunar (1/6g) (11, 12) gravity, this downward drainage caused by the lower levels of gravity occurred much more slowly than under 1-G conditions and allowed fluid to collect around the tubing before it drained downward toward the bottom of the chamber. Bubble formation was observed and documented during testing and during later video analysis. It is unknown what effect these bubbles had on the overall results of the experiment. The casting results from both martian and lunar gravity confirmed the effect of fluid collection around the tubing of the delivery system and revealed no observable or measurable difference between casts from martian or lunar gravity and microgravity. The casts revealed that the fluid created spherical shapes around the delivery systems, with little to no drainage patterns. Periods of hypergravity during the flight did not have any noticeable effect on the formation of the casts. The moisture meters placed in the center of the delivery systems recorded moisture levels of zero. The data also indicated that although no water reached the center of the test chamber, the water dispersed evenly across the dispersal ring (figure 10-6).

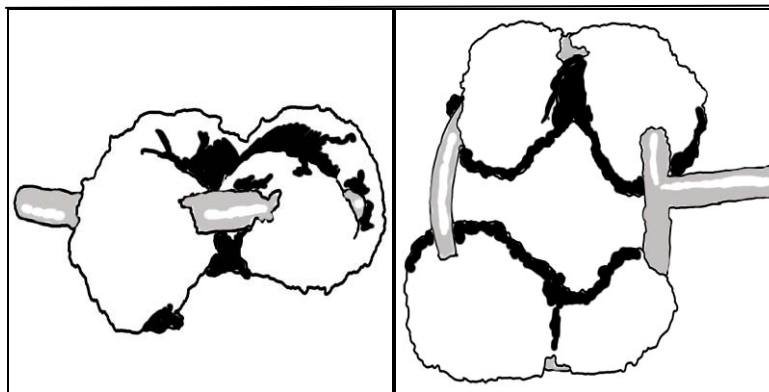


Figure 10-6. Cat litter cast (2 views) in lunar gravity. Saturated areas are shown in black.

The microgravity video results of systems one and two revealed that both systems operated within the expectations of the student design teams. Although bubble formation was again observed and documented during later video analysis, it is currently unknown what effect bubble formation had on the overall results of the experiment. The

microgravity video results revealed fluid absorption around the tubing in a spherical shape with no observable drainage. The castings formed by the cat litter verified these video results and revealed that the fluid created spherical shapes around the delivery systems much like those created during martian and lunar parabolas. Unlike the results during martian and lunar gravity, the systems did not disperse the water evenly throughout the test chamber. As figure 10-7 shows, there is a definite difference in water absorption between the left and right sides of the test delivery system.

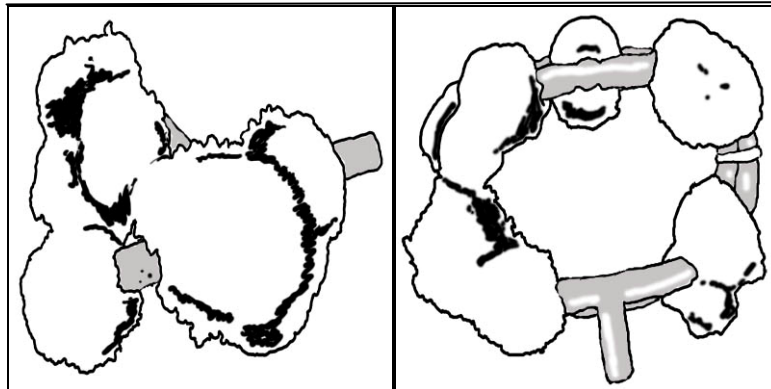


Figure 10-7. Cat litter casting of double-ring design in microgravity. Saturated areas are shown in black.

In phase 3 of the experiment, an 1100-mL chamber full of cat litter was supersaturated with 140 mL of water. The results showed that the water created the same spherical shapes created by phases one and two of the experiment. Moisture meter number 1, located on the outside of the ring, documented a reading of 7 out of 7, confirming that the corners of the chamber had been fully saturated. Moisture meter number 2, located in the center of the ring, indicated a reading of only 3 out of 7, indicating that although water reached the center of the chamber it did not reach full saturation. Once again, just as in phase one under lunar gravity and phase two under microgravity, no noticeable drainage patterns were observed; however, uneven saturation patterns were observed (figure 10-8).

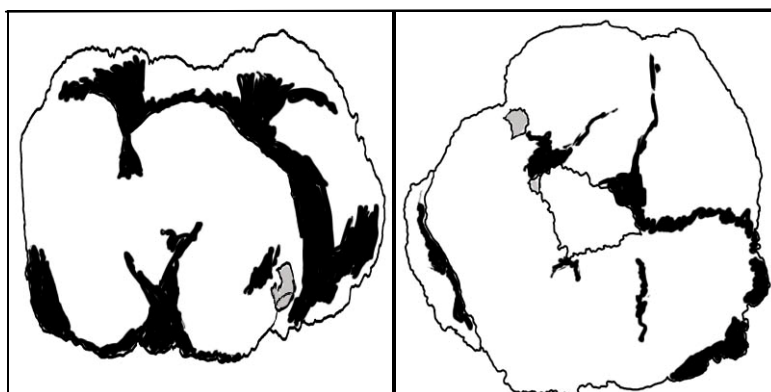


Figure 10-8. Supersaturation of single-ring design in microgravity. Saturated areas are shown in black.

DISCUSSION

It is well understood that some natural processes normal on Earth, such as drainage and percolation, do not occur in the microgravity environment experienced on the International Space Station.^{3, 6, 7, 8, 9} Design and testing teams involved in this research sought to understand how different water delivery systems dispersed water throughout the test chambers. This research team identified 2 outcomes that will need to be addressed when designing plant growth chambers for microgravity. First, proper drainage or water management will need continued research. Second, further research and development will be needed to deliver even saturation throughout the various growth media.

The result found that when 35 mL of water was injected into the system in a microgravity environment, the water gathered around the plastic tubing to form a spherical shape, and wedge-shaped casts were created by the downward flow of water in the test growth medium. These findings address important issues in plant and root health. It is well documented that roots of many plants need to have proper drainage to continue to grow and mature and that improper drainage is the cause of many plant ailments.⁷ The results of the current study showed that the lack of proper drainage in a microgravity environment presents a unique issue in the development of plant growth chamber design as well as development of the systems that supply these chambers with nutrients and water.

As stated in the results, during microgravity testing, the water being delivered gathered around the plastic tubing of the systems in spherical shapes. This result indicates that even saturation was not taking place. The systems did not spread equal amounts of water throughout the test chambers. Moisture meter data, as well as casting data, indicated that 35 mL was not enough water to allow any level of saturation in the center of the test chamber under microgravity conditions. Additionally, both the double-ring and single-ring systems did not produce even fluid flow throughout the test chamber. It is currently unknown why this effect was observed. Further research into the design and further analysis of the data are required to better understand this result. Only when a chamber was supersaturated with 140 mL of water did the moisture meters indicate that the water had indeed reached the center of the delivery ring and the surrounding test growth medium (cat litter) and had evenly dispersed throughout the test chamber.

CONCLUSION

The student design team as well as the teachers involved in this experiment and the C-9 reduced-gravity flight gained new insight and knowledge in the field of microgravity research and the importance of plant growth research for future space flights. This experiment and its results yielded data that require further study. It is the conclusion of the design team that further research is needed to better understand the nature of water dispersal systems in microgravity plant growth chambers. The test growth medium used in this study was clumping cat litter.¹⁰ This material was used because of its ability to hold water and create a 3-dimensional casting of the dispersal patterns of the water being injected into the systems. Data gathered from this experiment on water dispersal using

this type of modeling can lead to the conclusion that the water dispersal was uneven when compared to Earth-based, and lunar and martian gravity data. The design team understands that the water may behave differently in different growth media; thus, continued research in different types of growth media should be conducted along with delivery system testing and research.

The student-designed protocol that was developed for ground testing was adapted by the students and flight team for short-duration microgravity flight. This protocol proved to be very effective, as each portion of the experiment was conducted and successfully completed within the time allotted, thus producing results for further student analysis.

RESOURCES

1. Adobe Creative Suite 2 Photo Shop 2006
2. NASA Engineering Design Challenge, Lunar plant growth chamber, <http://www.nasa.gov/audience/foreducators/plantgrowth/home/>
3. Off-Planet Plants; http://nasaexplores.nasa.gov/search_nav_9_12.php?id=03-014&gl=912
4. Orbital Technologies Corporation (<http://www.orbitec.com>)
5. Orbital Technologies Corporation Space Garden (<http://www.spacegarden.net>)
6. Plants in Space; http://nasaexplores.nasa.gov/search_nav_9_12.php?id=01-048&gl=912
7. Root Problems on Plants in the Garden and Landscape, Stephen Nameth and Jim Chatfield, Ohio State University Fact Sheet, <http://ohioline.osu.edu/hyg-fact/3000/3061.html>
8. Study of Problematic Space Bubbles Electrified, Robert Roy Britt, 11/17/1999, http://www.space.com/scienceastronomy/generalscience/space_bubbles_991117.html
9. The Boiling Blob; http://nasaexplores.nasa.gov/search_nav_9_12.php?id=03-048&gl=912
10. Tidy Cats Scoop Blend for Multiple Cats <http://hpd.nlm.nih.gov/cgi-bin/household/brands?tbl=brands&id=18017002>
11. World Book at NASA, Mars, http://www.nasa.gov/worldbook/mars_worldbook.html
12. World Book at NASA, Moon, http://www.nasa.gov/worldbook/moon_worldbook.html
13. (Personal communication, Dr. Robert N. Bowman Senior Scientist, Lockheed Martin Mission Services, NASA Ames, 10/14/2007)

PHOTOGRAPHS

JSC2008EO24244 to JSC2008EO24248
JSC2008EO24254
JSC2008EO24261
JSC2008EO24268
JSC2008EO25805 to JSC2008EO25806
JSC2008EO25828
JSC2008EO25854 to JSC2008EO25856
JSC2008EO25872 to JSC2008EO25873

VIDEO

- Zero G flight week March 6–15, 2008, Masters: 734532 and 734533

Videos available from Imagery and Publications Office (GS4), NASA JSC.

CONTACT INFORMATION

Project Lead: Daniel Loewen
Alice Worsley School, Fresno, California
Office: (559) 495-3778
dloewen@fcoe.org

TITLE

NASA Educator Astronaut Teacher Program – Capillary Conundrum

FLIGHT DATE

March 11–12, 2008

PRINCIPAL INVESTIGATOR

Cindy Hasselbring, Milan High School

CO-INVESTIGATORS

Wendy Benya, Milan High School

Brad Baden, Milan High School

Alana O’Neal, Milan High School



GOAL

The goal of our experiment was to determine if and how capillary action works under various gravitational force conditions.

OBJECTIVES

- Form a hypothesis about how the diameter of the glass tubing will affect the distance the water travels.
- Form a hypothesis about how the density of the liquid will affect capillary action.
- Explain how gravity affects water.
- Discuss why water rises up a glass tube when the tube is placed in water.
- Explain capillary action.
- Discuss how capillary action acts in plants and explain how plants depend on capillary action.

- Predict the effect of lunar and martian reduced gravity, and hypergravity, on capillary action. (How high will water move up the column in reduced and hypergravity situations compared to normal Earth gravity?)

MATERIALS

- Two sets of 6 glass tubes mounted in 2 troughs
- Plexiglas® covers over trough
- 500 mL of distilled water in each trough
- 25 drops of methyl blue to color water
- 2 video cameras and tapes
- Fluorescent lights
- Transparent grids behind tubes for measurement (in millimeters)
- 10 g granulated plant food

METHODS

After deciding to study the effect of capillary action on plants, we needed to find an efficient way to test the effect of tube diameter and water density that could easily be done in both the classroom and in microgravity aboard the C-9 flight. We elected to use a 6-tube capillary apparatus purchased from Sciencefair.com. Students in the biology and FST (Functions, Statistics, and Trigonometry) classes tested the capillary action of plain distilled water (colored with methyl blue) and distilled colored water with plant food added. We put 500 mL of liquid in the capillary action apparatus and then measured how high the liquid rose in each tube. At first, we measured the height every 30 s for 5 min to see if time had any effect on how high the water rose. We checked the height every 30 s to correlate the results with the time frame for each parabola on the flight. However, we found no height difference between the 30-s check and the 5-min check. We calculated consistent results from the student experiments and also had a chance to see the effect of air bubbles in some of the tubes. Air bubbles in the tubes retarded how high the liquid rose and we were forced to find ways to remove the bubbles. The best way we found was to “flick” the tube to force the bubble up and out. Once all of the data were collected, the FST students used the formula for capillary action to predict what would happen in hyper-, reduced-, and zero-gravity situations.

$$h = \frac{2T}{\rho r g}$$

The above formula is used for capillary action where h = height of liquid, T = surface tension, ρ = density of liquid, r = radius of tube, and g = gravity.¹

The next step was to develop a way to perform the same experiment on board the C-9 flight. The apparatus had to be doubly contained to prevent any liquid from escaping while the plane was in parabolic flight. We also had to be able to see the liquid move while the force of gravity was changing every few seconds. We decided to use Velcro® to fasten our apparatus to the bottom of a clear Plexiglas box, and then placed that box in a second clear Plexiglas box. We attached a grid printed on a plastic transparency behind

each apparatus to enable us to measure the height of the liquid in each tube. Last, we placed the 2 boxes in a third box constructed of Lexan®, plywood, and steel. We mounted two video cameras to record the results and installed backlighting to help us see the liquid move more easily. It was our original intention to take the measurements during the flight, but we found the effects of gravitational changes on our bodies made this difficult to do. We measured our results from DVDs made from the video recordings instead. This allowed us to replay our results slowly and make more accurate measurements.



Figure 11-1. Biology students perform the capillary action lab in class. They are measuring the height of a water column in one of the troughs.



Figure 11-2. The experiment loaded on the plane. In the foreground are video cameras attached to the power source. In the background are the 2 troughs contained in the Plexiglas boxes with backlighting behind them.

We repeated the same experiment under 4 different gravity conditions during the C-9 flight. These were martian gravity, lunar gravity, reduced gravity, and hypergravity. We did the experiment on 2 separate flights and collected data using 2 video cameras. We flew for a total of 64 parabolas: 6 martian, 6 lunar, and 52 reduced gravity. The hypergravity data were collected at the bottom of each parabola.

RESULTS

Students in 5 different classes ran the experiment under Earth gravity conditions. We calculated the average of all of our readings under Earth conditions and then also averaged the results for each of the gravity conditions we experienced on the C-9 flight. The results are shown in tables 11-1 and 11-2, and graphically in figures 11-3 and 11-4.

Table 11-1. Height of distilled water colored with methyl blue in tubes of different diameter under different gravity conditions.

| Gravity Condition | Water height in 0.5 mm tube diameter | Water height in 1.0 mm tube diameter | Water height in 1.5 mm tube diameter | Water height in 2.0 mm tube diameter | Water height in 2.5 mm tube diameter | Water height in 3.0 mm tube diameter |
|----------------------------|--------------------------------------|--------------------------------------|--------------------------------------|--------------------------------------|--------------------------------------|--------------------------------------|
| Hypergravity | 0 mm |
| Earth | 34 mm | 30.2 mm | 15.4 mm | 14.2 mm | 4.3 mm | 2.9 mm |
| Martian | 38 mm | 10 mm | 8.5 mm | 3 mm | 1.5 mm | 1 mm |
| Lunar | 38.5 mm | 14.5 mm | 12 mm | 4 mm | 1 mm | 1 mm |
| Reduced (near zero) | 65+ mm | 51.6 mm | 19.8 mm | 10.8 mm | 2.6 mm | 15.4 mm |

Table 11-2. Height of distilled water with 10 g of plant food and colored with methyl blue, in tubes of different diameter under different gravity conditions.

| Gravity Condition | Water height in 0.5 mm tube diameter | Water height in 1.0 mm tube diameter | Water height in 1.5 mm tube diameter | Water height in 2.0 mm tube diameter | Water height in 2.5 mm tube diameter | Water height in 3.0 mm tube diameter |
|---------------------|--------------------------------------|--------------------------------------|--------------------------------------|--------------------------------------|--------------------------------------|--------------------------------------|
| Hypergravity | 0 mm |
| Earth | 9 mm | 4 mm | 7 mm | 2 mm | 1 mm | 1 mm |
| Martian | 15 mm | 10.5 mm | 10 mm | 5.5 mm | 1 mm | 3.5 mm |
| Lunar | 22 mm | 15 mm | 13 mm | 5 mm | 1 mm | 4 mm |
| Reduced (near zero) | 65+ mm | 17 mm | 41.3 mm | 26.8 mm | 13.4 mm | 32 mm |

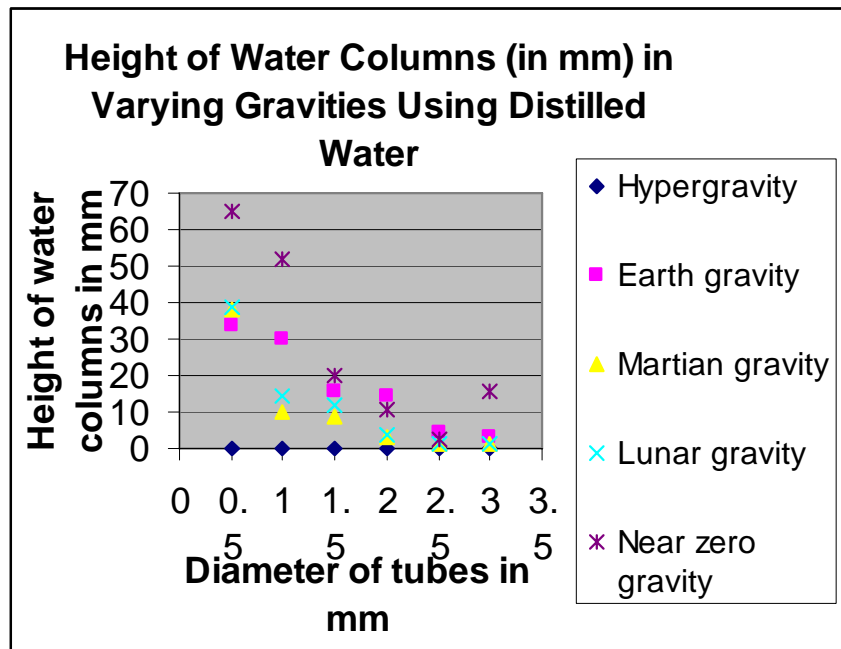


Figure 11-3. Average height of water column in each tube under different gravity conditions.

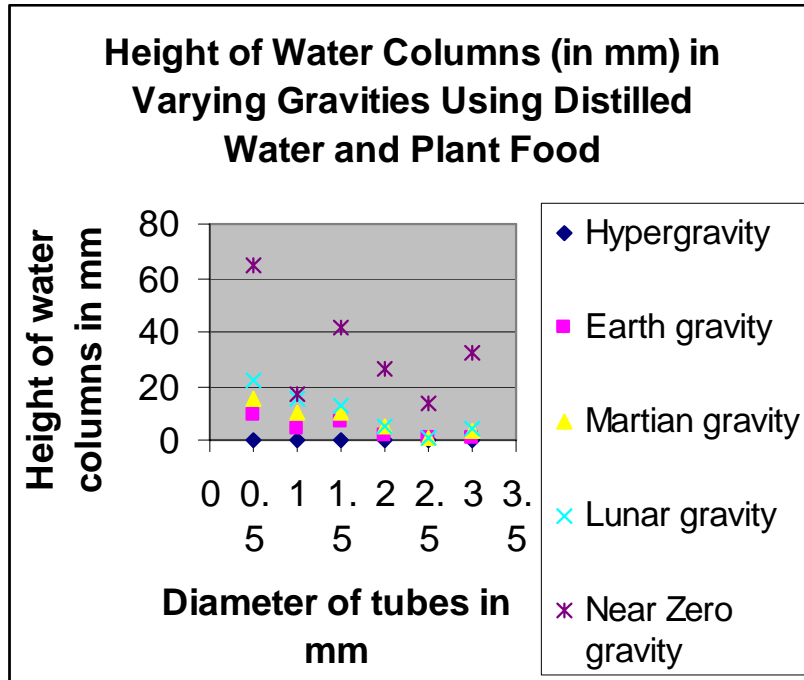


Figure 11-4. Average height of the column of a water and plant food mixture in each tube under different gravity conditions.

DISCUSSION

The Biology and FST classes discovered that in Earth gravity, the larger the diameter of the glass tube, the shorter the height of the water column (figures 11-3 and 11-5).

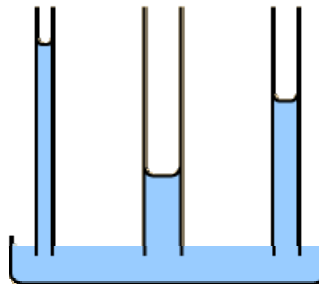


Figure 11-5. In Earth gravity, the larger the diameter of the glass tube, the shorter the height of the water column (<http://hyperphysics.phy-astr.gsu.edu/Hbase/surten2.html>)

The FST classes then predicted the heights of the water columns in various reduced gravities based on the equation for capillary action. We realized that the heights of the water columns would vary indirectly with the specific gravity. As gravity was reduced, the height of the water column would increase. For example, because martian gravity is 1/3 Earth’s gravity, during a martian gravity parabola, the water column should increase to 3 times the height it was in Earth’s gravity. Because the moon’s gravity is 1/6 that of the Earth, the water column’s height should increase 6 times during the lunar parabolas. The students made the prediction that during “zero” gravity, the water in each tube would

go all the way to the top. Although this did not occur in every tube during every “zero gravity” parabola, several water columns did reach the top throughout the course of the flights.

Our data may be somewhat exaggerated by the effects of the flight. The apparatus was strapped to the fuselage and not allowed to experience free fall. This may have decreased the transition period from one gravity condition to the next. In general what we found was that the water column rose higher in reduced gravities than in Earth gravity. The effect of tube diameter and water density also diminished as gravity was reduced. We did notice that fluid in the tubes of 1 mm and 1.5 mm diameter did not move as much as expected because of the formation of air bubbles, which blocked the upward progress of water. We found that in a few parabolas, some water columns rose to the top of the tubes in reduced gravity. However, because of cohesive forces, the water did not escape. In general, the smaller diameter tubes were more prone to air bubbles. The plant food and water mixture tended to go higher than water alone in the larger diameter tubes in reduced gravities. Our data would have been more accurate if we had prevented the formation of air bubbles that prevented water from climbing, using a device such as a screen, as mentioned in other experiments.²

According to our results, in reduced gravity, plants should have no difficulty taking in nutrients through capillary action. Because of this we did not deem it necessary to correlate plant root diameters to the diameters of the tubes used in the experiment. At first glance, it may seem that plants with smaller diameter roots would have more difficulty taking up nutrients, but plants do not have the same problem with air bubbles that we had with the capillary tubes. According to our data, as gravity decreased, the height of the water columns using plant food and water increased more dramatically. The presence of nutrients may enhance capillary action in reduced gravities. This may allow plants to take in nutrients more efficiently. More studies need to be done on long-term plant growth in reduced-gravity environments to see if the lack of gravity affects plant orientation during growth. Many plants are geotropic and grow up in response to gravity. If there is no gravitational pull on the plant, will the plant grow normally if all of its nutrient, water and light needs are met?

REFERENCES

1. <http://hyperphysics.phy-astr.gsu.edu/Hbase/surten2.html>
2. http://www.nasa.gov/mission_pages/station/science/capillary_flow.html

PHOTOGRAPHS

JSC2008EO25288 to JSC2008EO25291
JSC2008EO25799 to JSC2008EO25800
JSC2008EO25872 to JSC2008EO25873
JSC2008EO25862
JSC2008EO25868 to JSC2008EO25869

VIDEO:

- Zero G flight week March 6–15, 2008, Masters: 734532 and 734533

Videos available from Imagery and Publications Office (GS4), NASA JSC.

CONTACT INFORMATION

Cindy L. Hasselbring
Milan High School
200 Big Red Drive
Milan, MI 48160
734-439-5066
hasselbr@milan.k12.mi.us

TITLE

NASA Educator Astronaut Teacher Program – Effect of Microgravity on the Lateral Movement of Hair Cell Bundles (HCB) within the Otolithic Membrane

FLIGHT DATE

March 11–12, 2008

PRINCIPAL INVESTIGATORS

Deepak Ravindranathan, North Carolina School of Science and Mathematics

Eric Xu, North Carolina School of Science and Mathematics

Kevin Li, North Carolina School of Science and Mathematics

Aswin Lingachary, North Carolina School of Science and Mathematics

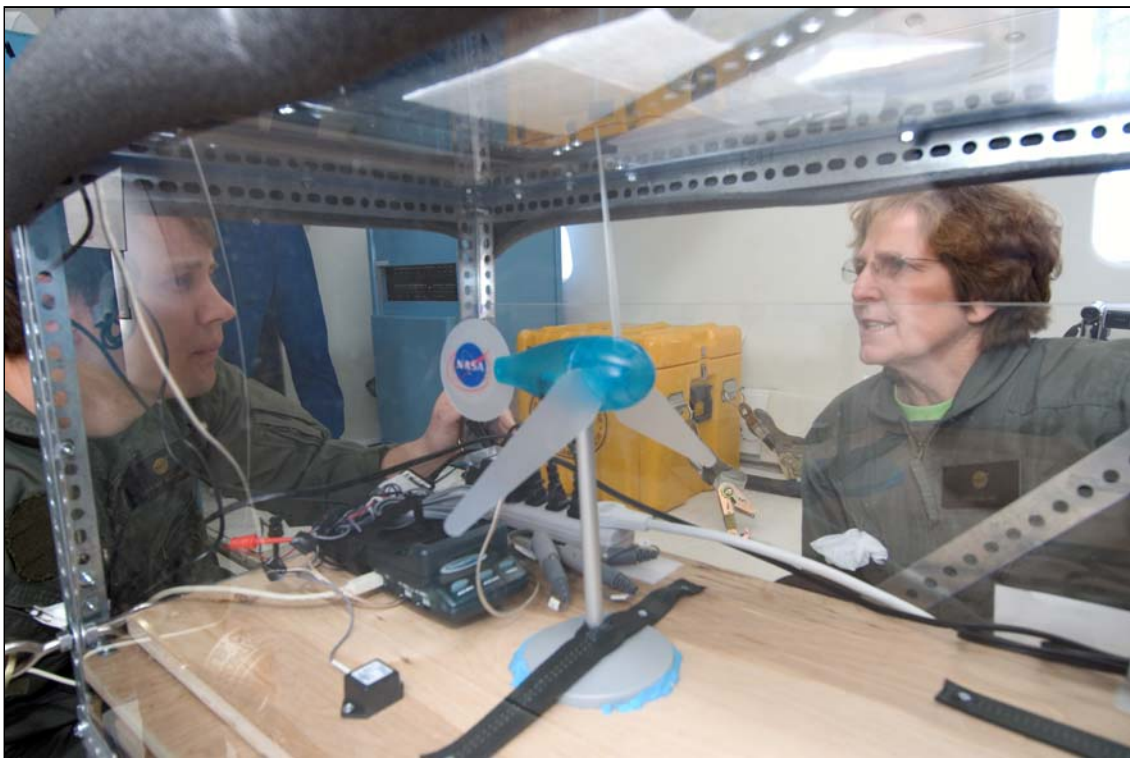
Andrew Guo, North Carolina School of Science and Mathematics

Amy Kim, North Carolina School of Science and Mathematics

Elizabeth Deerhake, North Carolina School of Science and Mathematics

Myra Halpin, North Carolina School of Science and Mathematics

Robert Gotwals, North Carolina School of Science and Mathematics



INTRODUCTION

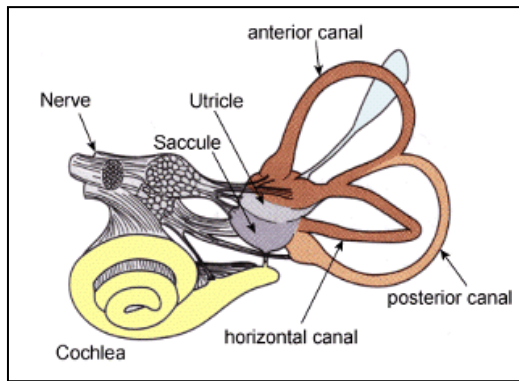
Space Motion Sickness

Space motion sickness is experienced by 60 to 80 percent of space travelers during their first 2 to 3 days in microgravity and by a similar proportion during their first few days after return to Earth. The primary accepted cause of space motion sickness at the beginning and end of space missions is called the sensory conflict hypothesis. Sensory

conflict is thought to arise from a mismatch between expected and actual sensory inputs from the vestibular system. Past research indicates that head movements, especially in the pitch and roll planes, may be the dominant stimuli to induce space motion sickness. Different head movements result in discordant nerve signals that are transmitted from the hair cell bundles (HCBs) to the central nervous system. Then, the central nervous system integrates the disrupted information from both the semicircular canal and the otolithic membrane (OM) to determine the spatial orientation as well as eye and body movements. It is thought that the conflict between vestibular mechanisms of the inner ear and eye movement result in symptoms of space motion sickness.¹

Vestibular System

The bony labyrinth is a system of cavities in the ear that contains sensors for the auditory and vestibular systems of the ear, which are responsible for the sensation of balance. Inside the bony labyrinth is the membranous labyrinth, housing the vestibular system.



The vestibular system is composed of 2 systems, the semicircular canal system and the otolithic organs, as shown in figure 12-1. The otolithic organs consist of 2 membranous sacs called the utricle and the saccule. The utricle is arranged transversely, sensing lateral acceleration, and the saccule is arranged vertically, sensing vertical acceleration. The macula is a thickened gelatinous layer inside each sac. On each macula is a hair bundle made up of neurons from the eighth nerve.

Figure 12-1. Drawing of vestibular system,
<http://www.physpharm.fmd.uwo.ca/undergrad/sensesweb/>

These hair cells project into a gelatinous layer called the otolithic membrane (OM), which contains calcium carbonate crystals. Every time hair cells bend, the tips open and accept K⁺ ions the gel in which they are imbedded. This depolarization releases neurotransmitters from eighth nerve, which consequently sends signals the brain, resulting in the sensation of lateral or vertical acceleration.²

Hair Cell Bundles

Hair cell bundles are responsible for the functioning of the vestibular system. An HCB, located in the OM, consists of stereocilia, which are connected to each other by a system of links. Figure 12-2 shows the

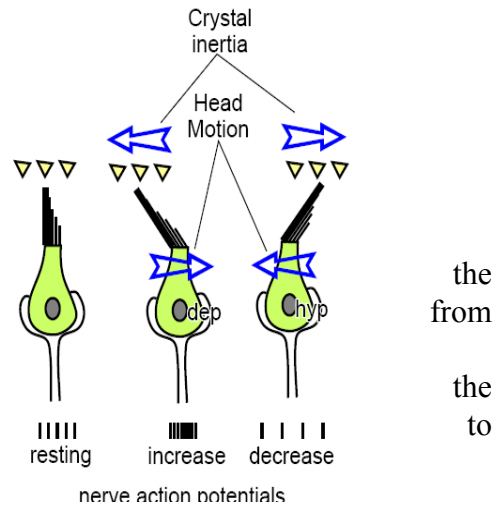


Figure 12-2. Drawing of vestibular system
http://www.physpharm.fmd.uwo.ca/undergrad/sensesweb

displacement of the OM (represented by triangles [crystals]) due to gravity or inertial acceleration that causes the stereocilia (tapered top of each hair cell) to deflect in the direction that the gel moves. The acceleration of the OM causes motion in the HCB relative to the gel. The forces exerted on the HCB due to its interaction with the moving environment result in deformation of the HCB, and cause the stretching or shortening of the special fine strands called tip links. These links are located between shorter and longer stereocilia, and connect their tips. The stereocilia of the HCB have varying heights, so when the HCB is deflected by a force, the links connecting the tips of the stereocilia will open and close. The opening and closing of the tip links regulates the mechano-electrical transduction channels, located in the cell's membrane, which are responsible for gating the transduction current.³

Otolithic Membrane, the Gelatinous Layer

The OM, shown in figure 12-3, into which the HCBs extend, is formed by 2 distinct layers: an upper, gelatinous layer and a lower subcupular "meshwork." While the gelatinous layer is limited to the macula region in the center of the otolith organ, the lower layer covers the entire surface of the otolith organ. The large spaces of the saccule and utricle cavities are filled by endolymph fluid. The OM itself has finely textured "rocks" or calcium carbonate particles, called otoliths, embedded in the gelatinous layer. This upper layer is composed of tightly arranged fibers that provide its gel-like texture. The membrane has a honeycomb structure with openings approximately 5 μm in diameter into which the hair cells extend. The gelatinous layer has been hypothesized to be precipitated from the endolymph fluid while the subcupular meshwork is secreted by sensory epithelium below the otolith membrane.⁴

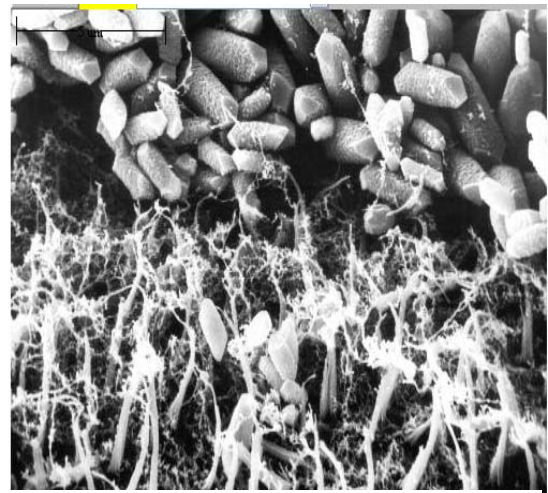


Figure 12-3. Electron micrograph of otolith membrane.

Previous Work

Several studies have been done on ear rocks and how microgravity affects the composition, size, and symmetry of these otoliths. Anken et al. utilized a drop-tower experiment to investigate how microgravity induced motion sickness in fish, using larval cichlid fish. The investigators considered whether asymmetry, which refers to the differences between the left inner ear stones and the right inner ear stones, contributed to whether an organism experiences motion sickness. According to their results, the specimens that experienced motion sickness had greater otolith asymmetry than the specimens that did not exhibit any motion sickness.⁶ Beier investigated whether altered gravity affected the growth of the inner ear otoliths in cichlid fish, and they determined that the otoliths decreased in size and asymmetry after being exposed to low gravity. However, continued investigation is needed to fully conclude whether otoliths play a significant role in inducing motion sickness, particularly in humans.⁷ Previous studies

indicate that utricular function is severely if not completely compromised in individuals lacking calcite ear rocks. The naturally occurring mutant head-tilt mouse completely lacks otoliths in both the utricle and the saccule. Hoffman et al. (2006) aimed to see if afferent synapses were still present in the utricular hair cells of these mice. An absence of synapses would indicate an atrophic relationship between the stimulus of hair cells and the afferent synapse. Utricular function was tested by briefly submerging the mice in water. The normal mice successfully oriented themselves toward the surface of the water and could swim. The mutated mice had no sense of orientation and could only somersault or roll in the water before being rescued. By examining the utricular hair cells of the mice under an electron microscope, the investigators were able to determine that afferent synapses were present even in the complete absence of otoliths. This suggests that the formation and maintenance of hair-cell synapses is not affected by stimulation of hair cells.⁸ Boyle et al. have studied the consequence of exposure to microgravity on the otolith organs using toadfish. In this study, the responses of vestibular nerve afferents supplying the utricular otolith organ to inertial accelerations in 4 toadfish were recorded sequentially for 5 days after 2 NASA Shuttle orbital flights. The results indicated that the magnitude of response to an applied movement was on average 3 times greater than for controls within the first day after landing. The conclusion stated that the reduced gravitational acceleration in orbit induced an increased sensitivity of utricular afferents. By 30 hours after landing, the responses of flown toadfish were statistically similar to those of controls. The time recorded for the nerve afferents to return to normal sensitivity corresponded to the reported time that astronauts took to recover from vestibular disorientation.⁹

While previous researchers using live organisms have investigated the effects of microgravity on vestibular nerve afferents, we propose a novel investigation of HCB movements in microgravity. In association with studies involving organisms, lateral acceleration data will elucidate the mechanisms of space motion sickness. The purpose of this study is to determine how reduced gravitational fields affect the vestibular system and cause motion sickness by constructing a scale model of the macula and exposing it to a microgravity environment.

METHODS AND MATERIALS

For this study, we constructed an enlarged model of the vestibular system on a scale of 1 to 10^6 . In this model, 2 layers of gel that represented the OM were placed in a plastic container into which the HCB simulants extended. The HCB simulants were fiber optics fibers, which extended through the gel into the container from the bottom.

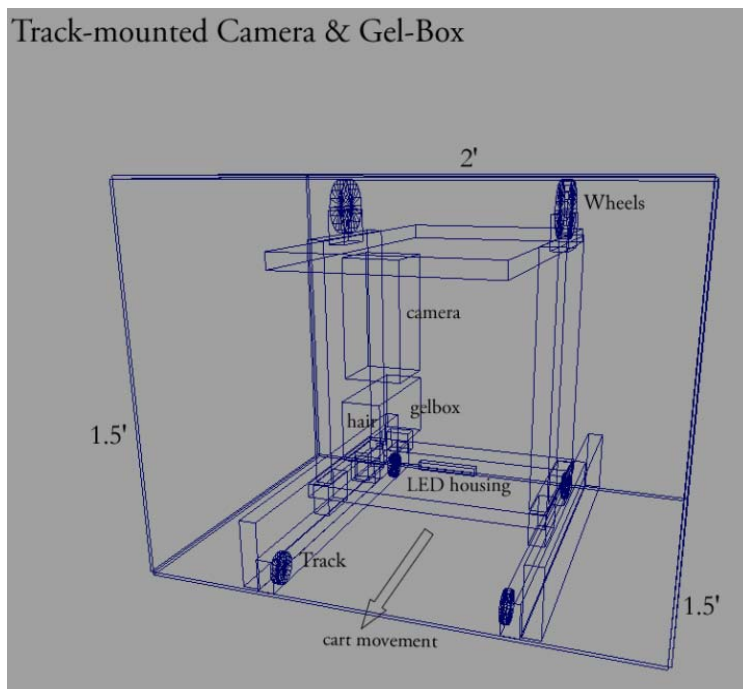


Figure 12.4. Computer-generated picture of the model of a macula

A red light-emitting diode (LED) was placed adjacent to the ends of the fibers beneath the box, to illuminate the tips of the fibers in the superior layer of gel. This was thought to provide a means of measuring the movement of the HCB simulants when the model underwent lateral acceleration. A digital video camera was suspended above the gel box and mounted in the model, as can be seen in figure 12-4. A small grid, with 0.5-cm blocks, was placed under the gel box to provide the reference scale. The lateral acceleration of the OM was modeled using a movable container, shown in figure 12-4. The dimensions of the exterior box that was placed in the payload were 16" × 15" × 12.5". In this exterior box was a second container open on 2 sides. The interior box was able to move laterally on drawer tracks within the exterior box. This simulated the lateral acceleration of the utricle in the human head. The model of the OM moved perpendicular to the direction of the plane, ensuring that lateral acceleration, not acceleration due to the movement of the aircraft, was measured by the accelerometer. Acceleration measurements were taken using a low-G accelerometer linked to a laptop computer outside the box, and data were collected using LoggerPro software.

Synthesis of Copolyacrylamide-Acrylate Polymer Gel

To model the OM, 2 copolyacrylamide-acrylate polymer gels with varying viscosities were synthesized. Because the OM contains 2 gel-like layers in which the more viscous layer floats on top of the less viscous layer, 2 different protocols were utilized to synthesize each gel layer. To synthesize the top layer, 0.9000 g of sodium acrylate (97%, Aldrich), 2.8450 grams of acrylamide (Fisher Scientific), and 0.1550 g of N, N'-methylene bisacrylamide (99%, Aldrich) were added to 30 mL of distilled water in a 100-mL beaker. Then the reagents were dissolved using a Fisher Scientific sonicator and

constant stirring. When all the reagents were completely solvated, 0.05 g of ammonium peroxy-disulfate (Fisher Scientific) was added. The solution was then transferred into the plastic gel box in a water bath of temperature around 50 to 60 °C. Then, 0.05 g of sodium sulfite (Fisher Scientific) was added while the solution was gently stirred, and gelation occurred almost immediately. After gelation, the box was removed from the water bath and cooled to room temperature. The bottom layer was synthesized by first adding 2.7000 g of sodium acrylate (97%, Aldrich), 8.5350 g of acrylamide (Fisher Scientific), and 0.4650 g of N, N'-methylene bisacrylamide (99%, Aldrich) to 210 mL of distilled water in a 500-mL beaker. Then the reagents were dissolved using a Fisher Scientific sonicator and constant stirring. Once all the reagents were completely solvated, 0.15 g of ammonium peroxydisulfate (Fisher Scientific) was added. The solution was transferred into the plastic gel box in a water bath of temperature around 50 to 60 °C. Then 0.15 g of sodium sulfite (Fisher Scientific) was added while the solution was gently stirred. Gelation occurred almost immediately. After gelation, the box was removed from the water bath and cooled to room temperature. After the gel layers were successfully synthesized, the top layer gel was transferred on top of the bottom layer gel.



Figure 12.5. Photograph of the pebbles embedded on the top layer.

Pebbles that had a density similar to that of the calcite rocks, were placed on the top layer of the gel (figure 12-5). These pebbles provided mass to the top layer and increased the lateral inertia of the gel when it moved laterally.

The model was flown on 2 separate flights of the C-9 microgravity aircraft. Video footage was captured on each flight. Using the Logger Pro image analysis software, the pebbles were used as reference points to record displacement. Only the video segments that displayed movement of the pebbles in microgravity were chosen. The intended method was to analyze the movement of the red-illuminated optic fibers, but for the most part, it was very difficult to see this in the video. Thus, it was appropriate to use the pebbles as a measure of movement.

Data Analysis

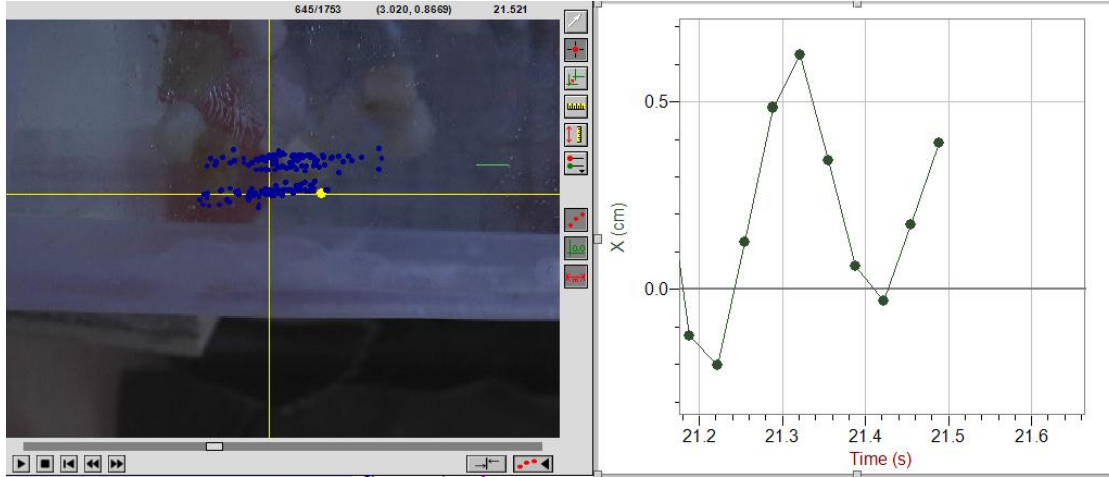


Figure 12-6. A screenshot of the video analysis software.

Video analysis software, which showed the position of the pebbles and a graph showing their displacement (figure 12-6), was used to analyze the data. The left half of the screenshot displays blue dots, which are the positions of one chosen pebble at each frame. The grid is used to provide scaling for the picture. Each block on the grid represents 1 centimeter. A yellow axis is used to generate a graph (right half of the screenshot), which shows the horizontal displacement, X (cm), of the pebble.

RESULTS

The numerical data from table 12-1 establish that movement of the pebbles and gel occurred in microgravity. The following data describe the movement of the pebbles on the gel. In flight 1, the pebbles had an average displacement of 0.3904 cm, and in flight 2, they had an average displacement of 0.5978 cm. The graphs of data points reflecting the position of the pebbles showed trends of oscillation. The periods of time in which data points changed in one direction indicated linear acceleration of the pebbles. The calculated standard deviations also indicated that, for each flight, the displacements had relatively low variability. The average for the second flight, on which more pebbles were added, was higher than the average for the first flight.

Table 12-1. Displacement of the pebbles on Flight 1 and Flight 2.

| Flight 1 Video 3 | cm | Average (cm) | Flight 1 Video 4 | cm | Average (cm) | Flight 2 Video 2 | cm | Average (cm) |
|---------------------|--------|-----------------|---------------------|--------|-----------------|---------------------|--------|-----------------|
| Section 1 | 19.5 | 20.5 | Section 1 | 10.04 | 10.6 | Section 1 | 4.07 | 4.673 |
| Min | 0 | | Min | -0.14 | | Min | -0.074 | |
| Max | 0.395 | | Max | 0.279 | | Max | 0.543 | |
| Displacement | 0.395 | | Displacement | 0.419 | | Displacement | 0.617 | |
| Section 2 | 22.1 | 23.1 | Section 2 | 11.16 | 11.271 | Section 2 | 5.506 | 6.006 |
| Min | -0.007 | | Min | -0.044 | | Min | -0.217 | |
| Max | 0.55 | | Max | 0.333 | | Max | 0.237 | |

| | | | | | | | | |
|---------------------|--------|------|---------------------------------------|---------|------|---------------------|--------|--------|
| Displacement | 0.557 | | Displacement | 0.377 | | Displacement | 0.454 | |
| Section 3 | 24.2 | 25.2 | Section 3 | 3.94 | 4.31 | Section 3 | 18.182 | 18.483 |
| Min | 0.063 | | Min | -0.071 | | Min | -0.125 | |
| Max | 0.43 | | Max | 0.231 | | Max | 0.55 | |
| Displacement | 0.367 | | Displacement | 0.302 | | Displacement | 0.675 | |
| Section 4 | 26.4 | 27.1 | Section 4 | 5.64 | 5.81 | Section 4 | 19.52 | 20.019 |
| Min | 0.029 | | Min | -0.0285 | | Min | 0.046 | |
| Max | 0.342 | | Max | 0.186 | | Max | 0.6 | |
| Displacement | 0.342 | | Displacement | 0.2145 | | Displacement | 0.554 | |
| Section 5 | 28.1 | 28.6 | Section 5 | 7.11 | 7.24 | Section 5 | 21.22 | 21.487 |
| Min | 0.064 | | Min | -0.228 | | Min | -0.206 | |
| Max | 0.355 | | Max | 0.174 | | Max | 0.393 | |
| Displacement | 0.291 | | Displacement | 0.402 | | Displacement | 0.599 | |
| | | | | | | | | |
| Average | 0.3904 | | Average | 0.3429 | | Average | 0.5798 | |
| | | | | | | | | |
| | | | Average for Microgravity (cm): | | | | | |
| | | | 0.4377 | | | | | |

DISCUSSION AND CONCLUSION

The results show that movement of otolithic rocks occurred in the simulated vestibular system in a state of microgravity. However, it was expected that, because of microgravity, the pebbles would float rather than remain embedded in the surface of the gel. This did not occur, and the pebbles stayed on the gel and exhibited only lateral displacement in microgravity with the gel. In addition, an increase in the mass of the pebbles caused an increase in displacement of the pebbles. This may be due to the fact that the added mass of the pebbles increased the inertia of the top of the gel. Thus, when the gel system linearly accelerated, the top portion of the gel accelerated more slowly, but resulted in an increase in displacement of the pebbles in reference to the gel system. Since the tips of the fiber optic hairs moved in conjunction with the pebbles and the top gel layer, increasing the total mass of the pebbles increased the displacement of the fiber hairs as well.

It could be said that the mass of the rocks in each ear may be one factor in determining why different people have different experiences with space adaptation. The movement of the gel, which in turn caused the movement of both the pebbles and the fiber optic HCB in the inner ear model, indicated that head movements may be the dominant stimulus for causing space motion sickness.

Although this research was not able to fully explain the problem of motion sickness, several further investigations can be conducted to study this problem. Research needs to be conducted to determine if indeed the pebbles rise above the gel. In addition, plans include constructing a model of the macula of the saccule, to be positioned perpendicular to the model of the utricular macula. We also want to use potentiometers as part of the model to measure voltage, since this would give a much better understanding of the movement of pebbles and gel.

ACKNOWLEDGMENTS

We would like to thank the NASA Reduced-Gravity Program for their approval of this project and for providing the C-9 microgravity flights to help conduct these experiments. We would also like to thank Wyle's Ms. Rachel Brady for her guidance and supervision of this project. Our thanks are also due to Dr. Myra Halpin and Mr. Robert Gotwals for writing the proposal, supervising the construction of the model, providing the necessary materials, editing the paper, and conducting the actual experimentation on the microgravity flights. We would also like to extend our appreciation to the students in the NCSSM Research in Chemistry class for all their contributions, as this project would not have been possible without them.

REFERENCES

1. Heer, Martina and William Paloski. "Space motion sickness: Incidence, etiology, and countermeasures." Autonomic Neuroscience: Basic and Clinical. 129 (2006) 77-79.
2. "Lecture 10 – Balance." The Physiology of the Senses: Transformations for Perception and Action. <http://www.physpharm.fmd.uwo.ca/undergrad/sensesweb/>
3. Kondrachuk, Alexander V. "Models of otolithic membrane-hair cell bundle interaction." Hearing Research. 166 (2002) 96-112.
4. Saitoh, Setsuo and Juro Yamada. "Ultrastructure of the Sacculus Epithelium and the Otolithic Membrane in Relation to Otolith Growth in Tilapia, *Oreochromis niloticus*." Transactions of the American Microscopical Society. 108 (1989).
5. Kondrachuk, Alexander V. "Models of otolithic membrane-hair cell bundle interaction." Hearing Research. 166 (2002) 96-112.
6. Anken, R., et al. "Otolith asymmetry and kinetotic behavior of fish at high-quality microgravity: A drop-tower experiment." Advances in Space Research. 38 (2006) 1032-1036.
7. Beier, M., et al. "Effect of hypergravity on carboanhydrase reactivity in inner ear inocytes of developing cichlid fish" Advances in Space Research. 33 (2004) 1386-1389.
8. Hoffman, Larry F., et al. "Afferent synapses are present in utricular hair cells from otoconia-deficient mice." Hearing Research. 222 (2006) 35-42.
9. Boyle, Richard, Allen F. Mensinger, Kaoru Yoshida, Shiro Usui, Anthony Intravaia, Timothy Tricas, and Stephen M. Highstein. Neural Readaptation to Earth's Gravity Following Return From Space. J. Neurophysiol. 86: 2118-2122, 2001.

PHOTOGRAPHS:

JSC2008EO25205

JSC2008EO25210 to JSC2008EO25218

JSC2008EO25236

JSC2008EO25221

JSC2008EO25224 to JSC2008EO25226

JSC2008EO25794
JSC2008EO25796 to JSC2008EO25798
JSC2008EO25801 to JSC2008EO25803
JSC2008EO25872 to JSC2008EO25873

VIDEO:

- Zero G flight week March 6–15, 2008, Masters: 734532 and 734533

Videos available from Imagery and Publications Office (GS4), NASA JSC.

CONTACT INFORMATION

Dr. Myra Halpin
North Carolina School of Science and Mathematics
1219 Broad Street
Durham, North Carolina 27705
919-416-2764
halpin@ncssm.edu

TITLE

NASA Educator Astronaut Teacher Program – The Effects of Microgravity on the Motion of Stereocilia in the Semi-Circular Canals of the Inner Ear

FLIGHT DATE

March 11–12, 2008

PRINCIPAL INVESTIGATORS

Patrick Tenorio, North Carolina School of Science and Mathematics
Jonell Watson, North Carolina School of Science and Mathematics
Saji Wickramasekara, North Carolina School of Science and Mathematics
Darren Zhu, North Carolina School of Science and Mathematics
Myra Halpin, North Carolina School of Science and Mathematics
Robert Gotwals, North Carolina School of Science and Mathematics



INTRODUCTION

The human vestibular system is responsible for helping the body maintain balance.⁴ It is found in the ear and consists of 2 primary receptor systems: the semicircular canals, and the utricle and saccule.³ The utricle and saccule measure linear acceleration through the shifting of hairs in a gel, while the semicircular canals measure angular acceleration (any tilting of the head) through the sloshing of fluid against hairs at the ends of the canals' tubes. The information obtained through the vestibular system is transmitted to the brain through nerve fibers attached to the hairs, and controls subconscious behaviors such as

the vestibulo-ocular reflex,³ which allows the eyes to stay fixed on a distant object should the head move.

The vestibular system evolved in Earth's gravity (1-G environment). Its function is impaired when the body is exposed to dramatically different magnitudes of gravitational acceleration, as is the case with astronauts in space. Information from the system conflicts with that obtained visually, resulting in disorientation and motion sickness.

Exploration of the effects of reduced gravitational environments on the human vestibular system could provide scientists with greater knowledge of the physical mechanisms in the ear that cause alterations in human visual perception. A greater understanding of the functions of the vestibular system has the potential for improving motor functions and mobility for humans in response to information obtained visually. In particular, this could significantly aid astronauts in reducing symptoms of dizziness and motion sickness, allowing greater ease in living and working in microgravity environments.⁸

Background on the Vestibular System

The vestibular system of the inner ear, composed of 3 mutually orthogonal semicircular canals and the otolith organs, maintains balance through determination of acceleration and body position.¹ Specifically, angular acceleration is detected by the semicircular canals²; while linear acceleration is determined by the otolith organs, and the canals and otolith organs together give the body a sense of position and balance.

Each of the 3 semicircular canals is positioned orthogonally to the others; thus the canals are able to identify body movements along all 3 axes,⁷ with the lateral canal detecting rotation about the y-axis, the superior canal detecting rotation about the x-axis, and the posterior canal detecting rotation about the z-axis. Each of these canals is filled with a fluid called endolymph, which is primarily a mixture of Na⁺, K⁺, and Cl⁻ ions,⁶ and is lined with a mucous substance. At the end of the canals is a bulblike structure, the ampulla, which leads into the utricle.¹

Inside each ampulla is a bundle of hair cells, known the stereocilia, which project up together into a mucous membrane known as the cupula.⁷ When angular acceleration occurs, the inertia of the endolymph causes the hair bundles to move accordingly, sending a signal to neurons on the other side of the hair bundles and allowing the brain to determine both the magnitude and direction of acceleration.^{2,5} Interestingly, these hair bundles move only when angular acceleration or deceleration first occurs; if a constant angular acceleration is maintained, then the hair bundles “relax” – thus, when one suddenly stops after constant angular acceleration, the hair cells are significantly directed in an opposite direction, causing dizziness, as a result of the sudden, subsequent neuron signal.⁷ In addition, recent studies have shown that the vestibular system is also able to differentiate between passive and active head movements, such as entire body rotations versus solely head rotations, respectively, although the underlying mechanisms of this process remain undetermined.²

Studies have shown that several factors contribute to the signals sent by the semicircular canals. First, research has shown that semicircular canals are nearly the same size in all animals, perhaps indicating that the particular dimensions of the canals may be either special or optimized for their function.⁷ Furthermore, the canals have particular size ratios in comparison to each other, which also may indicate the role of size in functionality. The composition of the endolymph and the amount of it contained in the canals also seems to serve some type of utility, as variations of endolymph have been found to result in such symptoms as vertigo and dizziness.⁵

Background on Motion Sickness

Motion sickness is most commonly attributed to a disruption or misinterpretation of the conduction of neural transmissions between the vestibular systems of the inner ear and the brain. In particular, it occurs when sensory inputs contradict the brain's prediction based on past experience.⁴

Because altered gravitational fields affect how fluid behaves in the vestibular systems of the inner ear, they can lead to motion sickness and its symptoms, including nausea, vomiting, mild vertigo, dizziness, cold sweating, and "reduction of orthostatic tolerance," or the inability to maintain an erect standing posture.⁴ Thus, most astronauts who are subjected to micro- or hypergravity display these characteristics, even after only short periods in space. Space flight-induced motion sickness can pose a substantial threat to the safety of astronauts or others who participate in space flights because it disrupts their normal functions and reaction times. In case of emergency, some who are more sensitive may be unable to react or function properly and be in danger because of it.

The 2 major proposed hypotheses concerning the cause of motion sickness in space are the fluid shift hypothesis and the sensory conflict hypothesis.⁸ The fluid shift hypothesis explains the imbalance in the vestibular system on the basis of fluid loss and cerebral blood flow. However, this hypothesis has been largely discounted because simulation models, such as lying in a bed tilted with the head down, do not cause the main space motion sickness symptoms.

The second hypothesis, the sensory conflict hypothesis, explains vestibular imbalance on the basis of the loss of signals usually sent by otolith organs. Because of the change in gravity, the otolith organs are tilted differently, and the loss of normal tilt signals causes a conflict in anticipated and actual otolith signals.⁸ These changes are particularly obvious in the pitch and roll planes and result in discordant signals during the integration of the angular acceleration signals from the semicircular canals and the linear acceleration and gravity signals from the otolith organs. This integration usually maintains spatial orientation and stabilizes eye and body movements.

Though all of the causes of motion sickness are not fully known, there is speculation that both cerebral blood flow and gastrointestinal hormone release may have impacts on space-induced motion sickness. After exposure to nauseogenic stimuli, such as spinning chairs or centrifuges, subjects who develop nausea show a considerable decrease in

cerebral blood flow and pancreatic polypeptide, and an increase in blood pressure and intestinal secretions.³ Though these hypothesized factors may contribute to the development of motion sickness, there is not enough experimental evidence to fully support them.

Because motion sickness in space can cause potentially detrimental effects on astronauts and others who are subjected to altered gravitational fields, various methods of preventing its development have been utilized, administered both orally and intramuscularly. However, most pharmaceuticals used for motion sickness create undesirable effects such as drowsiness and sedation. In recent experimental research, the use of virtual reality training has proved fairly effective in preparing astronauts or cosmonauts for space travel by simulating sensory conflicts that mimic those that occur in space.³

Procedure



A model of the semicircular canals was created from Tygon tubing with a $\frac{5}{8}$ -inch outer diameter and $\frac{1}{2}$ -inch inner diameter mounted onto a 9.0 cm \times 3.0 cm \times 3.7 cm block in the center of a wooden base. To simplify data collection, the model was scaled to be 15.9 times larger than the actual human semicircular canals. The 1:15.9 scale ratio was calculated by measuring the inner diameter of the Tygon tubing and determining the actual diameter of the canals found in the inner ear. The

lengths of each the 3 semicircular canals were also found: 12 mm for the lateral canal, 18 mm for the posterior canal, and 15 mm for the superior canal. Using the same scale ratio as for the inner diameter, the canal lengths were scaled to 190.50 mm for the lateral, 285.75 mm for the posterior, and 238.125 mm for the superior.



Once the Tygon tubing was measured and cut, the ampulla of each canal, the part containing the cilia that sends information to the brain about movement, was created by expanding a specific end of the canal. This was achieved by clamping one end of the tube shut and stopping the other except for a small plastic hose connecting the tubing to an argon gas pump. First, the end of the Tygon tubing determined to be the ampulla was softened in a hot water bath, and the whole tube was pumped with argon gas between

14 and 18 psi to create a bulbous swelling analogous to that found in the semicircular canals. In these bulbs, cilia, made from strings about 1 inch long, were placed inside using sealant. The semicircular canals were then attached to a larger, thicker, swollen Tygon tube, representing the utricle.

Though in the vestibular system a lining of mucus lies between the vascular fluid and the outer membranes, this was not included in this experiment because of the lack of sufficient information about its composition. The entire model was consequently filled with a solution of 1 mM NaCl, 130 mM KCl, and 30 mM KHCO₃ to model the composition of the endolymph. This resulted in a solution containing 1mM Na⁺, 160 mM K⁺, 131 mM Cl⁻, and 30 mM KCO₃⁻.

To monitor the movement of the cilia, 3 video cameras, each focused on a distinct set of cilia, were utilized. The cameras were mounted on 7.2 cm × 17.8 cm × 1.7 cm wooden block bases and aimed at their respective bulbs via furniture hinges. The use of furniture hinges allowed the adjustment of angles used to observe the cilia.

As a control, the experiment was simulated under normal gravitational conditions. To do so, the semicircular canals were rotated in each of the 3 dimensions in a normal 1-G environment, so that we could observe how each of the hair bundles acts under normal conditions. The cameras were used here to record movement of the cilia.

In microgravity, the cameras were again used to record movement of the cilia for the duration of the flight, but this time the movement came from the plane itself, and not manipulation of any one canal. After the operators placed the board with the canals into the containment box, they turned the video cameras on. During the flight, they verbally indicated their position in the parabola, and the audio feed from the videos taken served as time markers for the different positions of the plane and levels of reduced gravity. The cameras were synchronized with one another and analyzed in accordance with data from the accelerometer that was also being flown.

All video data were transferred to a computer and processed using image analysis software. The use of software capable of frame-by-frame manipulation enabled quantitative determination of the displacement of each set of stereocilia. We expect that a comparison with ground data sets that have undergone similar analysis will yield a mathematical model of the effects of microgravity on the movement of the cilia.

RESULTS AND DISCUSSION

The lateral and posterior semicircular canals, which had red and green hairs, displayed minimal hair movement during flight. However, the superior semicircular canal, which had black hairs, displayed significant movement in 70- to 80-s intervals except for certain 2- to 4-min intervals when the plane was changing direction. This movement may be attributed to the contact of the hair clusters and the gas bubbles during the times when the gas bubbles moved. Since the superior semicircular canal was the highest positioned canal in the model, most of the air bubbles stayed in this canal. For this reason, the

interaction between the gas bubbles and the hair clusters may be the sole cause of any hair movement found in the canals. For example, consider the position of the air bubble at 6-s intervals from 9:40 min into flight and 10:05 min into flight (figure 13-1).



Figure 13-1. Movement of an air bubble in the semicircular canal model.

In the beginning frame (1), the air bubble is more spread out and lies on the right side of the canal, away from the hair cluster. As the position of the air bubble moves to the position shown in the last frame, the air bubble almost completely encloses the hair cluster, forming a more spherical shape. This movement of the air bubble is thought to be the cause of the significant hair movement that was seen through these times.

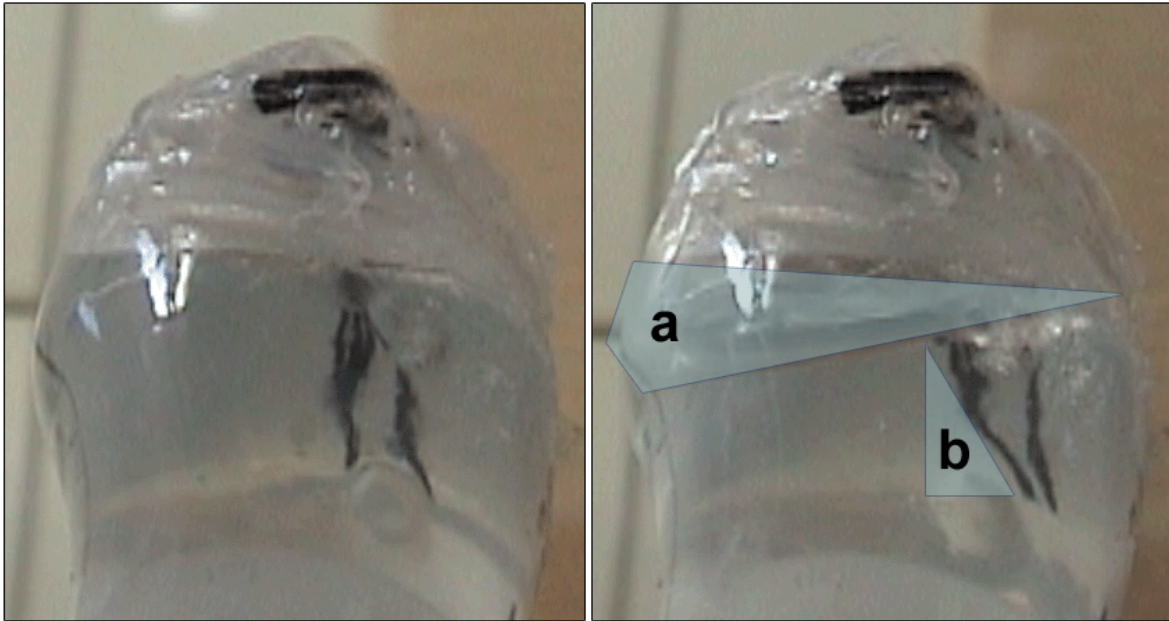


Figure 13-2. Area a represents the change in water level between the times when the water bubble is spread out and when the water bubble is spherical. Area b represents the displacement of the hairs at the same time. The correlation between the movement of the water bubble and movement of the hair supports our conclusion.

This may be attributed to the air bubbles being more likely to be present in the superior canal since it was the canal positioned highest in the model. In the photos of all 3 canals, the posterior and lateral canals showed no significant air bubbles, and probably as a result, there was no movement. This may not be just because of the height of the superior canal, but also because of the angle of the superior canal. All 3 canals were positioned orthogonally to each other, so perhaps the angle of the superior canal allowed air bubbles to exist in the fluid near the cluster of hairs.

We can interpret the movement of the air bubbles as a model for the movement of the dissolved gases in the ear. The hair clusters moved with the bubble when it changed position. More specifically, the bubble's position depended on the position of the plane. At intervals it turns around (for up to 7 min each time), and these intervals corresponded to times when the hair clusters did not move. For example, no movement was observed between 33:50 and 40:00 for the black hair cluster. This matches the turn-around at this time. This also makes sense because there were no visible pockets of air near the green or red hair clusters. We can conclude that the hair clusters moved because of the air pockets in the canals, and because an air pocket was near the black hair cluster, the cluster moved.

CONCLUSION

Space adaptation syndrome is a form of motion sickness, the cause of which is attributed to the vestibular system of the inner ear. More specifically, problems arise from the 3 mutually orthogonal semicircular canals inside the vestibular system. These canals typically convey motion in all 3 planes of motion. Under the influence of a microgravity environment, the dynamics and behavior of the fluids making up this system seem to be

critical to understanding space motion sickness. In this study of a model of the semicircular canals, the cilia in the superior canal displayed significant motion. This can be attributed to the position of the canal; as the highest canal, it had significantly more turbidity given that (unlike in the other canals) the cilia were not usually completely engulfed in fluid. Thus, a small pocket of air was responsible for the aberrant cilia movement under microgravity conditions. This air pocket holds a number of implications for the study of space adaptation syndrome. First, it is vital to note that what may be occurring is that all the gases present in the inner ear are coalescing in this region. From studying the pressure of this gas-liquid system, it may be possible to elucidate the relationship between pressure and sensitivity of vestibular receptors. This will require significant data collection in an Earth-gravity environment to establish a basis of comparison. In addition, determining how to artificially manipulate the sensitivity of vestibular receptors is an important obstacle to overcome once fluid and gas interactions with them are understood. From this study, however, we are able to conclude that coalescing of gases in the semicircular canals results in an air pocket that causes aberrant movement of stereocilia.

REFERENCES

1. Coulter, Gary R., Gregory L. Vogt. "The Effects of Space Flight on the Human Vestibular System." *Web of Life - NASA's Fundamental Space Biology Outreach Program*. 2002. NASA. 21 February 2008. <<http://weboflife.nasa.gov/learningResources/vestibularbrief.htm>>.
2. Cullen, Kathleen E., Jefferson E. Roy. "Signal Processing in the Vestibular System During Active Versus Passive Head Movements." *J Neurophysiol* 91(2004): 1919-1933.
3. Duwell, P., E. Jungling, M. Westhoffen, A. Luckhoff. "Potassium Currents in Vestibular Type II Hair Cells Activated by Hydrostatic Pressure." *Neuroscience* 116(2003): 963-972.
4. Heer, Martina, William H. Paloski. "Space Motion Sickness: Incidence, Etiology, and Countermeasures." *Autonomic Neuroscience: Basic and Clinical* 129(2006): 77-79.
5. Kassemi, M., D. Deserranno, J.G. Oas. "Fluid-Structural Interactions in the Inner Ear." *Computers and Structures* 83(2005): 181-189.
6. Ray, Chester A., Keith M. Hume, Samuel L. Steele. "Sympathetic nerve activity during natural stimulation." *Am J Physiol Regulatory Integrative Comp Physiol* 275(1998): 1274-1278.
7. Squires, Todd M. "Optimizing the Vertebrate Vestibular Semicircular Canal: Could We Balance Any Better?" *Physical Review Letters* 93(2004): 198106-1 -198106-4.
8. Yates, B. J., I. A. Kerman. "Post-Spaceflight Orthostatic Intolerance: Possible Relationship to Microgravity-Induced Plasticity in the Vestibular System." *Brain Research Reviews* 28(1998): 73-82.

PHOTOGRAPHS

JSC2008EO25205
JSC2008EO25210 to JSC2008EO25218
JSC2008EO25236
JSC2008EO25221
JSC2008EO25224 to JSC2008EO25226
JSC2008EO25794
JSC2008EO25796 to JSC2008EO25798
JSC2008EO25801 to JSC2008EO25803
JSC2008EO25872 to JSC2008EO25873

VIDEO

- Zero G flight week March 6–15, 2008, Masters: 734532 and 734533

Videos available from Imagery and Publications Office (GS4), NASA JSC.

CONTACT INFORMATION

Dr. Myra Halpin
North Carolina School of Science and Mathematics
1219 Broad Street
Durham, North Carolina 27705
919-416-2764
halpin@ncssm.edu

TITLE

NASA Educator Astronaut Teacher Program – Soil Porosity at Reduced Gravity

FLIGHT DATES

March 13–14, 2008

PRINCIPAL INVESTIGATOR

Loren Lykins, Carlisle High School

CO-INVESTIGATOR

Susan Kappen, Carlisle High School

Charla Jordan, Carlisle High School

Steve Stegall, Carlisle High School

MENTORS

Alma Tapia, NASA Johnson Space Center

Jonathan Neubauer, NASA Johnson Space Center



GOAL

To determine the percent soil porosity in lunar and Mars soil simulants and other soil types, at Earth gravity, moon gravity, Mars gravity, and microgravity.

OBJECTIVES

We hope to evaluate quantitatively the effects of gravity on recently disturbed soils of different particle sizes.

METHODS AND MATERIALS

We used anhydrous samples of martian and lunar soil simulants from Orbital Technologies Corporation (“Orbitec”) in addition to crushed lava rock, potting soil, and talc. The samples were sealed in plastic graduated cylinders. We used 30 grams of each sample type, except that we used 15 grams of the potting soil because of its lower bulk density.

Particle density was determined by measuring the mass of a sample of soil. The sample was then placed in a graduated cylinder to determine its overall volume. Water was added to fill in the spaces between the particles. The volume of the added water was subtracted from the total soil volume, leaving the soil particle volume. Soil particle density was subsequently determined by dividing soil mass by the soil particle volume. These densities were used later in determining the soil porosity.

Soil bulk density at Earth gravity was determined by placing a known mass of each soil type in a plastic graduated cylinder. The cylinder was sealed, inverted, and then returned to an upright position. The volume was recorded and used to calculate overall soil density by dividing the soil mass by the volume. The experiment was repeated using the pictured device (figure 14-1) for lunar gravity, Mars gravity, and microgravity parabolas on the C-9. The aircraft accelerometer was visible in each of the data photographs, so good associations could be made between changes in soil volume and percentages of Earth gravity. Percentage soil porosity was calculated using the equation:

$$100\% - [(bulk\ density / particle\ density) \times 100].$$

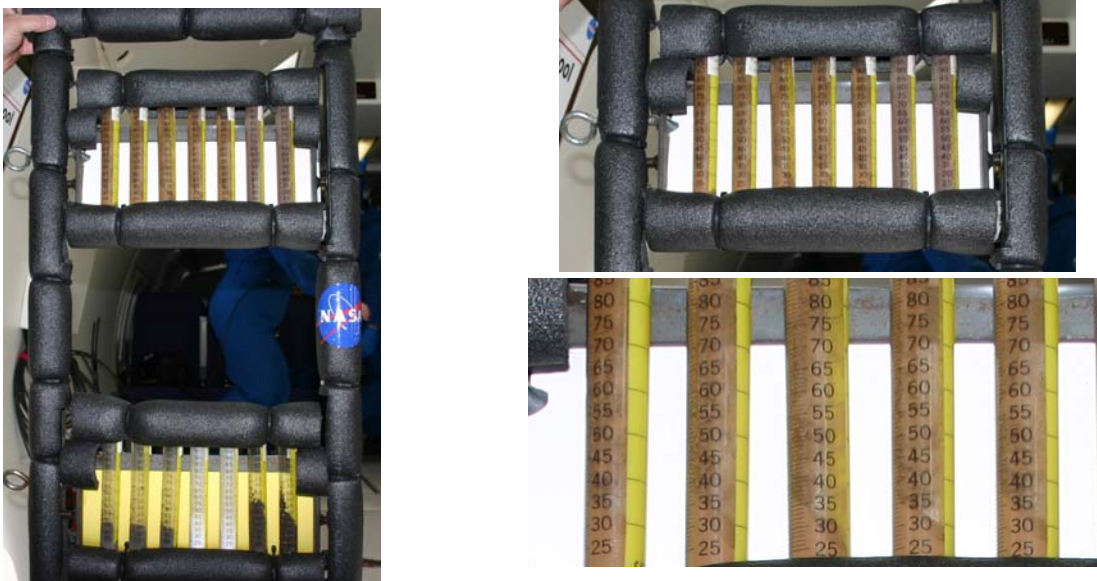


Figure 14-1. Increasing magnifications of soil samples at 0.05 Earth gravity.

RESULTS

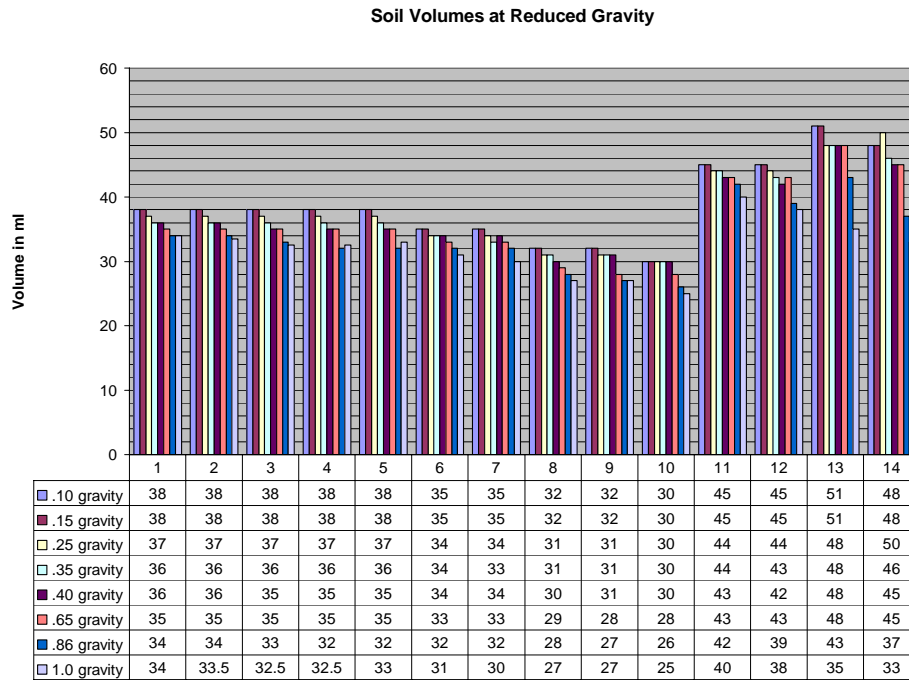


Figure 14-2. Soil bulk volume associated with fractions of Earth gravity, from data collected on NASA's C-9 aircraft and in the classroom. Samples 1–5, Orbitec Mars Simulant; samples 6–7, crushed lava rock; samples 8–10, Orbitec Lunar Simulant; samples 11–12, talc; samples 13–14, potting soil).

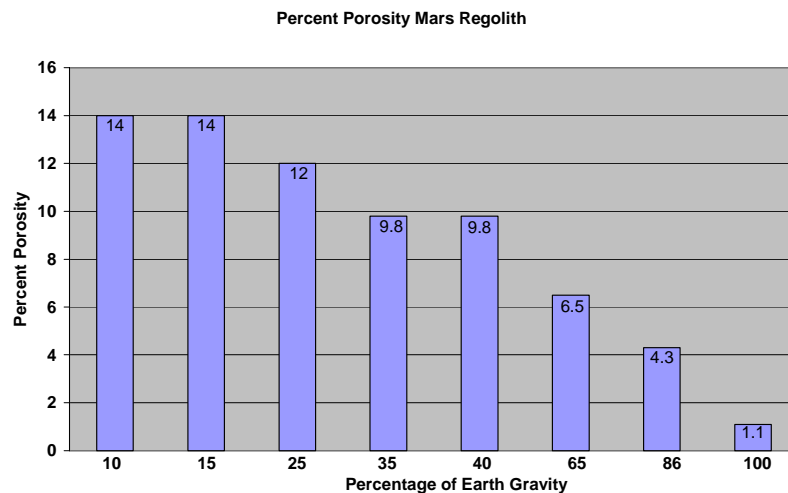


Figure 14-3. Percentage porosity of Mars soil simulant plotted against percentage of Earth gravity, from data collected on NASA's C-9 aircraft and in the classroom. The percentage porosity was found to increase as relative gravity decreased. The range of percent porosity for this soil was found to be 9.75% between 10% and 100% Earth gravity.

Crushed Lava Rock Porosity

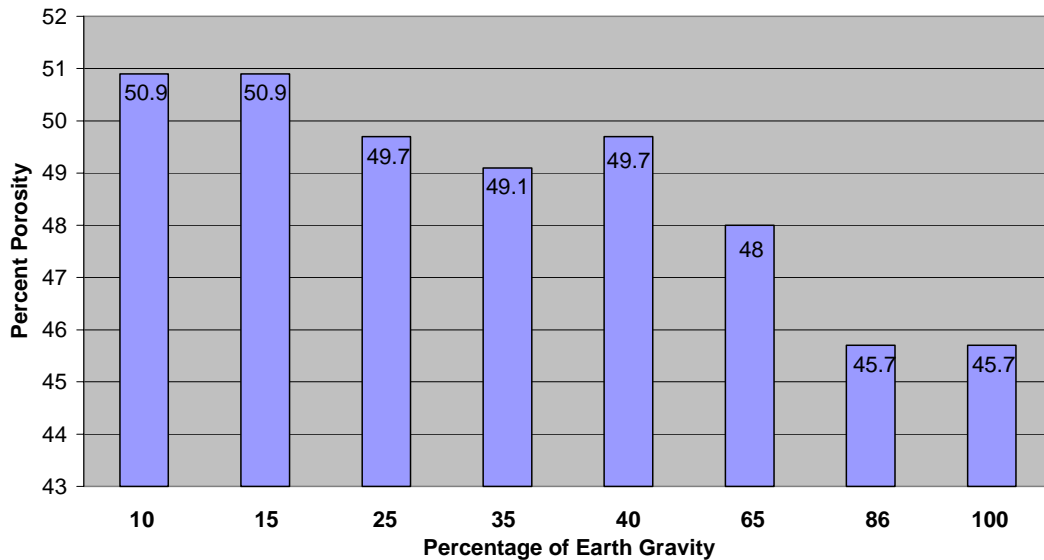


Figure 14-4. Percentage porosity of crushed lava rock plotted against percentage of Earth gravity, from data collected on NASA's C-9 aircraft and in the classroom. The percentage porosity was found to increase as relative gravity decreased. The range was found to be 5.2% in the crushed lava rock (<5 mm particle size) between 10% and 100% Earth gravity.

Percent Porosity Lunar Regolith

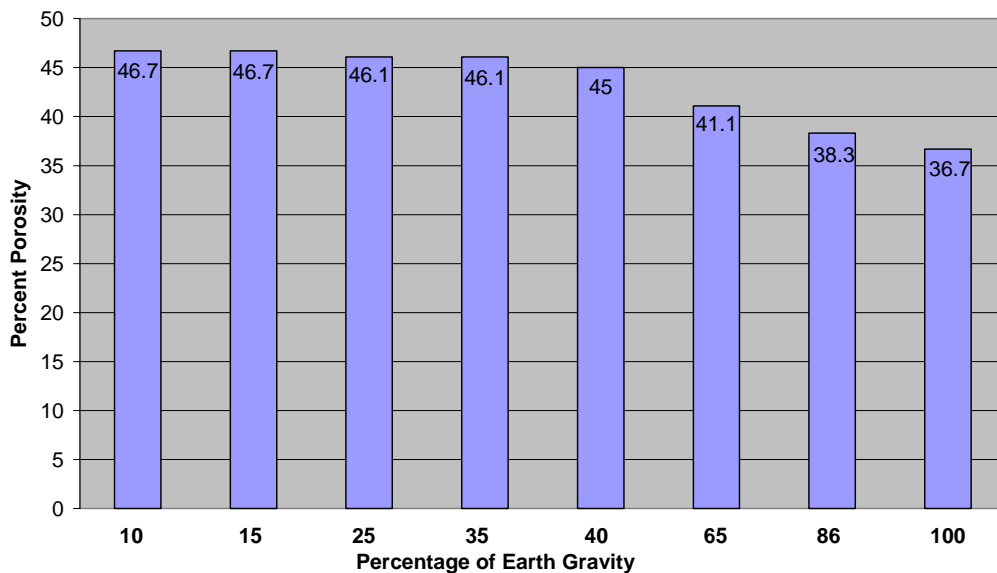


Figure 14-5. Percentage porosity of lunar soil simulant plotted against percentage of Earth gravity, from data collected on NASA's C-9 aircraft and in the classroom. The percentage porosity was found to increase as relative gravity decreased. The range was found to be 8.4% in the Orbitec lunar regolith between 10% and 100% Earth gravity.

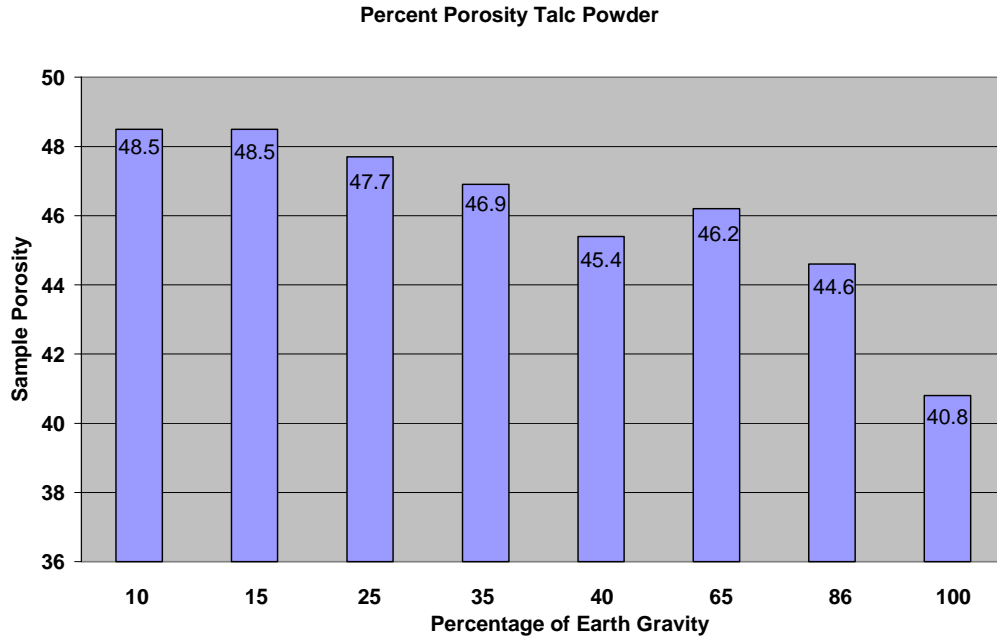


Figure 14-6. Percentage porosity of talcum powder plotted against percentage of Earth gravity, from data collected on NASA's C-9 aircraft and in the classroom. The percentage porosity generally increased as relative gravity decreased. The range was found to be 3.9% in the talcum powder between 10% and 100% Earth gravity.

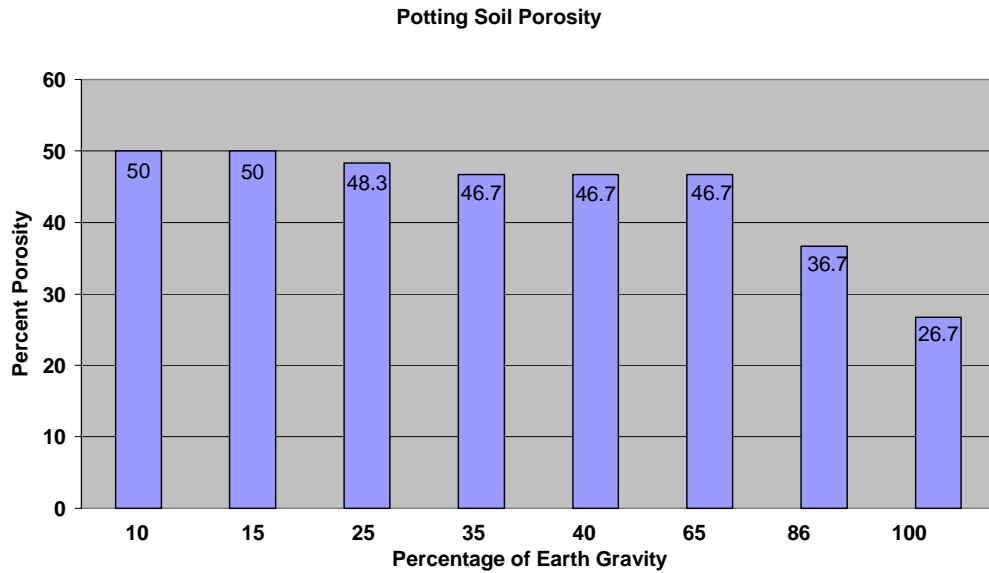


Figure 14-7. Percentage porosity of potting soil plotted against percentage of Earth gravity, from data collected on NASA's C-9 aircraft and in the classroom. The soil percentage porosity was found to increase as relative gravity decreased. The range was found to be 13.3% in the potting soil between 10% and 100% Earth gravity.

DISCUSSION

All soil samples showed an increase in volume and a subsequent increase in soil porosity as the percentage of Earth gravity acting on the soil decreased (figure 14-2). The potting soil (particle size <10 mm) had the greatest porosity range with a range of 13.3% between 1 Earth gravity and 0.1 Earth gravity (figure 14-7). Mars regolith (particle size <1 mm) had a range of 9.75% (figure 14-3), lunar regolith (particle size <1 mm) had a range of 8.4% (figure 14-5), crushed lava rock (particle size <5 mm) had a range of 5.2% (figure 14-4), and the talcum powder (particle size < 0.1 mm) showed the smallest range of porosity at 3.9% (figure 14-6). Differences in bulk density at 1 G for these sample types can be attributed in part to soil particle size, with smaller particles leaving less space for air. The differences in the porosity ranges among soil types at different fractions of Earth gravity could have been caused by a number of factors including particle size, surface attractions, and electrostatic charges; however, there was a direct association between the percentage porosity range and particle size.

CONCLUSION

Percent porosity for each of the tested soil types was found to increase in reduced gravity. The percent increase in porosity showed an association with the relative gravity. The magnitude of the increase varied among soil types, but might be related to particle size. Changes in soil porosity could influence water and nutrient absorption and retention by the soil and the capacity to support plant growth.

REFERENCES

- Assouline, S., J. Tavares-Filho, and D. Tessier. 1997. Effect of compaction on soil physical and hydraulic properties: Experimental results and modeling. *Soil Sci. Soc. Am. J.* 61:390–398.
- Baumgartl, T., and B. Koeck. 2004. Modeling volume change and mechanical properties with hydraulic models. *Soil Sci. Soc. Am. J.*
- Stang, F., and R. Horn. 2005. Modeling the soil water retention curve for conditions of variable porosity. *Vandose Zone J.* 4:602-613.

PHOTOGRAPHS

JSC2008EO26659
JSC2008EO26689
JSC2008EO26771 to JSC2008EO26780
JSC2008EO26888 to JSC2008EO26897
JSC2008EO26900
JSC2008EO26906 to JSC2008EO26908
JSC2008EO27212
JSC2008EO27308 to JSC2008EO27309
JSC2008EO27312
JSC2008EO27321
JSC2008EO27322

VIDEO

- Zero G flight week March 6–15, 2008, Masters: 734532 and 734533

Videos available from Imagery and Publications Office (GS4), NASA JSC.

CONTACT INFORMATION

Loren Lykins
Carlisle High School
lykinsl@carl.sprnet.org
(903) 861 3811 ext. 118

TITLE

NASA Educator Astronaut Teacher Program – Physics of Plant Growth in Micro, Lunar, and Martian Gravity

FLIGHT DATE

March 13–14, 2008

PRINCIPAL INVESTIGATOR

Luther Richardson, Columbus High School & Auburn University

CO-INVESTIGATORS

Kristen Painting, NASA Johnson Space Center
Scott Chandler, St. Elmo Center for Gifted Children
Carol Mashburn, St. Elmo Center for Gifted Children
Troy McGarr, Richards Middle School
Avery Baggett, University of Pennsylvania



GOAL

The goal of this experiment is to test a series of responses of common plants in lunar, martian, and microgravity environments to possible conditions in a greenhouse on the moon or Mars, or in transit to those places. Since the students who are working on this experiment could be the first humans to colonize the moon and Mars, this experiment is especially applicable, as they would need to grow plants for food and other resources.

OBJECTIVES

This experiment's objectives are to find evidence for significant differences in different gravity environments in the response of plant leaves to a thermal stimulus.

The normal pressure gradients that exist in the stems and leaves of a plant on Earth will behave differently in a reduced-gravity environment. Literature has been found that shows a real effect of microgravity on the transpiration rate of plants. Introducing the added variable of heat will make the temperature changes that occur in the fleshy parts of the plants more pronounced in lower gravity and less pronounced in hypergravity. The goal of this experiment is to make quantitative measurements that will lead to other investigations to understand the physics of energy transfer in plants through fluids.

The reaction of fluid flow in plants in a reduced-gravity environment to the application of thermal radiation will be measured and compared to normal gravity results. Fluid flow in reduced gravity can be predicted using the physics of fluids, but plants offer their own set of new variables. Lunar and martian parabolas will produce as much data as the microgravity parabolas in terms of how the plants react to thermal radiation in these environments.

Students from elementary, middle, and high school are included in this study. Stage 1 involves students coming up with questions we could answer on the NASA plane involving the chosen concepts. This step has already been completed. In stage 2, the students will make actual measurements, based on the questions of the previous stage, with different plant leaves and stalks to find an ideal candidate for the flight experiments. Stage 3 includes the final building of the experiment structure based on what was learned in stage 2. This third stage also includes implementation of the Outreach plan, for which student groups will travel to other schools to present their experiment, and teachers will be introduced to the NASA Engineering Design Challenge. A Web site has been established at <http://rg08.columbus2space.org> to include summaries of what the students from the different schools come up with so the development of the experiment can be shared with students from each school. Stage 4 is the final report and Student Exposition where parents, media, and other schools will be invited to participate in a series of presentations related to what was found in this experiment, and what students from other schools were able to do with the Engineering Design Challenge.

METHODS AND MATERIALS

An infrared camera (7.5 to 15 μm wavelengths) provided the primary data for this experiment. The average temperature of a region of plant leaf was recorded 15 times per second as a video file with embedded average temperature displayed. A thermal response was generated using a 125-W plant grow light, which was either switched on at the beginning of a reduced-gravity parabola or at the beginning of a hypergravity period.

Video analysis of the video recorded by the infrared camera provided a plot of temperature change for each trial. The plot shows 2 distinct parts: heating and cooling.

The heating segment is linear and the cooling is quadratic for the purposes of the mathematical models applied.

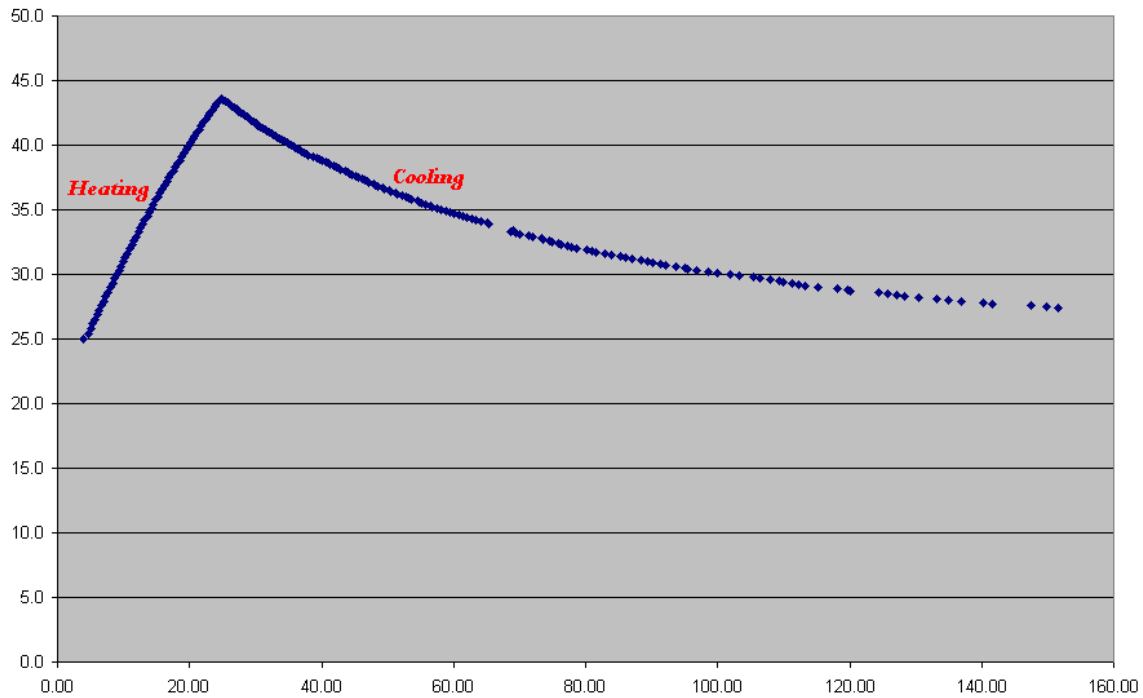


Figure 15-1. Temperature change for each trial. The plot shows 2 distinct parts: heating and cooling.

Since the heating portion is mostly linear ($R^2 > 0.98$), the beginning and end points were used to calculate the change in temperature for a specific change in time, or $\frac{\Delta T}{\Delta t} \rightarrow \left[\frac{^{\circ}\text{C}}{\text{s}} \right]$

The cooling of the leaves as viewed by the infrared camera shows a quadratic relationship of the form

$$T(t) = T_0 + \beta t + \alpha t^2$$

Given 3 values of temperature and time, the constants for this model can be found. The equations, in terms of the boundary conditions, are

$$\alpha = \frac{(t_1 - t_0)(T_2 - T_0) - (t_2 - t_0)(T_1 - T_0)}{(t_2 - t_0)(t_1 - t_0)(t_2 - t_1)} \text{ and}$$

$$\beta = \frac{(T_1 - T_0)}{(t_1 - t_0)} - \frac{(t_1 - t_0)(T_2 - T_0) - (t_2 - t_0)(T_1 - T_0)}{(t_2 - t_0)(t_2 - t_1)}$$

These constants were used to normalize a predicted change in temperature over a 120-s period to be compared per trial in each gravity environment. The final result was a comparison of the average predicted response with some statistics addressing the reliability of the measurements.

Measurements of CO₂ concentration and relative humidity during each gravity environment were made to corroborate changes in the local environments.

The types of sensors used in this experiment are listed in the table below.

Table 15-1. Experiment sensors and equipment.

| | |
|---------------------------------|---|
| FLIR EX320 IR camera | This camera has an RCA video output, which is fed through an analog-to-digital converter into a laptop and is recorded as video at 15 frames per second. The camera has an algorithm that calculates the average temperature of all the pixels in a central rectangle within 0.1 degrees Celsius. |
| DataTaker DT800 Logger | This is a 48-channel 16-bit data logger. It is used to take high-resolution data throughout the flight from a variety of sensors. |
| Relative humidity | Two of these sensors measure relative humidity inside the containment area away from the plants and heat lamp and also right underneath the leaf being treated. |
| CO ₂ module (Figaro) | Two of these sensors measure CO ₂ concentration inside the containment area away from the plants and heat lamp and also right underneath the leaf being treated. |

Plant #1 and Plant #2 were both potted plants purchased locally in Houston. They are shown in figure 15-2.



Plant #1



Plant #2

Figure 15-2. Plants used in this experiment.

RESULTS



Experiment in flight during heating



Leaf plate with embedded sensors

Figure 15-3. Hardware used in this experiment.

The raw data collected from the 11 trials are shown in the table below.

Table 15-2. Data from 11 trials.

| Trial | Temp1 | Temp2 | ΔT | Time heat | Temp3 | Time cool | Gravity |
|--------------|--------------|--------------|-----------|------------------|--------------|------------------|----------------|
| 1 | 20.2 | 22.9 | 2.7 | 15.54 | 20.5 | 120 | Martian |
| 2 | 19.8 | 31.0 | 11.2 | 46.8 | 21.3 | 120 | Lunar |
| 3 | 18.6 | 24.8 | 6.2 | 23.2 | 19.9 | 120 | Micro |
| 4 | 19.1 | 24.8 | 5.7 | 23.2 | 19.9 | 120 | Micro |
| 5 | 19.0 | 23.1 | 4.1 | 15.13 | 19.7 | 120 | Micro |
| 6 | 19.6 | 24.1 | 4.5 | 19.13 | 20.7 | 74 | Micro |
| 7 | 20.7 | 32.4 | 11.7 | 60.67 | 23.2 | 94 | Hyper |
| 8 | 19.1 | 26.2 | 7.1 | 19.67 | 21.2 | 120 | Micro |
| 9 | 20.8 | 28.2 | 7.4 | 21.07 | 22.1 | 120 | Micro |
| 10 | 21.9 | 38.2 | 16.3 | 58.73 | 27.0 | 77 | Hyper |
| 11 | 27.0 | 40.7 | 13.7 | 52.2 | 28.6 | 120 | Hyper |

Temp1 = initial average temp. of the leaf, Temp2 = peak temp., Temp3 = final temp. after cooling.

These data were used to calculate the heating gradients of the leaves during heating and cooling. These calculations were discussed in the methods section, and the results are shown in the table below.

Table 15-3. Heating gradients of leaves during heating and cooling.

| G-level | Heating | Cooling | | |
|-----------------|---------------------------------|----------------|----------|---------------------------------|
| | $\Delta T / \Delta t$ [deg C/s] | Alpha | Beta | 120s ΔT (normalized) |
| 0 Plant #1 | 0.27 | 0.000283 | -0.07484 | -4.9 |
| | 0.25 | 0.000253 | -0.07124 | -4.9 |
| | 0.27 | 0.000235 | -0.05652 | -3.4 |
| | 0.24 | 0.000269 | -0.06584 | -4.1 |
| 1.8 Plant #1 | 0.19 | 0.000435 | -0.13904 | -10.4 |
| 0 Plant #2 | 0.36 | 0.000360 | -0.0849 | -5.0 |
| | 0.35 | 0.000506 | -0.11156 | -6.1 |
| 1.8 Plant #2 | 0.28 | 0.000673 | -0.19786 | -14.1 |
| | 0.26 | 0.001038 | -0.22541 | -12.1 |

These results were statistically compared for each plant in micro- and hypergravity for both heating and cooling.

Plant #1 Heating

Microgravity: Average $\Delta T / \Delta t = 0.2575 \text{ deg C/s}$, standard deviation (SD) = 0.015

Hypergravity: Average $\Delta T / \Delta t = 0.19 \text{ deg C/s}$

Percent Change = -26%

Plant #1 Cooling

Microgravity: Average ΔT (normalized) = -4.3, SD = 0.73

Hypergravity: Average ΔT (normalized) = -10.4

Percent Change = -142%

Plant #2 Heating

Microgravity: Average $\Delta T / \Delta t = 0.355 \text{ deg C/s}$, SD = 0.0071

Hypergravity: Average $\Delta T / \Delta t = 0.27 \text{ deg C/s}$, SD = 0.014

Percent Change = -24%

Plant #2 Cooling

Microgravity: Average ΔT (normalized) = -5.55, SD = 0.78

Hypergravity: Average ΔT (normalized) = -14.1, SD = 1.38

Percent Change = -136%

Data from the CO₂ and relative humidity sensors were collected for 2 parabolas of reduced gravity. CO₂ showed a 5% drop in concentration and relative humidity showed an 11% drop in value during the applications of heat. The control sensors showed no change during these times.

Measurements of temperature were within 0.1 deg C, and measurements of time were within 0.33 s. Given an average change in temperature of 15 deg C, and an average change in time measurement of 20 s, the error in $\Delta T / \Delta t = \pm 1\%$.

DISCUSSION

These results show some statistically significant changes in both heating and cooling. However, several issues arose during the experiment that limited the value of the results. Most notable was the lack of a normal gravity trial. In the numerous practice trials completed before flight, the thermal response of various plants was very consistent as long as nothing changed between trials, specifically, the positioning of the leaf relative to the view of the infrared camera. During the experiment flight, a problem arose with the data logger, which led to a lack of time to complete a normal gravity trial during one of the turn-around periods of flight. In retrospect, the data logger data could have been sacrificed for a more complete set of infrared data.

Another issue was the placement of the leaf in the camera's field of view during the lunar and martian parabolas. Small changes had to be made before the microgravity parabolas since a gap was left in the initial placement. A solution to this would have been more time in experiment trial practice on the ground. Placement of the leaves is a subtle action, but it is important for validity of the data. Although data were collected during lunar and

martian parabolas, the values cannot be compared to the other data since a different part of the leaf was used and some background gaps occurred in those data.

Even without the normal gravity control data, the results showed a significant change in plant response in the micro- and hyper-gravity parts of the flight.

CONCLUSION

The leaves of 2 different plants showed significant changes in thermal response in both heating and cooling in microgravity and hypergravity environments. Microgravity heating was more pronounced than hypergravity heating. It is speculated that the lack of gravity changed pressure gradients in the plant leaves, enhancing the physics behind their heat transfer capability through the fluids in the leaves. Cooling differences were opposite. Plants in hypergravity cooled down faster than plants in microgravity. In microgravity, once the fluids in the plants were heated, the lack of gravity took away convective effects that would have helped in cooling. With hypergravity, the convective effects would be enhanced, as the data showed.

The plants were very different in leaf type, and the rates of heating and cooling showed this. However, the percent differences between micro- and hypergravity were very consistent. This same experiment would be worth flying again with procedural improvements to include sensor data with adequate normal gravity data to quantify the extent of different plant responses in different gravity environments. This sort of data taken for different plants would provide valuable insight to anyone planning on maximizing growth and plant health in the gravity environments associated with space travel and future inhabitants of the lunar and martian long-term bases.

E-mail discussions with Dr. Ray Wheeler at Kennedy Space Center revealed other possibilities for these results. Heating and cooling will be greatly affected by the convection of air around the leaves. In the absence of gravity and with no air circulation, heating would be more pronounced in a local area since convection would not occur. Hot air would stay around the leaf. This would also support the idea of cooling in microgravity taking more time. These results would have been less ambiguous had the sensor suite been operable throughout the flight. Also, Dr. Wheeler suggested trying to measure internal pressures of the plant during parabolas to definitively answer what was happening to the plant and not just its environment. It would be very challenging to get reliable readings for these pressures, but it might warrant a future experiment flight.

The ambiguity of these conclusions points out the difficulty in measuring changes in plants over small amounts of time. However, this investigation points out directions for future experiments to help understand the effects of different gravity environments on plants.

REFERENCES

Kitaya, Y., Kawai, K., Tsuruyama, I., Takahashi, H., Tane, A., Hoto, E., Saito, T. and Saito, T. The Effect of Gravity on the Surface Temperature of Plant Leaves. *Plant, Cell, and Environment* (2003) 26, 497-503.

Olszyk, D. and Tibbitts, T. Stomatal Response and Leaf Injury of *Pisum sativum* L. and SO₂ and O₃ Exposures. *Plant Physiology* (1981) 67, 545-549.

Ksenzhek, O., Pretova, S., and Kolodzazhny, M. Electrical Properties of Plant Tissues. Resistance of a Maize Leaf. *Bulg. J. Plant Physiol* (2004) 30 (3-4), 61-67.

Hyman, J., Graham, E., Hansen, M., and Estrin, D. Imagers as Sensors: Correlating Plant CO₂ Uptake with Digital Visible-Light Imagery. *Proceedings of the 4th International Workshop on Data Management for Sensor Networks (DMSN 07)*, 2007, Austria.

PHOTOGRAPHS

JSC2008EO26703 to JSC2008EO26713

JSC2008EO26855

JSC2008EO26859 to JSC2008EO26861

JSC2008EO26880 to JSC2008EO26884

JSC2008EO26917 to JSC2008EO26918

JSC2008EO27246 to JSC2008EO27250

JSC2008EO27279

JSC2008EO27287 to JSC2008EO2789

JSC2008EO27296 to JSC2008EO27298

JSC2008EO27302 to JSC2008EO27306

JSC2008EO27322

VIDEO

- Zero G flight week March 6–15, 2008, Masters: 734532 and 734533

Videos available from Imagery and Publications Office (GS4), NASA JSC.

CONTACT INFORMATION

Luther Richardson

lrich@physics.auburn.edu

TITLE

NASA Educator Astronaut Teacher Program – Project MEGA (Microgravity Experimental Growth Activity)

FLIGHT DATE

March 13–14, 2008

PRINCIPAL INVESTIGATOR

Bradley J. Neu, Lubbock High School

CO-INVESTIGATORS

Joy Buchok, Lubbock High School

Chad Haskins, Lubbock High School

Sharron Story, Lubbock High School



GOAL

The goal of the investigation was to determine if the amount of gravity affects crystal growth.

OBJECTIVES

The objective of the investigation was to measure the temperature, speed of growth, electron micrograph images, and x-ray diffraction of sodium acetate crystals as they formed from a supersaturated solution upon being disturbed in hyper- and microgravity.

METHODS AND MATERIALS

Sodium acetate solution found in commercially available hand warmers

Temperature probe and data collection software

Laptop computer

Camera

Ruler

X-ray diffraction equipment courtesy of MIT

Scanning electron microscope courtesy of Hitachi

RESULTS

The maximum temperature of the samples ranged from 36 to 49.5 °C but was not consistent in hyper- or microgravity. The rate of growth in microgravity ranged from 0.68 to 1.14 cm/s. The rate of growth in hypergravity ranged from 0.64 to 1.0 cm/s. Finally, MIT's x-ray diffraction analysis when the spectral samples were overlaid showed no difference between the samples.

DISCUSSION

The rate of crystal growth appeared to be unaffected by gravity. The temperature differences between micro- and hypergravity were random, the rate of growth was slightly slower in hypergravity but only by 0.05 cm/s, and the x-ray analysis proved to have no spectral variances. Hitachi provided a series of scanning electron micrographs, which also showed no difference in the crystal structure.

CONCLUSION

Our conclusion is that crystals are not affected by the intensity of the gravitational field.

PHOTOGRAPHS

JSC2008EO26655 to JSC2008EO26657

JSC2008EO26682 to JSC2008EO26683

JSC2008EO26911 to JSC2008EO26913

JSC2008EO26918

JSC2008EO27214

JSC2008EO27218 to JSC2008EO27219

JSC2008EO27224

JSC2008EO27227

JSC2008EO27238

JSC2008EO27234 to JSC2008EO27235

JSC2008EO27322

VIDEO

- Zero G flight week March 6–15, 2008, Masters: 734532 and 734533

Videos available from Imagery and Publications Office (GS4), NASA JSC.

CONTACT INFORMATION

Bradley J. Neu
Lubbock High School
2004 19th Street
Lubbock, TX 79401
806-766-1444
806-766-1469 Fax

TITLE

NASA Educator Astronaut Teacher Program – Uptake of Nutrients by Plants in Microgravity

FLIGHT DATE

March 13–14, 2008

PRINCIPAL INVESTIGATOR

Angela M. Krause-Kuchta, Menomonie High School

CO-INVESTIGATORS

Ryan E. Ruegnitz, Menomonie High School
Deanna M. Suilmann, Menomonie High School



GOAL

The goal of this investigation was to determine the effect of microgravity and other reduced-gravity fields on the uptake of nutrients by plants.

OBJECTIVES

Through this investigation, students will

- gain an appreciation for the value of space exploration
- understand the scientific process
- utilize a variety of skills necessary to conduct research
- understand the concept of microgravity and how objects function in microgravity
- recognize the vital connection between Science and Social Studies

METHODS AND MATERIALS

Our experiment utilized a customized housing design that contained a chamber for water with an opening for the stem of a *Dieffenbachia* sp. plant. The hole was sealed to avoid leakage of water. The water chamber had a rubber stopper through which a syringe was inserted to withdraw samples of the water. Food coloring was added to the water to simulate the presence of nutrients. Since nutrient uptake is by simple diffusion, we utilized the diffusion of the food coloring to represent individual nutrients essential to the plant. During the microgravity portions of each parabola of the flight, 1-mL samples of the colored water were drawn from the chamber. On the ground, similar samples were collected in a control experiment to compare with our flight data. The plant, in its customized housing, was spun on a large turntable (merry-go-round) to simulate the hypergravity portion of flight. After this was done, samples were drawn after entering normal Earth gravity. The relative concentration of the food coloring in each sample was determined using a Milton Roy Spec 20 spectrophotometer.



RESULTS

| Standard (%) | % Transmittance | Absorbance |
|--------------|-----------------|------------|
| 100.00 | 88 | 0.055 |
| 96.00 | 88 | 0.058 |
| 92.00 | 90 | 0.048 |
| 88.00 | 90.2 | 0.045 |
| 84.00 | 86 | 0.068 |

| | | |
|-------|------|-------|
| 80.00 | 82.5 | 0.082 |
| 76.00 | 87.3 | 0.06 |
| 72.00 | 95 | 0.021 |
| 68.00 | 82.5 | 0.092 |
| 64.00 | 87 | 0.061 |
| 60.00 | 85 | 0.07 |
| 56.00 | 91.9 | 0.038 |
| 52.00 | 95.5 | 0.02 |
| 48.00 | 87.9 | 0.058 |

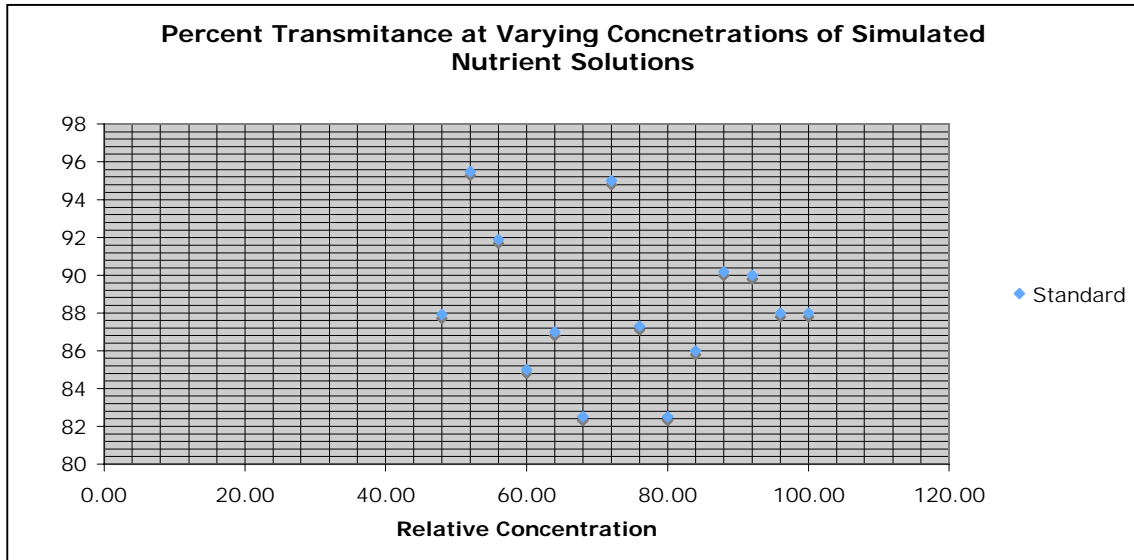


Figure 17-1. Percent transmittance at different concentrations of simulated nutrient solutions.

Table 17-2. Data from flight and ground-based experiments.

| Flight Sample Data | | |
|---|------------------------|-------------------|
| Test Tube Number / Parabola Number | % Transmittance | Absorbance |
| 1 | 100% | 0 |
| 2 | 100% | 0 |
| 4 | 99.90% | 0 |
| 5 | 99.90% | 0 |
| 6 | 99.90% | 0 |
| 7 | 99.90% | 0 |
| 8 | 99.90% | 0 |
| 9 | 100% | 0 |
| 10 | 99.90% | 0 |
| 11 | 100% | 0 |
| 12 | 100% | 0 |
| 13 | 100% | 0 |
| 14 | 99.90% | 0 |
| 15 | 100% | 0 |
| 16 | 100% | 0 |
| 17 | 100% | 0 |
| 18 | 100% | 0 |
| 20 | 99.90% | 0 |
| 21 | 100% | 0 |
| 22 | 99.90% | 0 |
| 23 | 99.90% | 0 |
| 24 | 99.90% | 0 |
| 25 | 99.90% | 0 |
| 26 | 99.90% | 0 |

| Ground-Based Samples | | |
|--|------------------------|-------------------|
| Test Tube Number / Trial Number | % Transmittance | Absorbance |
| 36 / 0 (initial) | 100% | 0 |
| 37 / 1 | 100% | 0 |
| 40 / 2 | 100% | 0 |
| 41 / 3 | 100% | 0 |
| 42 / 4 | 100% | 0 |
| 43 / 5 | 100% | 0 |
| 46 / 6 | 100% | 0 |
| 52 / 7 | 100% | 0 |
| 53 / 8 | 100% | 0 |
| 54 / 9 | 100% | 0 |

DISCUSSION

At the start of this project, we recognized the value of plant growth experiments for space. The use of plants has many applications in long-duration space flight. Growing a variety of plants will provide food and oxygen for astronauts as well as act in bioremediation of wastes. Furthermore, plants will play an integral part in maintaining crew morale. Being in a room with plants reduces stress and promotes a sense of calm by reducing blood pressure and heart rate. Additionally, we have recognized that research done in space can greatly improve life on Earth. As technologies have advanced, agricultural practices have benefited. Living in a semi-agricultural community, we feel it is important to look at various impacts on plant growth in a variety of environs. One problem associated with agricultural practices in our community and surrounding locations is agricultural runoff, which has led to severely eutrophic conditions in our waterways. We had hopes of applying the findings of our research to this dilemma. In the analysis of our data, however, we saw no difference in the uptake of food coloring (simulating nutrients) between the plants in flight and our control plant on the ground. While slight variation is seen in the flight data (100%-99.90%), we suspect that this is simply variance in the reading of the spectrophotometer by the observer. This variance of 0.10% follows no pattern to signify that nutrients have actually been taken up. We suspect, however, that the lack of noticeable difference between the flight and ground data may be due to the short duration in which the plants experienced microgravity. We will do additional research utilizing significantly longer periods of time to determine if changing gravitational fields will affect nutrient uptake. To do so, we will place a plant in simulated hypergravity for 24 hours, measuring the concentration of color in the water at the start and end of the time period. Additionally, we will have a control plant in normal Earth gravity and will determine the change in concentration of color in the water during the same 24-hour period.

Our research was important for many other reasons. The most significant was witnessing our students' engagement in their education. Each stage of the process (development of the experiment, conduct of the experiment, and analysis) has had a positive impact on a variety of learners. The project was a natural fit for Biology classes, but was a wonderful addition to Social Studies classes as well. This opportunity allowed our students and us to explore the connection between history and science. Interestingly, we found that the connection runs very deep. Especially now, after returning from the Reduced-Gravity Flight experience, we find ourselves interjecting information about the experiment, the trip to NASA, or the flight into our everyday lessons. Students are curious about the results of the experiment and often stop by our classrooms to ask about the findings.

CONCLUSION

In conclusion there is no noticeable difference in the effectiveness of nutrient uptake by plants in Earth gravity and plants in reduced gravitational fields.

PHOTOGRAPHS

JSC2008EO26665 to JSC2008EO26666
JSC2008EO26884
JSC2008EO26686
JSC2008EO26853
JSC2008EO26858
JSC2008EO26901 to JSC2008EO26902
JSC2008EO26918
JSC2008EO27213
JSC2008EO27225
JSC2008EO27228
JSC2008EO27301
JSC2008EO27322

VIDEO

- Zero G flight week March 6–15, 2008, Masters: 734532 and 734533

Videos available from Imagery and Publications Office (GS4), NASA JSC.

CONTACT INFORMATION

Angela M. Krause-Kuchta
Menomonie High School
1715 5th Street West
Menomonie, WI 54751
(715)-232-2606
angela_krause@msd.k12.wi.us

TITLE

Transgenic Arabidopsis Gene Expression System and
Advanced Biological Research System

FLIGHT DATES

March 18–21, 2008

PRINCIPAL INVESTIGATORS

Robert Ferl, University of Florida
Anna-Lisa Paul, University of Florida



GOAL AND OBJECTIVES

- 1) To obtain a replicate data set characterizing the extent of thermal variation on the surface of Arabidopsis leaves during parabolic flight. The C-9 parabolic flight experiments conducted in 2006 and 2007 were very successful in this endeavor; these experiments demonstrated that if air is not allowed to circulate, the difference in surface leaf temperature can vary by 2 to 4 °C between the 0-G and 2-G segments of the parabola. These experiments were repeated using a Fluke thermal imaging device and plants engineered with gene reporters that are designed to reveal changes in gene expression in response to heat-induced stress. Data were collected in the form of digital images and tissue-specific patterns of reporter gene expression.
- 2) To develop further understanding of the numerous genes associated with auxin metabolism. Genetic analyses were performed after the April 2003 KC-135 and March 2006 C-9 experiments. The results from these analyses indicated that numerous genes associated with auxin metabolism are upregulated in response to parabolic flight (22,000-gene array chips from Affymetrix™). Several of these genes have been implicated in gravity sensing. The genetic analyses from plants studied on this flight will contribute to the dissection of this response. Plants engineered with gene reporters designed to respond to variations in auxin metabolism were also used to gather tissue-specific gene expression data.
- 3) To test the Advanced Biological Research System (ABRS) Condensate Recovery System. The ABRS hardware will support the APEX-Cambium payload operations by providing environmental control as well as condensate recovery. The ABRS Condensate Recovery System uses a finned Cold Sink design that has not previously been tested in microgravity. Movement of water across the Cold Sink fins was observed to give insight into the efficiency of the Condensate Recovery System design.

METHODS AND MATERIALS

- 1) A thermal imaging device was used to monitor the surface temperature of Arabidopsis leaves during a series of parabolic flights (figure 18-1). Data were collected in the form of digital images and corresponding numeric values. The thermal imaging device utilized was the Fluke Ti30. The Ti30 imager provides fast image scanning and radiometric measurements on a large LCD screen. Images and corresponding numerical information will be analyzed with accompanying reporting software.

The Ti30 was used in a free-float scenario as well as mounted to the aircraft floor. A single plant was imaged for 10 parabolas. At the turnarounds, the position of the plate was changed so that a new plant was in the imaging field. In this way, 4 replicate plants were qualitatively and quantitatively analyzed during a typical flight of 40 parabolas. Variations of the experiment among the flight days included imaging plants of various ages and various tissues in the plants.



Figure 18-1. Thermal imaging device on March 2008 flight.

- 2) The plants utilized for the genetic analysis experiments were flown as seedlings (9 to 20 days old) on Petri plates (figure 18-2). All plants were contained in BioTransporter (BT) containers. On each flight day, harvests were performed during the turnarounds. Plants were removed from their growth support medium using forceps and were placed in capped tubes of stain (x-gluc) or preservative (RNAlater®) solution. A small number of additional plants were placed in Kennedy Space Center Fixation Tube (KFT) hardware during parabolas to test a mesh barrier design in the KFT plant sample tube section.



Figure 18-2. Harvest of plants from Petri plates.

- 3) The ABRS is the hardware that will contain the Transgenic Arabidopsis Gene Expression System (TAGES) experiment on the International Space Station. The Condensate Recovery System circulates air across a finned Cold Sink. Blowers on the Cold Sink induce forced convection throughout the entire plant growth chamber, thus

cooling the chamber. The Cold Sink is part of a closed chilled water loop that also includes a peristaltic pump, water reservoir, and humidification pouch (external to the plant growth chamber). A condensation collection sponge is located beneath the Cold Sink fins to absorb excess moisture. The ABRs C-9 Condensate Recovery System was mounted on an aluminum base plate (figure 18-3) and was beneath a clear polycarbonate lid to enable viewing of water moving along the fins and to prevent leakage of water outside of the system. Mistifiers were used to spray water across the Cold Sink fins during the 0-G portion of each parabola. A laptop computer was connected to the Condensate Recovery System for control of the peristaltic pump for misting and for the blowers. A video camera was used to record the movement of water across the Cold Sink fins.



Figure 18-3. ABRs hardware setup (left) and colored water passing along Cold Sink fins.

RESULTS

- 1) Thermal imaging device: Surface temperature changes were successfully recorded during the parabolas. Data from the thermal imager are still being analyzed to determine if temperature variations in plants of different age and tissue type were statistically significant.
- 2) Genetic analyses: As with previous flights, results from these studies indicated that numerous genes associated with auxin metabolism are upregulated in response to parabolic flight. The genetic analyses of plants studied on this flight are ongoing and will contribute to the dissection of this parabolic flight response. The mesh barrier testing of the KFT hardware was successful, and the hardware will be implemented for the flight experiment.
- 3) ABRs: Water was observed moving along the fins as anticipated. The C-9 flights confirmed that the design of the Condensate Recovery System will meet the established requirements.

CONCLUSION

As in our previous experience, the C-9 investigations have proven invaluable in studying the *Arabidopsis* plant's response to parabolic flight and microgravity. Additionally, the

validation of the ABRS Condensate Recovery System design gives the engineering team the confidence that the current design will meet the on-orbit requirements for this payload.

PHOTOGRAPHS

JSC2008EO27341 to JSC2008EO27363

JSC2008EO27518 to JSC2008EO27547

JSC2008EO27548 to JSC2008EO27559

JSC2008EO27625 to JSC2008EO27651

VIDEO:

- Zero G flight week March 17–21, 2008, Master: 306415

Videos available from Imagery and Publications Office (GS4), NASA JSC.

CONTACT INFORMATION

For more information on the TAGES science, contact
Rob Ferl, PhD, or Anna-Lisa Paul, PhD
University of Florida Department of Horticultural Science
1253 Fifield Hall
Gainesville, FL 32601-0690
(352) 392-1928 x301

For more information regarding the ABRS hardware, contact
David Reed, Mail Code: BIO-3, Kennedy Space Center, FL 32899
(321) 861-2980 voice
David.W.Reed@nasa.gov

TITLE

Human Vestibular Orientation in Variable Force Backgrounds –
Flight Week 2

FLIGHT DATE

March 18–21, 2008

PRINCIPAL INVESTIGATOR

James R. Lackner, Brandeis University

Paul DiZio, Brandeis University



OBJECTIVES

The experiment we conducted during March 18–21, 2008, in parabolic flights on board the C-9 was a continuation of our effort to develop a predictive model of human vestibular orientation and movement control in variable force backgrounds. We conducted 3 experiments, which will be designated by their project names as follows:

1. Vestibular Orientation.
2. Limb Mass Adaptation
3. Weight / Mass Estimation

All procedures were approved by the Brandeis Committee for the Protection of Human Subjects (CPHS) as well as by the JSC CPHS.

BACKGROUND

Experiment 1, *Vestibular orientation*. The overall goal of this project is to develop a 3-dimensional model of static spatial orientation. This project is a continuation of the experiments we conducted in our previous parabolic flights, July 31–August 2, 2007. The specific aim of these experiments is to collect the first comprehensive data set assessing the subjective vertical as a function of static body tilt in all 3 cardinal axes, in different force backgrounds, using a single technique for indicating the vertical. During July 31–August 2, 2007, we tested 3 subjects in parabolic flight. The goal for the March 18–21, 2008, week was to test an additional 4 subjects. Subjects were tested in a multi-axis tilt device that could orient them in pitch, yaw, and roll. Each subject was blindfolded and securely strapped into the device. Movements between positions were brief and naturalistic. Each dwell position was held for 5 s, during which perceived vertical was indicated with a joystick held in both hands. Static tilts included 1) all 3 cardinal axes; 2) the full range of possible tilt angles, 0 through 360°; 3) multiple force backgrounds – 0 G, 1 G, and 1.8 G. This data set, when analyzed, will allow the development and evaluation of the first true 3-dimensional model of static orientation.

Experiment 2, *Limb mass adaptation*. The overall goal of the project is to understand control of body movement in non-terrestrial force backgrounds, when subjects are wielding objects or wearing loads. The specific aim of this experiment is to understand how altering arm mass affects arm movement control. Six subjects were tested in the previous flights, July 31–August 2, 2007. Eight additional subjects were tested this flight week, March 18–21, 2008. Subjects executed planar reaching movements while either holding a hollow cylinder or the same shape cylinder loaded with a mass of 500 g. Movements were performed only in 0 G. A magnetic tracking system was used to collect kinematic data about the arm. When the data are processed, we hope to learn the time course required for subjects to internalize the mass perception.

Experiment 3, *Weight / mass estimation*. The overall goal of this experiment is to understand how estimates of the mass and weight of hefted objects are affected by different force backgrounds and by whether or not the observer is wearing a glove having the same mass as the hefted object. Subjects attempted to discriminate between 2 same-looking objects of slightly different mass lifted simultaneously with their right and left hands, in 0 G, 1 G, and 1.8 G, with and without wearing 300-g gloves on both hands. The masses ranged from 256 grams to 304 grams, in 8-g increments. Data collection involved manual (typed into a laptop computer) recordings of verbal responses.

METHODS

The specific procedures for each experiment were as follows:

Experiment 1, *Vestibular orientation*. Each subject was tested in parabolas 1 through 40 of one flight day. Three of the subjects selected for testing were experienced fliers who had never had any motion-sickness symptoms in parabolic flight. The fourth subject was tested on the fourth flight of her first week of parabolic flights, after we ascertained that

she is insusceptible to flight motion sickness. Subjects were blindfolded and tightly restrained in a motorized 2-axis device capable of tilting them in pitch (horizontal medial-lateral body axis), roll (horizontal anterior-posterior body axis) or recumbent yaw (horizontal foot-to-head body axis). Subjects wore earplugs and noise-canceling earphones and were listening to white noise to mask the sound of the aircraft as much as possible. The experimenter could interrupt the white noise to speak to the subject at any time. The experimenter triggered a 2-axis device movement when he or she judged that a stable 1.8-G or 0-G force period (during parabolas) or 1-G period (during straight-and-level flight) had been reached, by viewing accelerometer readout on our computer console. The 2-axis device moved to a randomly selected tilt angle, at 15° increments, about 1 of the 3 axes. Tilt velocity profiles were raised cosines with peak velocities of 100°/s and durations of 0.5 to 4 s. These profiles mimic natural head turns in speed and amplitude. When the tilt was complete, the subject heard a computer-generated command instructing him or her to indicate the subjective vertical by orienting a pointer held in both hands so that its top pointed “up.”

There were 2 tilts and 2 judgments in each 1.8-G and 0-G force phase during parabolas, as well as before flight in 1 G. Rests were given every sixth parabola, with the subject positioned upright.

Experiment 2, Limb mass adaptation. Each subject was tested in 20 parabolas of 1 flight day. Testing was done with the subject seated in any one of the standard aircraft seats on the right (starboard) side of the cabin. The portable work surface was secured to the arms of the chair with Velcro straps after takeoff. Marked on the table surface were a starting location for all reaches, and 2 target locations. In the 0-G phase of each parabola, the experimenter gave verbal commands for the subject to move from the start location to one of the targets, and to return when done. Ten movements per parabola were executed. In some parabolas, subjects made moves while holding a hollow cylinder, whereas in other parabolas the same shape cylinder was loaded with a mass of 500 g. A laptop computer collected kinematic data about the arm movement from a set of magnetic sensors mounted on cuffs worn on the arm.

Experiment 3, Weight / mass estimation. Each subject was tested in 20 parabolas of 1 flight day. Testing was done with the subject seated in any one of the standard aircraft seats on the left (port) side of the cabin. The tray with docked weights was secured to the subject's lap with Velcro straps after takeoff. Weights were identical-looking cylinders of different mass. A computer program selected 2 weights for the subject to compare, according to a modified staircase procedure. The subject would lift the 2 weights identified by lit LEDs, heft them, and report which one was heavier, or if they were perceived as weighing the same. The experimenter would record the answer and order the subject to put down both weights and take the next pair. The procedure was also completed in 1 G, before and after flight.

RESULTS, DISCUSSION, AND CONCLUSION

Preliminary analysis of the Vestibular Orientation experiment indicates that the quality and quantity of data collected are sufficient to consider data collection complete. Firm conclusions are not yet possible, but 2 notable features appear in the data: 1) Variability of the haptic subjective vertical increased dramatically with pitch and roll tilts beyond $\pm 90^\circ$ from the upright position, but there was no comparable change in variability during recumbent yaw axis tilts, in 1-G and 1.8-G force backgrounds. 2) In 0 G, subjects were not disoriented but instead had a firm sense of the vertical, although the direction varied with preceding tilt axis and angle.

Preliminary analysis of the Limb Mass Adaptation experiment indicated that changes in vertical displacement and horizontal velocity were the main kinematic consequences of altering the mass of the arm in 0 G. This is surprising because in 0 G, wielding or wearing the added load alters the dynamics in the plane of the movement (horizontal) but does not alter vertical loading.

Preliminary analysis of the Weight / Mass Estimation experiment indicated that subjects are able to discriminate identical-looking objects of different mass in 0 G. The discrimination thresholds and comparative analysis across G-levels, as well as glove conditions, are forthcoming.

ACKNOWLEDGEMENTS

This work is supported by Air Force Grant # FA9550-06-1-0102 and NASA Grant # NNNJ04HJ14G.

PHOTOGRAPHS:

JSC2008EO27366 to JSC2008EO27415

JSC2008EO27478 to JSC2008EO27517

JSC2008EO27560 to JSC2008EO27591

JSC2008EO27652 to JSC2008EO27689

VIDEO

- Zero G flight week March 17–21, 2008, Master: 306415

Videos available from Imagery and Publications Office (GS4), NASA JSC.

CONTACT INFORMATION

Dr. James R. Lackner, Director
Dr. Paul DiZio, Associate Director

lackner@brandeis.edu
dizio@brandeis.edu

Ashton Graybiel Spatial Orientation Laboratory
Brandeis University MS 033
Waltham MA 02454-9110
Tel: 781-736-2033
Fax: 781-736-2031

TITLE

Undergraduate Program – Multimission Space Suit EVA Drink Bag Filling Process

FLIGHT DATE

April 9, 2008

PRINCIPAL INVESTIGATOR

Steven C. Martinez, Auburn University

CO-INVESTIGATORS

Braxton Kinsey, Auburn University

Nathan Bussey, Auburn University

Brian Davis Jr., Auburn University



GOAL

To provide NASA’s astronaut corps a working centrifugal separation system that will allow air-tight filling of EVA bags.

OBJECTIVES

To prove that a centrifugal rotation system to separate air and water will be successful in providing a feasible solution to the EVA bag filling process problem.

Microgravity Program Introduction

NASA’s Reduced-Gravity Student Flight Opportunities Program (RGSFOP), also known as Microgravity University, along with Auburn University, gave the opportunity to a

selected group of students to design, construct, and present an experiment that will be tested on board NASA's C-9 Reduced-Gravity Plane, "Weightless Wonder," or as it is more affectionately known, "Vomit Comet." Steven Martinez (Student Lead), Braxton Kinsey, and Nathan Bussey, along with their faculty advisor Dr. Ahmed Anwar, have ventured out under the additional guidance of NASA engineers Mr. Robert Trevino and Ms. Jessica Vos in providing a solution to an actual problem faced by today's astronauts while in a microgravity environment. To achieve this goal, funding was provided by the Alabama Space Grant Consortium.

Auburn University's Reduced-Gravity (Microgravity) Flight Team worked in collaboration with NASA engineers to help in the design and testing of the Multi-Mission Space Extra Vehicular Activity (EVA) Suit. NASA's countdown to Shuttle retirement and aggressive schedule for the completion of the International Space Station is a pressing matter for the tasks at hand. The current NASA schedule calls for 16 more Shuttle flights through 2010. For this reason, NASA's pilots, mission specialists and engineers know that time is of the essence and every minute of work while in space is indispensable to meet all deadlines. Here is where the AUMG Team steps in, helping in the development of new-generation spacesuits that will allow mission crewmembers to perform EVAs for longer periods.

Flight Team members learned the basics of systems engineering from NASA professionals and applied technical knowledge to solve the problem presented to us by the Microgravity Program.

METHODS AND MATERIALS

Our team set out to design, build, and test a multi-mission spacesuit drink bag filling process that could remove air from drinking water quickly and be used for both 0 G and 1/6 G surface EVAs. The time overhead and crew workload needed to fill and remove air from drinking water before installing it in the suit is currently a major time-consuming item that affects the Work Efficiency Index. This is mainly a 0-G problem, but it may also apply to lunar 1/6 G conditions, which will also be tested by our team while we are on board the NASA aircraft. EVA drink bags will definitely be required during surface EVAs because the expected workloads are large.

To achieve our goals, we designed a centrifugal rotation mechanism that would separate air from water.

NASA's current approach to solving this problem is to spin the bags and separate the air from the water by hand, which costs crewmember time and energy. Our team has designed a mechanism to resolve this problem through utilization of a centrifugal rotation mechanism that separates water and air. Additionally we used air-tight intravenous (IV) fluid bags to serve in place of the drinking bags. By having these bags pre-vacuum sealed, we reduced the number of air bubbles from the water bag filling process.

FLIGHT TESTING AND RESULTS

During flight testing, our team was able to test a total of 4 bags. Three of these bags showed promising results in verifying that our filling process mechanism worked successfully. During the process, one of the bags had a leak (therefore, this bag could not retain water adequately), but the other 3 bags were filled with the water from the reservoir pods. Looking at the photographic and data evidence, it seems that if a larger reservoir of water were to be used, the IV bags would be filled completely with water, leaving only a negligible air pocket in the in/out flow line.



Figure 20-1 shows an example of the bags tested. The amount of air originally in the bag seemed to be negligible. The photograph shows more air in the bag due to the insertion of hot glue to seal the bag, which displaced more air into the bag.

DISCUSSION

From the results, we were able to determine that creating a centrifugal air / water separation mechanism for EVAs is a good approach conceptually. Our team is currently discussing possibilities of improvement to the design. After experiencing the microgravity environment we are now able to look at the problem with a better view and less guessing. Among the experiment modifications to consider are

- Higher quality video collection devices
- The use of flow valves for flow measurements
- Modification of the pods for a more efficient draining method (possibility of some type of hydraulic accumulator)

Regarding the experiment apparatus (not the actual testing device),

- The access door should be modified for faster and simpler access.

- Larger fitted Plexiglas panes should be ordered. (This will provide a safer and more water-tight device that should comply with Reduced-Gravity Operations standards.)
- Motor power control should be mounted alongside the laptop, as originally designed.
- The addition of at least one camera to record all actions and procedures performed during flight would provide better action and results analysis.

Our team is confident that with the flight experience we have gained and modifications to the apparatus, we will be able to provide a working system that will need further testing. For a more detailed report contact Steven Martinez at martist@auburn.edu.

PHOTOGRAPHS

JSC2008E033019
 JSC2008E033031 to JSC2008E033032
 JSC2008E033080 JSC2008E033092
 JSC2008E033109
 JSC2008E033120 to JSC2008E033121
 JSC2008E033124
 JSC2008E033147 to JSC2008E033148
 JSC2008E033080 to JSC2008E03384
 JSC2008E033148
 JSC2008E033242
 JSC2008E033246
 JSC2008E033261 to JSC2008E033266
 JSC2008E033277 to JSC2008E033280
 JSC2008E033282 to JSC2008E033286
 JSC2008E033338

VIDEO

- Zero G flight week April 7–11, 2008, Master: 734554

Videos available from Imagery and Publications Office (GS4), NASA JSC.

CONTACT INFORMATION

Team Members

Steven C. Martinez

Email: martist@auburn.edu

stevenmtz@prodeq.com.mx

Brian Davis Jr.

Email: davisb3@auburn.edu

Braxton Kinsey
Email: kinsebc@auburn.edu

Mentors

Ms. Jessica Vos
NASA Johnson Space Center
EC5/EVA Systems Integrated Test Lead
B7A R114, 281-244-1383
jessica.r.vos@nasa.gov

Mr. Robert Trevino
NASA Johnson Space Center
EC5/EVA Systems Integrated Test Lead
B7A R114, 281-244-1383
robert.c.trevino@nasa.gov

Faculty Advisors

Brian S. Thurow, PhD, Assistant Professor,
Department of Aerospace Engineering
211 Aerospace Engineering Building
Auburn University, AL 36849-5338

Ahmed Anwar, PhD, Assistant Professor,
Department of Aerospace Engineering
211 Aerospace Engineering Building
Auburn University, AL 36849-5338

TITLE

Undergraduate Program – Gravitational Effects on Human Immune Complexes and Flame Dynamics

FLIGHT DATE

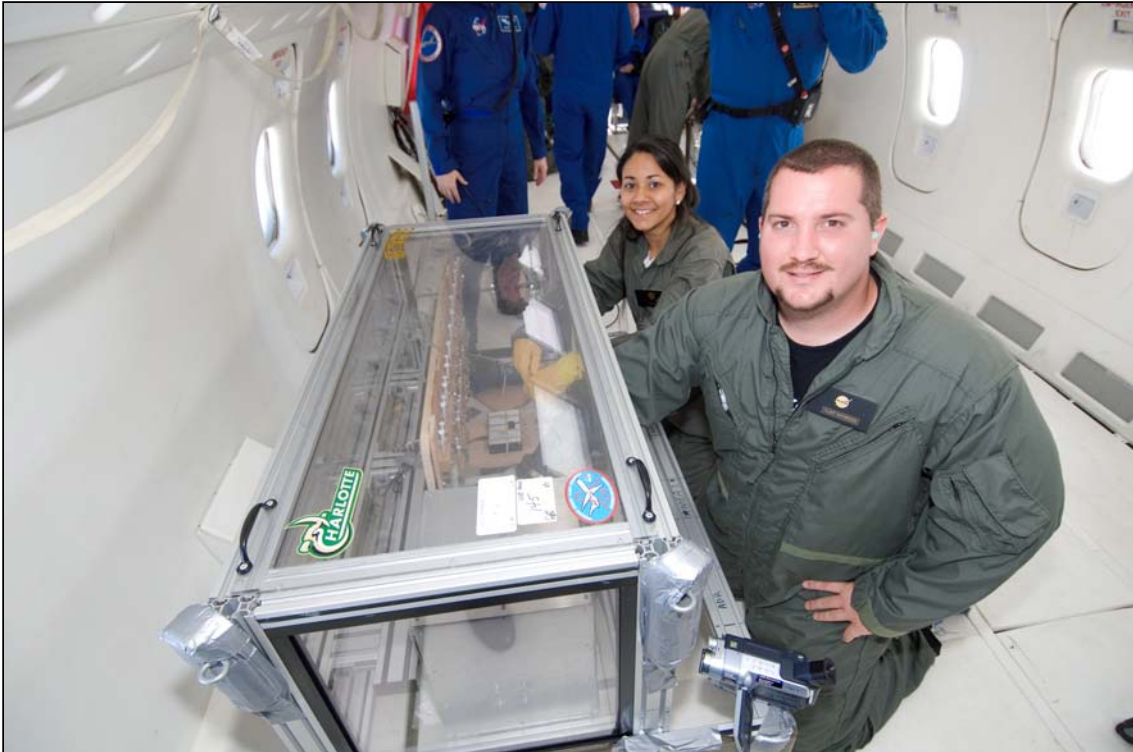
April 22–23, 2008

PRINCIPAL INVESTIGATORS

Timothy Ritter, University of North Carolina at Pembroke
Clinton Haywood, University of North Carolina at Pembroke
Samantha Schrock, University of North Carolina at Pembroke
Tala Smith, University of North Carolina at Pembroke
Lisa Walters; University of North Carolina at Pembroke

CO-INVESTIGATORS

Siva Mandjiny, University of North Carolina at Pembroke



GOAL

To determine if the force of gravity has an effect on the rate at which immune complexes are formed. To observe and visually record the physical changes of a flame as it passes through varying gravitational fields.

OBJECTIVES

We considered the following question for our principal investigation with this project: “What is the dependency of immune complex formation on gravitational force, if any?” We hypothesized that gravitational forces would change the convection flow in the fluid in which immune molecules are immersed, thus preventing the immune molecules from interacting the way they normally do. We predicted that the reaction rate would decrease because less molecular interaction would occur. In an attempt to prove our hypothesis, the University of North Carolina at Pembroke conducted a reaction to form human immune complexes during the 0-G portions of the parabolic curves provided by the flight of NASA’s C-9 aircraft. Since the immune system is known to be compromised during long-term space travel, this experiment was performed to test how decreases in gravitational fields change the way immune complexes are formed in the human body. Along with our primary research project, we also conducted a flame dynamics experiment as part of our outreach program. We visually recorded the changes in the physical characteristics of a flame while passing through both 0-G and 2-G portions of the parabola in hopes of stimulating youth interest in the sciences.

METHODS AND MATERIALS

To study the formation of immune complexes in vitro, we observed the reaction between human immunoglobulin G (IgG) and goat-derived anti-immunoglobulin G (A-IgG) in a sodium phosphate buffer. The buffer solution contained polyethylene glycol (PEG), which served as a catalyst to break down the structure of the water molecules and increase the rate of reaction. This was necessary because of the time constraint and limited periods in the 0-G gravitational field. To measure the rate at which the complexes formed after the IgG and A-IgG solutions had been combined, we used an Ocean Optics CHEMUSB4-UV-VIS consisting of a USB4000 spectrometer with a combination deuterium tungsten halogen light source and 1-cm cuvette holder interfaced with a PASCO Xplorer GLX Datalogger. This setup was used to record the absorption measurements during the approximately 20- to 25-s periods of 0 G.

While in flight, the experiment apparatuses were housed in a double-walled Plexiglas glove box, which allowed access by heavy-duty industrial-style rubber gloves. The Immune Complex Formation (ICF) apparatus was constructed using two 1-mL syringes secured to a wooden piece by a retaining block, figure 21-1. Each syringe had a 26-gauge needle secured to it. The 2 needles punctured a plastic cap, which was sealed to a standard CVD-UV plastic 1 cm × 1 cm × 4.5 cm (4.5 mL) cuvette. The top of each cuvette was secured to the wooden piece by an aluminum retaining strip. Each ICF apparatus was secured vertically to an ICF holder using industrial-style Velcro.

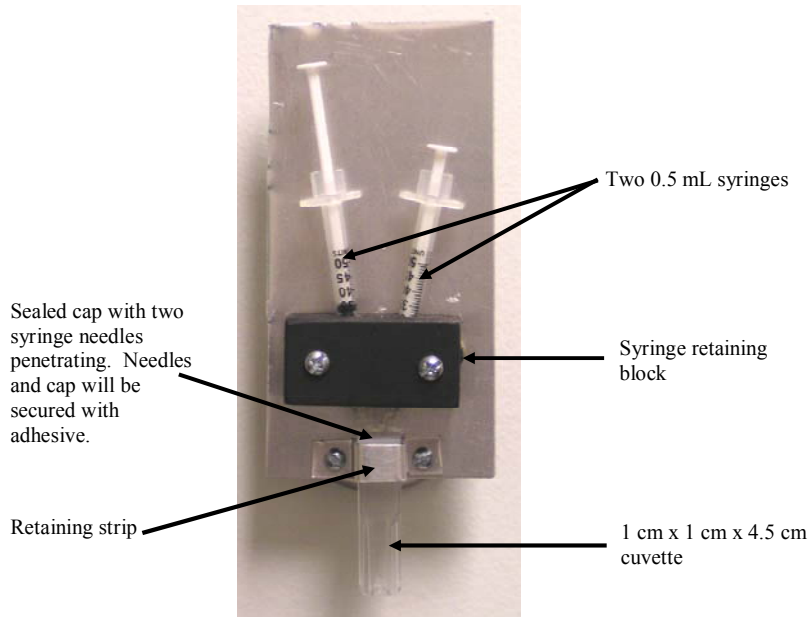


Figure 21.1. Immune Complex Formation (ICF) apparatus.

Between 0-G portions of the parabolas, one ICF was removed from the ICF holder and placed in the spectrophotometer. The IgG solutions had been pre-inserted into the cuvettes and upon entering the 0-G portion, the A-IgG was inserted and the absorption recorded over the 20- to 25-s period.

The Flame Dynamics apparatus consisted of a combustion containment chamber. The 10 in × 10 in × 12 in chamber was composed of 22-gauge aluminum sheets on 5 sides, with 1 side made of Lexan polycarbonate to allow the experiment to be visually recorded, figure 21-2. For access to the chamber, a 5-inch-diameter hole was cut in the right side of the box and covered by a 6-inch-diameter piece of 22-gauge aluminum attached using industrial-strength Velcro. A common emergency candle was inserted into a 0.75-in-wide × 2.5-in-long metal pipe mounted at a slight upward angle. The candle was lit using a non-pressurized liquid-fuel (Zippo) lighter.

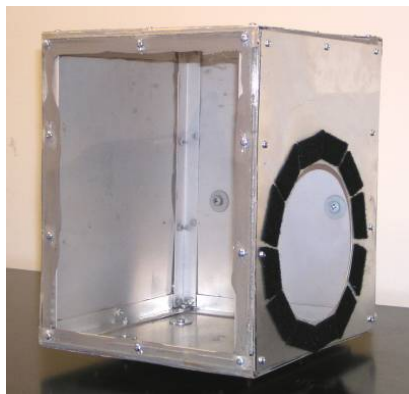


Figure 21-2. The Flame Dynamics apparatus utilized in the candle experiment, shown outside of glove box. Candle mount not shown.

RESULTS AND DISCUSSION

In the case of the immune complex experiment, the team experienced a catastrophic loss of flight data. Unfortunately, the data were not backed up immediately after the flight. During the trip from Houston back to North Carolina, all data stored on the GLX Datalogger were lost. Even though the team did not have any data to analyze, initial results were encouraging. Plots of the data were made and observed immediately after the flight on the GLX Datalogger. A non-quantitative analysis of these results did appear to validate our hypothesis, that the rate of reaction during flight was less than in the 1-G laboratory setting. However, no quantitative analysis was made in Houston, and thus all results for this part of the experiment, while encouraging, are qualitative.

In the case of the candle experiment the team had much more success. The apparatus worked rather well. The major problem was in lighting the candle if and when it was extinguished. The Zippo lighter did not function well in the 0-G environment of the aircraft and it was very difficult to ignite the lighter itself. When the candle was lit, it did demonstrate a variance in the shape and color of the flame as the aircraft went from micro- to hypergravity conditions. During the hypergravity portions of the flight the flame elongated considerably relative to its 1-G shape and size, while during the 0-G portions the flame became more spherical and shorter in length. These results were not a surprise and are what the team expected. All of these results were captured on video and will be added to future outreach presentations.

CONCLUSION

In the first experiment, we attempted to investigate the effects of microgravity on the immune system by looking at the binding rates of antigens and antibodies found in the human body. In this experiment, we observed the reaction between human immunoglobulin G (IgG) and goat-derived anti-immunoglobulin G (A-IgG) in a sodium phosphate buffer. The identical experiment was performed in 0 G and 1 G to determine if there is a gravitational effect on the rate of reaction. Because all flight data were lost, the 0-G results could not be compared to our 1-G samples. The second experiment, which was primarily an outreach demonstration, was much more successful. We were able to observe and record a candle flame in 0 G, 1 G, and 2 G. The video clearly shows the effects of a varying gravitational environment and will be incorporated into our outreach program.

REFERENCES

- Borchers AT, Keen CL, Gershwin ME. Microgravity and Immune Responsiveness: Implications for Space Travel. *Nutrition*, **18** (2002) 889–898.
- Dietrich DL, Ross HD, Shu Y, Chang P, Tien JS, *Combustion Science & Technology*, **156** (2000) 1-24.
- Ronney PD. Combustion Phenomena at Microgravity. In *Physics of Fluids in Microgravity*, ed. by R. Monti, Taylor & Francis Inc., New York, 2001.

Sonnenfeld G. The Immune System in Space and Microgravity. *Med Sci Sports Exerc*, **34** (2002) 2021–2027.

Sonnenfeld G, Butel JS, Shearer WT, Effects of the Space Flight Environment on the Immune System. *Rev Environ Health*, **18** (2003) 1–17.

Sonnenfeld G, Shearer WT. Immune Function during Space Flight. *Nutrition*, **18** (2002) 899–903.

Sundaresan A, Risin D, and Pellis NR, *J Appl Physiol*, **96** (2004) 2028-2033.

Wisniak J. *Indian Journal of Chemical Technology*, **7** (2001) 319-326.

PHOTOGRAPHS

JSC2008EO35707

JSC2008EO35716

JSC2008EO35730

JSC2008EO35752

VIDEO

- Zero G flight week April 21–25, 2008, Master: DV1465

Videos available from Imagery and Publications Office (GS4), NASA JSC.

CONTACT INFORMATION

Dr. Timothy M. Ritter
Dept. of Chemistry and Physics
University of North Carolina Pembroke
Pembroke, NC 28372
tim.ritter@uncp.edu.

TITLE

Undergraduate Program – Study of Damping Effects of Grass-like Crops in a Microgravity Environment

FLIGHT DATE

June 12–13, 2008

PRINCIPAL INVESTIGATORS

Jordan Addison, Lamar University
Tiffany Smith, Lamar University
Jonathan Sterling, Lamar University
Corey Wyble, Lamar University
Jiang Zhous, Lamar University



GOAL

The goal of the experiment is to study the damping effects of wheat and other flexible crop structures on a vibrating system in microgravity.

INTRODUCTION

The basis for this experiment is Dr. Jiang Zhou's Texas Space Grant Consortium New Investigators' Program Proposal: Feasibility Study of Synergistic Effect of Spacecraft Vibration Suppression and Crop Based Life Support. This study states that spacecraft can vibrate in the frequency range of 0.1 to 4 Hz.

METHODS AND MATERIALS

Grass-like crops, such as wheat, were used to determine if they provide useful information about the damping of low-frequency vibrations.

A shaker table was used to create these vibrations. The amount the wheat or grass-like crops damped the vibrations was recorded.

Testing was conducted on 2 flights aboard NASA's C-9 aircraft with approximately 30 microgravity parabolas per flight.

RESULTS AND DISCUSSION

As we have just completed the C-9 flight opportunities, data processing and analysis are continuing.

CONCLUSION

Preliminary observations suggest that grass-like crops do provide some vibration damping benefit. Ground-based experiments conducted for long-term study of the damping effect and the effect of vibration on the growth of the crops are being planned.

PHOTOGRAPHS

JSC2008EO46837
JSC2008EO46845 to JSC2008EO46846
JSC2008EO46858
JSC2008EO46866
JSC2008EO46873
JSC2008EO46893

VIDEO

- Zero G flight week June 5–14, 2008, Master: 738973

Videos available from Imagery and Publications Office (GS4), NASA JSC.

CONTACT INFORMATION

Jonathan Sterling
crimsoncleansed@gmail.com
Lamar University

Appendix

Background Information about the C-9 and the Reduced-Gravity Program

The Reduced-Gravity Program, operated by the NASA Johnson Space Center (JSC), provides engineers, scientists, and astronauts alike a unique opportunity to perform testing and training in a weightless environment but without ever having to leave the confines of Earth orbit. Given the frequency of Space Shuttle missions, the construction and habitation of the International Space Station, and NASA's new mission to explore the moon and Mars, the Reduced-Gravity Program provides a truly ideal environment to test and evaluate space hardware and experimental procedures before launch.

The Reduced-Gravity Program was established in 1959 to investigate the reactions of humans and hardware during operations in a weightless environment. A specially modified C-9 turbojet, flying parabolic arcs, produces periodic episodes of weightlessness lasting 20 to 25 s. The C-9 is sometimes also flown to provide short periods of lunar (1/6) and martian (1/3) gravity. Over the last 35 years, approximately 100,000 parabolas have been flown in support of the Mercury, Gemini, Apollo, Skylab, Space Shuttle, and Space Station Programs.

Excluding the C-9 Flight Crew and the Reduced-Gravity Program Test Directors, the C-9 accommodates seating for a maximum of 20 other passengers. The C-9's cargo bay provides a test area that is approximately 45 feet long, 104 inches wide, and 80 inches high. The aircraft is equipped with electrical power, overboard venting system, and photographic lights. When requested and available, professional photography and video support can be scheduled to document activities during flight.

A typical flight lasts 2 to 3 hours and consists of 30 to 40 parabolas. The parabolas are flown in succession or with short breaks between maneuvers to allow time for reconfiguring test equipment.

For additional information about flight weeks sponsored by the Johnson Space Center's Human Adaptation & Countermeasures Division or other Reduced-Gravity Program opportunities, please contact

| | | |
|-------------------------------------|----|---|
| Todd Schlegel, MD | or | Dominic Del Rosso |
| Technical Monitor | | Lead Test Director |
| Human Adaptation & Countermeasures | | NASA Lyndon B. Johnson Space Center |
| NASA Lyndon B. Johnson Space Center | | Reduced-Gravity Office, Ellington Field |
| Mail Code: SK | | Mail Code: CC43 |
| Houston, TX 77058 | | Houston, TX 77034 |
| Telephone: (281) 483-9643 | | Telephone: (281) 244-9113 |

Explore the Zero Gravity Experiments and Aircraft Operations Web pages at:
<http://zerog.jsc.nasa.gov/> and <http://jsc-aircraft-ops.jsc.nasa.gov/>

| REPORT DOCUMENTATION PAGE | | | Form Approved OMB No. 0704-0188 | |
|--|---|--|---|----------------|
| Public reporting burden for this collection of information is estimated to average 1 hour per response, including the time for reviewing instructions, searching existing data sources, gathering and maintaining the data needed, and completing and reviewing the collection of information. Send comments regarding this burden estimate or any other aspect of this collection of information, including suggestions for reducing this burden, to Washington Headquarters Services, Directorate for Information Operations and Reports, 1215 Jefferson Davis Highway, Suite 1204, Arlington, VA 22202-4302, and to the Office of Management and Budget, Paperwork Reduction Project (0704-0188), Washington, DC 20503. | | | | |
| 1. AGENCY USE ONLY (Leave Blank) | 2. REPORT DATE September 2008 | 3. REPORT TYPE AND DATES COVERED NASA Technical Paper | | |
| 4. TITLE AND SUBTITLE C-9 and Other Microgravity Simulations | | | 5. FUNDING NUMBERS | |
| 6. AUTHOR(S) Prepared by: Space and Life Sciences Directorate Human Adaptation and Countermeasures Office | | | | |
| 7. PERFORMING ORGANIZATION NAME(S) AND ADDRESS(ES) Lyndon B. Johnson Space Center Houston, Texas 77058 | | | 8. PERFORMING ORGANIZATION REPORT NUMBERS S-1015 | |
| 9. SPONSORING/MONITORING AGENCY NAME(S) AND ADDRESS(ES) National Aeronautics and Space Administration Washington, DC 20546-0001 | | | 10. SPONSORING/MONITORING AGENCY REPORT NUMBER TM-2006-213727 | |
| 11. SUPPLEMENTARY NOTES | | | | |
| 12a. DISTRIBUTION/AVAILABILITY STATEMENT Available from the NASA Center for AeroSpace Information (CASI) 7121 Standard Hanover, MD 21076-1320 Category: 99 | | | 12b. DISTRIBUTION CODE | |
| 13. ABSTRACT (Maximum 200 words) This document represents a summary of medical and scientific evaluations conducted aboard the C-9 or other NASA sponsored aircraft from June 23, 2007, to June 23, 2008. Included is a general overview of investigations manifested and coordinated by the Human Adaptation & Countermeasures Division. A collection of brief reports that describe tests conducted aboard the NASA-sponsored aircraft follows the overview. Principal investigators and test engineers contributed significantly to the content of the report describing their particular experiment or hardware evaluation. Although this document follows general guidelines, the format of individual reports varies to accommodate differences in experiment design and procedures. This document concludes with an appendix that provides background information about the Reduced Gravity Program. | | | | |
| 14. SUBJECT TERMS Weightlessness, weightlessness simulation, parabolic flight, zero gravity, aerospace medicine, astronaut performance, bioprocessing, space manufacturing. | | | 15. NUMBER OF PAGES 160 | 16. PRICE CODE |
| 17. SECURITY CLASSIFICATION OF REPORT Unclassified | 18. SECURITY CLASSIFICATION OF THIS PAGE Unclassified | 19. SECURITY CLASSIFICATION OF ABSTRACT Unclassified | 20. LIMITATION OF ABSTRACT Unlimited | |
